

Review

Hubble Tension: The Evidence of New Physics

Jian-Ping Hu ¹ and Fa-Yin Wang ^{1,2,*}¹ School of Astronomy and Space Science, Nanjing University, Nanjing 210093, China; hjp2022@nju.edu.cn² Key Laboratory of Modern Astronomy and Astrophysics (Nanjing University), Ministry of Education, Nanjing 210093, China

* Correspondence: fayinwang@nju.edu.cn

Abstract: The Λ CDM model provides a good fit to most astronomical observations but harbors large areas of phenomenology and ignorance. With the improvements in the precision and number of observations, discrepancies between key cosmological parameters of this model have emerged. Among them, the most notable tension is the 4σ to 6σ deviation between the Hubble constant (H_0) estimations measured by the local distance ladder and the cosmic microwave background (CMB) measurement. In this review, we revisit the H_0 tension based on the latest research and sort out evidence from solutions to this tension that might imply new physics beyond the Λ CDM model. The evidence leans more towards modifying the late-time universe.

Keywords: cosmological parameters; cosmology; Hubble constant

1. Introduction

The cosmological constant (Λ) cold dark matter model (Λ CDM) is the simplest cosmological model and consistent with the most astronomical observations [1–14]. In the past 30 years, it has been the best model, and no better one has yet been presented to replace it. Despite its remarkable successes, the validity of the Λ CDM model is currently under intense investigation [13,15–17] (for reviews, see [18–23]). The fine tuning and coincidence problems are the most important theoretical difficulties [24–28]. The fundamental problem with the former is that there is a large discrepancy between the observations and theoretical expectations of Λ [24,26,29,30]. The latter is related to the observed vacuum energy density Ω_Λ and the matter energy density Ω_m , which are now nearly equal despite their dramatically different evolutionary properties. The anthropic principle, as a possible solution to these problems, states that these “coincidences” results from a selection bias towards the existence of human life in the context of a multiverse [31,32]. In addition to the above theoretical challenges, the two main components in the Λ CDM model, dark matter (DM) and dark energy (DE), are poorly understood. Moreover, there are also some tensions between the cosmological and astrophysical observations and the Λ CDM model, which include the Hubble tension [3,33–40] (5σ), growth tension [41–43] ($2\text{-}3\sigma$), CMB anisotropy anomalies [22,44–53] ($2\text{-}3\sigma$), cosmic dipoles [23,54–63] ($2\text{-}5\sigma$), Baryon Acoustic Oscillation (BAO) curiosities [64–66] ($2.5\text{-}3\sigma$), parity violating rotation of CMB linear polarization [67–70], small-scale curiosities [71–74], age of the universe [75], the Lithium problem [76] ($2\text{-}4\sigma$), the quasar Hubble diagram [77–81] ($\sim 4\sigma$), oscillating signals in short range gravity experiments [82,83], anomalously low baryon temperature [84] ($\sim 3.8\sigma$), colliding clusters with high velocity [85,86] ($\sim 6\sigma$), etc. More detailed information of these tensions can be found from Perivolaropoulos and Skara [21]. The H_0 tension emerged with the first release of *Planck* results [87], and has grown in significance in the past few years [3,33–40].



Citation: Hu, J.-P.; Wang, F.-Y. Hubble Tension: The Evidence of New Physics. *Universe* **2023**, *1*, 0. <https://doi.org/>

Received: 13 January 2023

Revised: 21 January 2023

Accepted: 6 February 2023

Published:



Copyright: © 2023 by the authors. Licensee MDPI, Basel, Switzerland. This article is an open access article distributed under the terms and conditions of the Creative Commons Attribution (CC BY) license (<https://creativecommons.org/licenses/by/4.0/>).

There have been many studies dedicated to finding out what causes the Hubble tension, but so far there is no convincing explanation. The reanalyses of the Planck observations and Hubble Space Telescope (HST) measurements demonstrate that the serious discrepancy of H_0 may not be caused by systematics (including photometric biases, environmental effects, calibration error, lens mass modelling biases, CMB foreground effects and so on) [35,40,46,88–94]. Hence, many researchers prefer to believe that the H_0 tension might be caused by new physics beyond the Λ CDM model [36]. So far, there has been a large number of modified models which adopted to resolve or relieve the H_0 tension, see [19,21] for a review of H_0 tension solutions. Although many extensions of Λ CDM can alleviate the H_0 tension, none are supported by the majority of observations [95,96]. There are many international conferences held on the H_0 tension, such as “Beyond Λ CDM”, “Hubble Tension Headache”, “Tensions between the Early and the Late Universe”, etc. [97]. “Beyond Λ CDM” in Oslo in 2015, a poll at the conference showed that 69% of participants believe that new physics is the most likely explanation. On the contrary, more than 50% of the participants of the “Hubble Tension Headache” conference held by the University of Southampton supported the explanation that there were still systematics unknown to us in the observational data. Theoretical Physics workshop (“Tensions between the Early and the Late Universe”) in July 2019 directed attention to the Hubble constant discrepancy. The workshop pointed out that “New results showed that it does not appear to depend on the use of any one method, team or source” [98]. To streamline the interaction between these different communities and promote the transparent transfer of information, participants also gave some reasonable suggestions. More details about the workshop are available at website: <https://www.kitp.ucsb.edu/activities/enervac-c19>. In a word, the research and discussion on the H_0 tension is still going on.

This review is organized as follows. In Section 2, we briefly introduce the H_0 tension, and then detail two methods for constraining H_0 , the CMB measurements and the local distance ladder. In Section 3, we discuss recent methods for estimating H_0 using otherwise independent observations. We also discuss a taxonomy of solutions to the H_0 tension in Section 4. Afterwards, from all the solutions to the H_0 tension, we sort out evidence that might imply new physics beyond the Λ CDM model and briefly introduce some of the proposed scenarios in Section 5. Finally, we give a brief conclusion and future prospects.

2. H_0 Tension

The local expansion rate of the universe H_0 is a fundamental value. It also determines the age of the universe; thus, it is important to determine it accurately. The accuracy of H_0 measurements has been improved as the number of probes has increased. A review of most well-established probes can be found in literature [99]. In general, the H_0 measurements can be estimated from the cosmological model utilizing the early universe measurements, or more directly measured from the local universe. Interestingly, the H_0 values measured by these two approaches are inconsistent. The discrepancy between the H_0 values measured from the local distance ladder and from the CMB is the most serious challenge to the standard Λ CDM model. This H_0 discrepancy is also known as “Hubble Tension” [87].

2.1. Constraints of H_0 from the CMB Measurements

The estimation of H_0 from the CMB data proceeds in three steps [100,101]: (1) determine the baryon density and matter density to allow for the calculation of the sound horizon size (r_s); (2) infer θ_s from the spacing between the acoustic peaks to determine the comoving angular diameter distance to last scattering $D_A = r_s/\theta_s$; (3) adjust the only remaining free density parameter in the model that D_A gives this inferred distance. With this last step complete, we now have $H(z)$ determined for all z , including H_0 ($z = 0$).

In 2013, Bennett et al. [100] provided $H_0 = 70.00 \pm 2.20$ km/s/Mpc through analysing the nine-year Wilkinson Microwave Anisotropy Probe (WMAP) observations. Meanwhile, the first data release of the *Planck* space observatory, which was operated by the European Space Agency (ESA), gave a precise result $H_0 = 67.40 \pm 1.40$ km/s/Mpc [87]. After that, a more accurate $H_0 = 67.40 \pm 0.50$ km/s/Mpc yielded by the *Planck* final data release is also in line with the *Planck*2013 results [3]. Researchers also consider adding the other observational data to constrain H_0 , *Planck*2018+lensing 67.36 ± 0.54 km/s/Mpc and *Planck*2018+lensing+BAO 67.66 ± 0.42 km/s/Mpc [3]. The main H_0 measurements are shown in Figure 1. In addition, there exists a lot of H_0 predictions adopting other CMB experiments from the ground, including the South Pole Telescope (SPTPol) [66,102] and Atacama Cosmology Telescope (ACT) [103]. These H_0 predictions are all consistent with the *Planck*2018 result [3].

2.2. Constrain H_0 from the Local Distance Ladder

At present, there has been a lot of methods in the local universe to estimate the Hubble constant based on the distance-redshift relation. These methods are usually undertaken by building a “local distance ladder”; the most common approach is to adopt geometry to calibrate the luminosity of specific star types. Cepheid variables are often employed to determine the distance of 10–40 Mpc [104,105]. Measuring longer distances requires other standard candles, for example SNe Ia, whose maximum redshift can reach 2.36 [2,7]. Quasars [106–115] and gamma radio bursts (GRBs) [5,10,14,116–128] offer the prospect of extending the Hubble diagram up to higher redshifts.

The first H_0 estimation, using the Cepheid variables and SNe Ia provided by the HST project, was 72 ± 8 km/s/Mpc [104]. A improved result, 74.3 ± 2.1 km/s/Mpc, was yielded by using a modified distance calibration [105]. After that, the SH0ES project, which started in 2005, also produces many H_0 results [34,35,39,129]. Based on the SH0ES data, H_0 results from numerous reanalyses using different formalisms, statistical methods of inference, or replacement of parts of the data-set are both in line with the previous results [130–136]. The latest H_0 result provided by the SH0ES collaboration shows that $H_0 = 73.04 \pm 1.04$ km/s/Mpc [40].

During the last few decades there has been remarkable progress in measuring the Hubble constant. The available technology and measurement methods determine the accuracy of this quantity. The main H_0 results up to 2022 obtained from the CMB measurements and the local distance ladder, as a function of the publication year, is shown in Figure 1. The uncertainties in these values have been decreasing for both methods and the recent measurements disagree by 5σ [40]. There is an obvious H_0 tension without physical explanations.

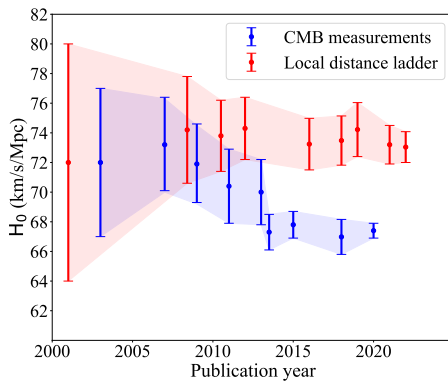


Figure 1. H_0 measurements from the early-time and the late-time observations. Blue points denote H_0 estimations from analyses of CMB data, including first year WMAP [137], three year WMAP [138], five year WMAP [139], seven-year WMAP [140], nine-year WMAP [100], Planck 2013 [87], Planck 2015 [33], Planck 2018 [3] and BAO [65]. Red points denote H_0 values measured by utilizing the local distance ladder including the Cepheid distance scale [104], Carnegie Hubble Program [105] and SH0ES [34,35,39, 40,129,141,142]. (Source: Figure 12 in Perivolaropoulos and Skara [21])

3. H_0 Arbitration

The *Planck* CMB measurements and the local ladder measurements both provide very precise constraints on cosmological parameters. However, as with any experimental measurement, they are not free from systematic errors. Hence, possible systematics in the *Planck* observations and the HST measurements are suspected to be responsible for the Hubble discrepancy in the early and late measurements. However, this possibility has been largely ruled out [35,40,46,88–92,94]. Since reanalyses of the *Planck* and local ladder measurements could not find a satisfactory answer to the H_0 tension, hope was pinned on other observations, such as quasar lensing [37,143], Megamaser [144–148], gravitational waves (GW) [149–151], fast radio bursts (FRBs) [152–156], tip of the red giant branch (TRGs) [157–159], BAOs [4,65], Type II supernovae [94], Ages of Old Astrophysical Objects [160,161], etc. [162]. These observations do not assume a cosmological model and are independent of the CMB and distance ladder measurements.

3.1. Quasar Lensing

Quasar lensing as an independent method can be used to estimate H_0 . With observed time delay $\Delta\tau_{obs}$ and lens mass model, H_0 can be inferred. The observed time delay is owing to the geometrical path length difference caused by the gravitational potential of the lens, which is associated with the path of the light rays from the vicinity of the lens to the observer [163]. The time delay distance $D_{\Delta t}$ inferred from $\Delta\tau_{obs}$ is actually a combination of angular diameter distances: [37]

$$D_{\Delta t} \equiv (1 + z_{lens}) \frac{D_d D_s}{D_{ds}}, \quad (1)$$

where z_{lens} is the lens redshift, D_d is the angular diameter distance to the lens, D_s is the angular diameter distance to the source, and D_{ds} is the angular diameter distance between the source and the lens. In the flat Λ CDM model, D_{ds} can be given as [164]

$$D_{ds} = \frac{c}{H_0(1 + z_s)} \int_{z_{lens}}^{z_s} (\Omega_m(1 + z')^3 + \Omega_\Lambda)^{-1/2} dz', \quad (2)$$

here, z_s is the redshift of source. Substitute z_{lens} and z_s into the following formula:

$$D_i = \frac{c}{H_0(1+z_i)} \int_0^{z_i} \sqrt{\Omega_m(1+z')^3 + \Omega_\Lambda} dz', \quad (3)$$

the expressions of D_d and D_s can be obtained. The time delay distance is primarily sensitive to H_0 , with weak dependence on other cosmological parameters. There were seven systems which provided the estimations of H_0 , as shown in the following Table 1. In addition, Wong et al. [37] and Millon et al. [143] utilize the multiple lens systems to constrain H_0 ; the former provides a result of $73.3^{+1.7}_{-1.8}$ km/s/Mpc and the latter provides a result of $74.0^{+1.7}_{-1.8}$ km/s/Mpc. Recently, Shajib et al. [165] updated the H_0 measurement ($78.3^{+3.4}_{-3.3}$ km/s/Mpc) derived from the lens RXJ1131-1231, and provided a new H_0 measurement ($74.2^{+1.6}_{-1.6}$ km/s/Mpc) for seven lenses. Their new measurement is in excellent agreement with those obtained in the past using standard simply parametrized mass profiles.

Table 1. Summary of the H_0 estimations derived from the quasar lensing systems.

Lens Name	z_d	z_s	H_0 (km/s/Mpc)	Reference
B1608+656	0.6304	1.394	$71.0^{+2.9}_{-3.3}$	[166,167]
RXJ1131-1231	0.295	0.654	$78.3^{+3.4}_{-3.3}$	[165,168,169]
HE0435-1223	0.4546	1.693	$71.7^{+4.8}_{-4.5}$	[169,170]
SDSS 1206+4332	0.745	1.789	$68.9^{+5.4}_{-5.1}$	[171]
WFI2033-4723	0.6575	1.662	$71.6^{+3.8}_{-4.9}$	[172]
PG1115+080	0.311	1.722	$81.1^{+8.0}_{-7.1}$	[169]
DES J0408-5354	0.597	2.375	$74.2^{+2.7}_{-3.0}$	[173,174]

3.2. Megamaser

Water megamasers residing in the accretion disks around supermassive black holes (SMBHs) in active galactic nuclei (AGNs) provide a unique way to bypass the distance ladder and make one-step, geometric distance measurements to their host galaxies [148]. The archetypal AGN accretion disk megamaser system is located in the nearby (7.6 Mpc) [147,175] Seyfert 2 galaxy NGC 4258 [176–178]. The Megamaser Cosmology Project (MCP) is a multi-year campaign to find, monitor, and map AGN accretion disk megamaser systems [179,180]. The primary goal of the MCP is to constrain H_0 to a precision of several percent through making geometric distance measurements to megamaser galaxies in the Hubble flow [144–146,181]. Distance measurements using the megamaser technique do not rely on the CMB or distance ladders measurements. Therefore, megamaser measurements provide an independent handle on H_0 estimates.

The MCP has so far published distances to six galaxies including UGC 3789 [145], NGC 6264 [144], NGC 6323 [146], NGC 5765b [182], NGC 4258 [147] and CGCG 074-064 [183]. The latest details of these six galaxies are shown in Table 2. In 2018, Braatz et al. [184] updated the published value to the UGC 3789 and obtained the H_0 estimation by using the first four galaxies, $H_0 = 69.3 \pm 4.2$ km/s/Mpc. Recently, Pesce et al. [148] applied an improved approach for fitting maser data and obtained better distance estimates for the first four galaxies. Combining all the distance measurements of galaxies and assuming a fixed velocity uncertainty of 250 km/s in connection with peculiar motions, they provided the H_0 estimation, $H_0 = 73.9 \pm 3.0$ km/s/Mpc, independent of the CMB and distance ladders measurements.

Table 2. The details of six galaxies. The H_0 estimations are obtained by assuming a fixed velocity uncertainty of 250 km/s. (Source: Tables 1 and 2 in Pesce et al. [148].)

Galaxy Name	Distance (Mpc)	Velocity (km/s)	H_0 (km/s/Mpc)	Reference
UGC 3789	$51.5^{+4.5}_{-4.0}$	3319.9 ± 0.8	$75.8^{+3.4}_{-3.3}$	[145]
NGC 6264	$132.1^{+21.0}_{-17.0}$	10192.6 ± 0.8	$73.8^{+3.2}_{-3.2}$	[144]
NGC 6323	$109.4^{+34.0}_{-23.0}$	7801.5 ± 1.5	$73.8^{+3.1}_{-3.0}$	[146]
NGC 5765b	$112.2^{+5.4}_{-5.1}$	8525.7 ± 0.7	$74.1^{+4.5}_{-4.4}$	[182]
NGC 4258	7.58 ± 0.11	679.3 ± 0.4	$73.6^{+3.1}_{-3.0}$	[147]
CGCG 074-064	$87.6^{+7.9}_{-7.2}$	7172.2 ± 1.9	$72.5^{+3.4}_{-3.2}$	[183]

3.3. Gravitational Wave

On 17 August 2017, the Advanced Laser Interferometer Gravitational-wave Observatory (LIGO) [185] and Virgo [186] detectors observed GW170817, a strong signal from the merger of a binary neutron-star system. Less than 2 seconds after the merger, a gamma-ray burst (GRB 170817A) was detected within a region of the sky consistent with the LIGO-Virgo-derived location of the GW source [187–189]. The detection of GW170817 in both gravitational waves and the electromagnetic (EM) waves heralds the age of the gravitational-wave multi-messenger astronomy.

With the luminosity distance fitted from the GW waveform and the redshift information from the host galaxy, GW can be treated as standard sirens to conduct research in cosmology. The GW amplitude depends on the chirp mass and luminosity distance of the GW source. The mass can be precisely determined by the phase measurement of the GW signal. Therefore, as long as the amplitude and phase information of the GW source are obtained at the same time, the corresponding luminosity distance can be given. The heliocentric redshift measurement, $z_{helio} = 0.009783$, was obtained from the optical identification of the host galaxy NGC 4993 [190]. The joint analysis of the GW signal from GW170817 and its EM localization led to the first H_0 estimation, $H_0 = 74^{+16}_{-8}$ km/s/Mpc (median and symmetric 68% credible interval) [149]. In this analysis, the degeneracy in the GW signal between the source distance and the observing angle dominated the uncertainty of the H_0 measurement. Tight constraints on the observing angle using high angular resolution imaging of the radio counterpart of GW170817 have been obtained [150]. Hotokozaka et al. [151] reported an improved measurement of $H_0 = 70.30^{+5.3}_{-5.0}$ km/s/Mpc by using these new radio observations, combined with the previous GW and EM data. Recently, using 47 GW sources from the Third LIGO-Virgo-KAGRA Gravitational-Wave Transient Catalog (GWTC-3), The LIGO Scientific Collaboration et al. [191] presented $H_0 = 68^{+12}_{-7}$ km/s/Mpc (68% credible interval) when combined with the H_0 measurement from GW170817 and its EM counterpart. Moreover, combining the GWTC-3 with the H_0 measurement from GW170817, Mukherjee et al. [192] provided a more compact H_0 result of $67^{+6.3}_{-3.8}$ km/s/Mpc.

3.4. Fast Radio Burst

FRBs are millisecond-duration pulses occurring at cosmological distances [193–195]. The total dispersion measure (DM_{obs}) of FRBs can provide a distance estimation to the source. The expanded form of DM_{obs} is as follows:

$$DM_{obs}(z) = DM_{MW} + DM_{IGM}(z) + \frac{DM_{host}(z)}{1+z}, \quad (4)$$

where DM_{IGM} represents the contribution of the intergalactic medium (IGM), DM_{MW} are contributed by the interstellar medium (ISM) and the halo of the Milky Way, and the DM_{host} is

contributed by the host galaxy. Considering a flat universe, the averaged value of DM_{IGM} is [196]

$$\langle DM_{IGM}(z) \rangle = \frac{A\Omega_b H_0^2}{H_0} \int_0^{z_{FRB}} \frac{f_{IGM}(z)f_e(z)(1+z)}{\sqrt{\Omega_m(1+z)^3 + 1 - \Omega_m}} dz, \quad (5)$$

where $A = \frac{3c}{8\pi G m_p}$ and m_p is the proton mass. The electron fraction is $f_e(z) = Y_H X_{e,H}(z) + \frac{1}{2}Y_{He}X_{e,He}(z)$, with hydrogen fraction $Y_H = 0.75$ and helium fraction $Y_{He} = 0.25$. Hydrogen and helium are completely ionized at $z < 3$, which implies the ionization fractions of intergalactic hydrogen and helium $X_{e,H} = X_{e,He} = 1$. The cosmological parameters Ω_m and Ω_b are the density of matter and the density of baryons, respectively. At present, there is no observation that can provide the evolution of the fraction of baryon in the IGM f_{IGM} with redshift. Shull et al. [197] provided an estimation of $f_{IGM} \approx 0.83$ [153]. Then, the dispersion measure-redshift relation allows FRBs to be used as cosmological probes. However, the degeneracy between DM_{IGM} and DM_{host} is the main obstacle for the cosmological application of FRBs. A reasonable method is to consider the probability distributions of DM_{IGM} [198,199] and DM_{host} [200].

Hagstotz et al. [152] presented the first H_0 estimation, $H_0 = 62.3 \pm 9.1$ km/s/Mpc, using the nine then available FRBs. Employing the probability distributions of DM_{IGM} [199] and DM_{host} [200] from the IllustrisTNG simulation, a more compact result, $H_0 = 68.81^{+4.99}_{-4.33}$ km/s/Mpc, was given by Wu et al. [153] using eighteen localized FRBs. These two H_0 estimations seem to favor the smaller H_0 value. After that, James et al. [154] show $H_0 = 73^{+12}_{-8}$ km/s/Mpc employing an updated sample of 16 Australian Square Kilometre Array Pathfinder (ASKAP) FRBs detected by the Commensal Real-time ASKAP Fast Transients (CRAFT) Survey and localised to their host galaxies, and 60 unlocalised FRBs from Parkes and ASKAP. Compared to previous FRB-based estimates, uncertainties in FRB energetics and DM_{host} produce larger uncertainties in the inferred value of H_0 . Furthermore, Hagstotz et al. [152] performed a forecast using a realistic mock sample to demonstrate that a high-precision measurement of the expansion rate is possible without relying on other cosmological probes. Another H_0 measurement, $H_0 = 70.60 \pm 2.11$ km/s/Mpc, was given by Liu et al. [155], employing a cosmological-model independent method. Recently, Zhao et al. [156] provided the first statistical H_0 measurements using unlocalized FRBs. They provided two H_0 measurements, $H_0 = 71.7^{+8.8}_{-7.4}$ km/s/Mpc and $H_0 = 71.5^{+10.0}_{-8.1}$ km/s/Mpc, which were obtained from the simulation-based case and the observation-based case, respectively. They also proposed that in the next few years, a 3% precision on the random error of the Hubble constant could be achieved using thousands of FRBs.

3.5. Tip of the Red Giant Branch

Compared to other standard candles, the tip of the red giant branch (TRGB) offers many advantages; for example, in the K-band they are ~ 1.6 magnitudes brighter than Cepheids. They have nearly exhausted the hydrogen in their cores and have just begun helium burning. Employing parallax methods, their brightness can be standardized. They thus can be regarded as the standard candles visible in the local universe. Instead of the Cepheid, the TRGB can be used as calibrators of SNe Ia. Freedman et al. [157] gave the Hubble constant result $H_0 = 69.8 \pm 0.8$ km/s/Mpc by measuring TRGB in nine SNe Ia hosts and calibrating TRGB in the large magellanic cloud. A consistent result, $H_0 = 69.6 \pm 0.8$ km/s/Mpc, was also given by Freedman et al. [158] using their revised measurement of the Large Magellanic Cloud TRGB extinction. After that, Freedman [159] combined several recent calibrations of the TRGB method, and are internally self-consistent at the 1% level. The updated TRGB calibration applied to a sample of SNe Ia from the Carnegie Supernova Project results in a value of $H_0 = 69.8 \pm 0.8$ km/s/Mpc.

We display H_0 measurements obtained from the recent observations in Table 3, and describe the correlation between the H_0 values and the published year in Figure 2. Combining Table 3 and Figure 2, it is easy to find that the measurements of the quasar lensing are tending to the SH0ES results as a whole. The H_0 measurements obtained from Megamaser, GW and FRB are more diffuse and have a large error which both covered the SH0ES results and CMB results. It is interesting that the H_0 values measured by TRGB have small errors and are between the SH0ES results and the CMB results. Collectively, these independent observations are currently unable to arbitrate the H_0 tension.

Table 3. H_0 measurements with the 68% confidence level derived from the recent observations.

Observation	H_0 (km/s/Mpc)	Reference	Observation	H_0 (km/s/Mpc)	Reference
Quasar lens	$73.3^{+1.7}_{-1.8}$	[37]	FRB	62.3 ± 9.1	[152]
Quasar lens	$74.0^{+1.7}_{-1.8}$	[143]	FRB	$68.81^{+4.99}_{-4.33}$	[153]
Quasar lens	$74.2^{+1.6}_{-1.6}$	[165]	FRB	$73.0^{+12.0}_{-8.0}$	[154]
Megamaser	69.3 ± 4.2	[184]	FRB	70.6 ± 2.11	[155]
Megamaser	73.9 ± 3.0	[148]	FRB	$71.5^{+10.0}_{-8.1}$	[156]
GW	$74.0^{+16.0}_{-8.0}$	[149]	TRGB	69.8 ± 0.8	[157]
GW + EM	$70.3^{+5.3}_{-5.0}$	[151]	TRGB	69.6 ± 0.8	[158]
GW	$68.0^{+12.0}_{-7.9}$	[191]	TRGB	69.8 ± 0.8	[159]
GW	$67.0^{+6.3}_{-3.8}$	[192]			

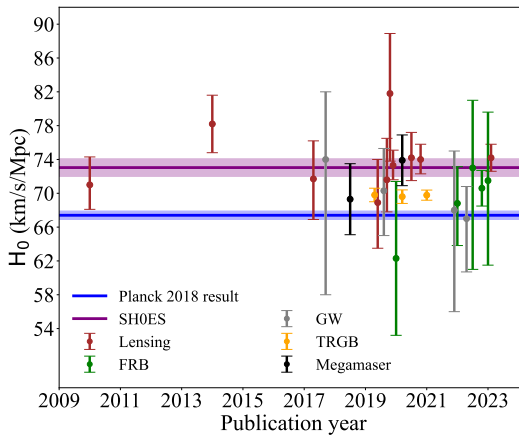


Figure 2. H_0 measurements in the late-time universe derived from other independent observations which include quasar lensing [37,143,165–172], FRB [152,153,156], GW [149,151,191,192], TRGB [157–159] and Megamaser [184]. The purple and blue regions correspond to the results of SH0ES [40] and Planck collaborations [3], respectively.

4. Solutions for the H_0 Tension

The case for an observational discrepancy between the early and late universe appears strong, is hard to dismiss, and merits an explanation. The analyses of possible systematics did not lead us to the cause of the Hubble tension [35,40,46,88–92,94]. The arbitration of H_0 given by otherwise independent observations also did not produce consistent results in favor of one side [37,143,149,151–153,159,184]. Hence, many researchers prefer to believe that the Hubble tension may be caused by new physics beyond the Λ CDM model [201]. Until now, a large number of theoretical solutions have been proposed to solve or relieve the H_0 tension. The detailed information can be found from these references [21,97,202].

4.1. Classification of Solutions to H_0 Tension

In the review article for H_0 tension, Di Valentino et al. [202] gave a detailed classification for the solutions of the H_0 tension. They divided all schemes proposed for solving the H_0 tension into 11 major categories with 123 subcategories, and some subcategories include several different schemes. The detailed classification results are as follows:

- (a) Early dark energy [203–205]:
 - (1) Anharmonic oscillations [206];
 - (2) Ultra-light axions [95,96,207–211];
 - (2.1) Dissipative axion [212];
 - (2.2) Axion interacting with a dilaton [213];
 - (3) Power-law potential [214];
 - (4) Rock ‘n’ roll [215];
 - (5) New early dark energy [216,217];
 - (6) Chain early dark energy [218];
 - (7) Anti-de Sitter phase [219,220];
 - (8) Gradusted dark energy [221];
 - (9) Acoustic dark energy [222,223];
 - (9.1) Exponential acoustic dark energy [223];
 - (10) Early dark energy in α attractors [224].
- (b) Late dark energy [225–227]:
 - (1) w CDM model [201,228–230];
 - (2) w_0w_a CDM or CPL parameterization [228,229,231];
 - (3) Dark energy in extended parameter spaces [232];
 - (4) Dynamical dark energy parameterizations with two free parameters [233,234];
 - (5) Dynamical dark energy parameterizations with one free parameter [235];
 - (6) Metastable dark energy [236–238];
 - (7) Phantom crossing [239];
 - (8) Late dark energy transition [240,241];
 - (9) Running vacuum model [242,243];
 - (10) Transitional dark energy model [244];
 - (11) Negative dark energy [245];
 - (12) Bulk viscous models [246–248];
 - (13) Holographic dark energy [249–252];
 - (13.1) Tsallis holographic dark energy [253];
 - (14) Swampland conjectures [254–258];
 - (15) Late time transitions in the quintessence field [259,260];
 - (16) Phantom braneworld dark energy [261];
 - (17) Frame-dependent dark energy [262];
 - (18) Chameleon dark energy [263,263,264].
- (c) Dark energy models with degrees of freedom and their extensions:
 - (1) Phenomenologically emergent dark energy [265–267];
 - (1.1) Generalized emergent dark energy [268,269];
 - (1.2) Modified emergent dark energy [270];
 - (2) Vacuum metamorphosis [271–273];
 - (2.1) Elaborated vacuum metamorphosis [271–273].
- (d) Models with extra relativistic degrees of freedom:
 - (1) Sterile neutrinos [274,275];
 - (2) Neutrino asymmetries [276];
 - (3) Thermal axions [277,278];
 - (4) Decaying dark matter [279–284];

- (4.1) Self-interacting dark matter [285,286];
(4.2) Two-body dark matter decays [287,288];
(4.3) Light gravitino scenarios [289–291];
(4.4) Decaying ‘Z’ [292];
(4.5) Dynamical dark matter [293];
(4.6) Degenerate decaying fermion dark matter [294];
(5) Neutrino–dark matter interactions [295–297];
(5.1) Neutrino–Majoron interactions [298–300];
(5.2) Feebly interacting massive particles (FIMPs) decay into neutrinos [301];
(6) Interacting dark radiation [301];
(7) Coupled DM–dark radiation scenarios [302,303];
(8) Cannibal dark matter [304];
(9) Decaying ultralight scalar [304,305];
(10) Ultralight dark photon [306,307];
(11) Primordial black holes [308–310];
(12) Unparticles [311].
- (e) Models with extra interactions:
 - (1) Interacting dark energy (IDE) [312];
(1.1) Interacting vacuum energy [313–317];
(1.2) Coupled scalar field [318];
(1.3) IDE with a constant DE equation of state [319–322];
(1.4) IDE with variable DE equation of state [273,323];
(1.5) Interacting vacuum scenario and IDE with variable coupling [321,324];
(1.6) IDE with sign-changing interaction [325];
(1.7) Anisotropic stress in IDE [326];
(1.8) Interaction in the anisotropic universe [327];
(1.9) Metastable interacting dark energy [236,238];
(1.10) Quantum field cosmology [316,328];
(1.11) Interacting quintom dark energy [329];
(2) Interacting dark matter [330,331];
(2.1) DM–photon coupling [332,333];
(2.2) DM–baryon coupling [334,335];
(3) DE–baryon coupling [336,337];
(4) Interacting neutrinos [338–340];
(4.1) Self-interacting neutrinos: [338,339,341–343];
(4.2) Self-interacting sterile neutrino model [344];
(4.3) Dark neutrino interactions [345,346].
- (f) Unified cosmologies:
 - (1) Generalized Chaplygin gas model [347];
(2) A new unified model [348];
(3) $\Lambda(t)$ CDM model [349];
(4) Λ -gravity [350,351].
- (g) Modified gravity [352]:
 - (1) $f(\mathcal{R})$ gravity theory; [353–356];
(2) $f(\mathcal{T})$ gravity theory [357–360];
(3) $f(\mathcal{T}, \mathcal{B})$ gravity theory [361,362];
(4) $f(Q)$ gravity theory [363,364];
(5) Jordan–Brans–Dicke (JBD) gravity [365];
(5.1) Brans and Dicke– Λ CDM [366,367];
(6) Scalar-tensor theories of gravity [368,369];

- (6.1) Early modified gravity [370,371];
- (6.2) Screened fifth forces [372,373];
- (7) ‘Uber-gravity’ [374,375];
- (8) Galileon gravity [376,377];
- (9) Nonlocal gravity [378,379];
- (10) Unimodular gravity [380];
- (11) Scale-dependent scenario of gravity [381];
- (12) VCDM [382,383].
- (h) Inflationary models [384]:
- (1) Exponential inflation [385,386];
- (2) Reconstructed primordial power spectrum [387,388];
- (3) Lorentzian quintessential inflation [389];
- (4) Harrison–Zel’dovich spectrum [390].
- (i) Modified recombination history [391]:
- (1) Effective electron rest mass [392,393];
- (2) Time varying electron mass [394];
- (3) Axi–Higgs model [395];
- (4) Primordial magnetic fields [396,397].
- (j) Physics of the critical phenomena:
- (1) Double- Λ CDM [398];
- (2) Ginzburg–Landau theory of phase transition [321];
- (3) Critically emergent dark energy [399].
- (k) Alternative proposals:
- (1) Local inhomogeneity [400,401];
- (2) Bianchi type I spacetime [402];
- (3) Scaling solutions [403–405];
- (4) CMB monopole temperature T_0 [406];
- (4.1) Open and hotter universe [407,408];
- (5) Super- Λ CDM [409];
- (6) Heisenberg uncertainty [410]
- (7) Diffusion [411];
- (8) Casimir cosmology [412];
- (9) Surface forces [413];
- (10) Milne model [414,415];
- (11) Running Hubble tension [416,417];
- (12) Rapid transition in the effective gravitational constant [418];
- (13) Causal horizons [419,420];
- (14) Milgromian dynamics [421];
- (15) Charged dark matter [422,423].

It can be observed that Di Valentino et al. [202]’s classification of schemes to alleviate the H_0 tension is very detailed. With help of this classification, we can quickly find out the solutions and corresponding articles we need. Recently, Perivolaropoulos and Skara [21] updated and optimized the classification scheme based on the latest research work. The new classification scheme is more concise than before. They divided all solutions into 5 major categories, each of which contained several sub-categories, for a total of 19 sub-categories. The detailed classification is as follows:

- (i) Late time deformations of the Hubble expansion rate $H(z)$:
- (1) Phantom dark energy [424];
- (2) Running vacuum model [425];
- (3) Phenomenologically emergent dark energy [426–428];

- (4) Vacuum phase transition [429];
- (5) Phase transition in dark energy [430].
- (ii) Deformations of the Hubble expansion rate $H(z)$ with additional interactions/degrees of freedom:
 - (1) Interacting dark energy [431–436];
 - (2) Decaying dark matter [437].
- (iii) Deformations of the Hubble expansion rate $H(z)$ with inhomogeneous or anisotropic modifications:
 - (1) Chameleon dark energy [438,439];
 - (2) Cosmic voids [440,441];
 - (3) Inhomogeneous causal horizons [419].
- (iv) Late time modifications: Transition or recalibration of the SNe Ia absolute luminosity:
 - (1) Gravity and evolution of the SNe Ia intrinsic luminosity [442];
 - (2) Transition of the SNe Ia absolute magnitude M at a redshift $z \simeq 0.01$ [443–445];
 - (3) Late (low-redshift) $w - M$ phantom transition [446–448].
- (v) Early time modifications of sound horizon:
 - (1) Early dark energy [449–457];
 - (2) Dark radiation [458–463];
 - (3) Neutrino self-interactions [340,464–466];
 - (4) Large primordial non-Gaussianities [409];
 - (5) Heisenberg's uncertainty principle [410];
 - (6) Early modified gravity [368–370].

Of course, the above classifications may not completely cover all the solutions to relieve H_0 tension. The proposal of new schemes never stops, such as the Weyl invariant gravity [467], Horndeski gravity [468], Λ_S CDM model [469,470], Early Integrated Sachs–Wolfe (eISW) effect [471], realistic model of dark atoms [472], information dark energy [473], $U(1)_{L_\mu - L_\tau}$ model with Majoron [474], etc.

Classification is a summary of previous research work on relieving the H_0 tension, which helps to find out the physical origin that causes the discrepancy in H_0 measurements. For the classification of solutions to the H_0 tension schemes, not all schemes fall perfectly into one of these categories [475]. At present, the proposed models and theories are usually divided into three categories: early-time model, late-time model and modified gravity. The boundary between the early-time models and late-time models is the recombination redshift ($z \sim 1100$). Detailed introduction of each scheme has been made in previous H_0 review literature [202] and Perivolaropoulos and Skara [21]. We will not repeat it here. In addition to categorizing so many solutions, there are several works that provide comparative analysis of solutions for H_0 tension, and discussion on the H_0 tension [388,475–485]. Schöneberg et al. [475] organized H_0 Olympic-like games for the relative success of seventeen models which have been proposed to resolve the H_0 tension, and gave a ranking. Finally, the early dark energy model, new early dark energy model, early modified gravity model and varying $m_e + \Omega_K$ model are the most successful of the models studied in the H_0 Olympic-like games.

According to the research and discussions on solving the H_0 tension, we tend to divide all of the solutions into two categories: one proposes a new cosmological model first, and then combines the existing early-time (for example, CMB) or late-time (for example, Cepheid) observational data-sets to constrain the cosmological parameters (including H_0). A higher H_0 value which is consistent with the SH0ES results can be given by utilizing the recent available observations. This category is the most common used to relieve the H_0 tension. We define such schemes as the sequential scheme. There is one thing to note here. Considering that the new model needs to introduce additional parameters, and the increase in the volume of the parameter space will make the final H_0 result incompact, this would amplify the extent

to which the new model mitigates the H_0 tension. Moreover, it is difficult to estimate the contribution of additional parameters to the degree of mitigation of the H_0 tension. The other is to use the Λ CDM model or model-independent methods, combined with the existing late-time observations center to find the H_0 singular behaviors which can be used to resolve or alleviate the H_0 tension. Compared to the sequential scheme, such a scheme should be called a reverse-order scheme. These H_0 singular behaviors might hint to new physics beyond the Λ CDM model, and still require new cosmological models to explain them. The proposal of the new cosmological model no longer directly alleviates the H_0 tension, but explains the H_0 singular behaviors. It seems that there is no need to worry about the problem of increasing the parameter space with the additional parameters. The former scheme has been elaborated in many review articles [21,202] and will not be repeated here. We will revisit the latter scenario, which might hint at new physics beyond the Λ CDM model, in the next section.

5. Evidence of New Physics Beyond the Λ CDM

According to previous analyses of the quasar lensing, Wong et al. [37] found that the inferred value of H_0 , which was estimated using the strongly-lensed quasar time delay (H0LiCOW), decreases with the lens redshift. The H0LiCOW H_0 descending trend is of low statistical significance at 1.9σ . Adding a new H0LiCOW H_0 result [174] (DES J0408-5354) reduces the statistical significance to 1.7σ [143], as shown in Figure 3. After that, the TDCOSMO IV re-analysis lowers the H_0 estimates and increases the error bar [486]. Hence, the significance of the H_0 descending trend may be lower, and it is not clear that the H_0 descending trend is not a systematically driven-by-analysis choice in its rather complicated pipeline [486]. Even so, this still provides a new diagnostic for the H_0 tension.

Motivated by the H0LiCOW results [37], Krishnan et al. [487] focused their attention mainly on late-time observations. They estimated the cosmological parameters in different redshift ranges by binning the observational data-sets ($z < 0.7$) comprising megamasers, CCs, SNe Ia and BAOs according their redshifts. The total data-set is divided into six parts. Then, they constrained the H_0 value for each of the bin, and using (\bar{z}, H_0) present the final result. The form of \bar{z} is written as [487]

$$\bar{z} = \frac{\sum_{n=1}^{N_i} z_n (\sigma_n)^{-2}}{\sum_{n=1}^{N_i} (\sigma_n)^{-2}}, \quad (6)$$

where σ_k denotes the error in the observable at redshift z_n . Finally, they found a similar H_0 descending trend in the Λ CDM model with a low statistical significance (2.1σ), as shown in the left panel of Figure 4. This result obtained by using the observation data completely independent of H0LiCOW is consistent with the H0LiCOW results to a certain extent.

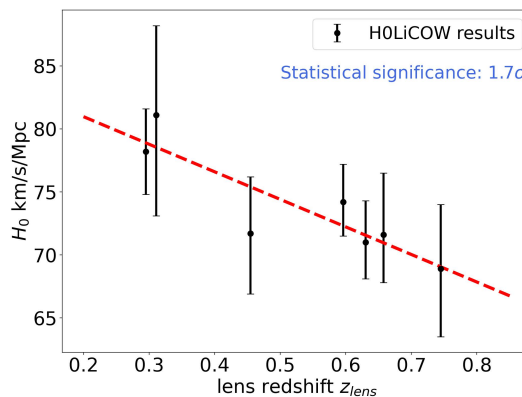


Figure 3. H_0 measurements from H0LiCOW. The trend of smaller H_0 value with increasing lens redshift has significance levels of 1.7σ . (Source: Figure 5 in Millon et al. [143].)

Based on the flat Λ CDM model and flat $w_0 w_a$ CDM model, a similar H_0 descending trend is also found by Dainotti et al. [417] using the Pantheon sample only. In this analysis, they set the absolute magnitude of SNe Ia so that $H_0 = 73.5$ km/s/Mpc, and they fix fiducial values for $\Omega_{0m}^{\Lambda\text{CDM}} = 0.298$ and $\Omega_{0m}^{w_0 w_a\text{CDM}} = 0.308$. The $g(z)$ function was used to describe the behavior of the H_0 descending. Its form is as follows:

$$g(z) = H_0(z) = \frac{\tilde{H}_0}{(1+z)^\alpha}, \quad (7)$$

where \tilde{H}_0 and α are free parameters, and α indicates the evolutionary trend. The $g(z)$ function is the standard for characterizing the evolution of many astrophysical sources and is widely used for GRBs and quasars [488–490]. In addition, they also considered four kinds of binning methods: 3 bins, 4 bins, 20 bins and 40 bins. Finally, they reduced the H_0 tension in the range of (54%, 72%) for both cosmological models and pointed out that the H_0 descending trend is independent of the cosmological model and number of bins. A more detailed result can be found from Table 1 in Dainotti et al. [417].

Here, we demonstrate their fitting results obtained from the 4 bins method in the flat Λ CDM model. The results of \tilde{H}_0 and α are 73.493 ± 0.144 km/s/Mpc and 0.008 ± 0.006 , respectively. Adopting the $g(z)$ function, they obtained $H_0(z = 1100) = 69.271 \pm 2.815$ km/s/Mpc, which can be used to reduce the H_0 tension effectively, as shown in the right panel of Figure 4. The reduction of the H_0 tension is 66%. A similar descending trend (i.e., H_0 decreasing as z_{min} increases) was also found by Horstmann et al. [61] and Ó Colgáin et al. [491] from the Pantheon sample. The constraints of $H_0(z_{min})$ are obtained by using the SNe Ia data larger than z_{min} .

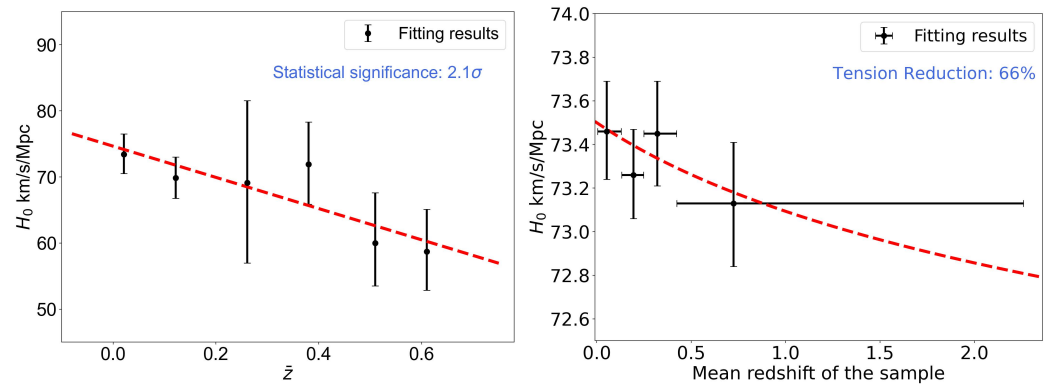


Figure 4. A similar H_0 descending trend obtained from the combined sample (including megamasers, CCs, SNe Ia and BAOs) and Pantheon sample. Left panel shows the result obtained from the combined sample. The statistical significance of descending trend is 2.1σ . Right panel shows the result of Pantheon sample which can reduce the H_0 tension by 66%. (Source: left panel, Figure 2 in Krishnan et al. [487]; right panel, Figure 5 in Dainotti et al. [417].)

After that, Dainotti et al. [492] made a further analysis for the H_0 evolution, which was described by Equation (7) combining the Pantheon sample and BAO data. The final results demonstrate that a descending trend with $\alpha \sim 10^{-2}$ is still visible in the combined sample. The α coefficient reaches zero in 2.0σ and 5.8σ for the Λ CDM model and $w_0 w_a$ CDM model, respectively. In addition, Colgáin et al. [493] performed an independent investigation in the Λ CDM model, adopting the composite sample consisting of $H(z)$, SNe Ia and quasars. In the end, they confirmed that the observations exhibit an increasing Ω_m (decreasing H_0) trend with

an increasing bin redshift and that such behaviour can arise randomly within the flat Λ CDM model with a lower probability $p = 0.0021$ (3.1σ).

At the same time, Perivolaropoulos and Skara [447] proposed a physically motivated new degree of freedom in the Cepheid calibrator analysis, allowing for a transition in one of the Cepheid modeling parameters R_w (Cepheid Wesenheit color-luminosity parameter) or M_w (Cepheid Wesenheit H-band absolute magnitude). This is mildly favored by the observational data and can yield a lower H_0 value. Their results may imply the presence of a fundamental physics transition taking place at a time more recent than 100 Myrs ago. The transition magnitude is consistent with the magnitude required for the resolution of the H_0 tension in the context of a fundamental gravitational transition occurring by a sudden increase in the strength of the gravitational interactions G_{eff} by about 10% [418] at a redshift $z_t \lesssim 0.01$. Such a transition would abruptly increase the absolute magnitude of SNe Ia by $\Delta M_B \simeq 0.2$ [241,418].

Using the publicly available SH0ES data described in Riess et al. [39], the extended analyses were given by Perivolaropoulos and Skara [444] in a detailed and comprehensive manner. They found that when an absolute magnitude M_B transition of the SNe Ia at $D_c \simeq 50$ Mpc (about 160 Myrs ago) can drop, the H_0 constraint drops from 73.04 ± 1.04 km/s/Mpc to 67.32 ± 4.64 km/s/Mpc, which is in full consistency with the Planck results. When the inverse distance ladder constraint on $M_B^>$ is included in the analyses, the uncertainties for H_0 reduce dramatically ($H_0 = 68.2 \pm 0.8$ km/s/Mpc) and the $M_B^>$ transition model is strongly preferred over the baseline SH0ES model in terms of the Akaike Information Criterion (AIC) [494] and the Bayesian Information Criterion (BIC) [495] model selection criteria. Similar hints for a transition behavior is found for the other three main parameters of the analysis (b_W , M_W and Z_W) at the same critical distance $D_c \simeq 50$ Mpc, even though in that case the H_0 estimation is not significantly affected [444]. In addition, Wojtak and Hjorth [496] also reanalysed the SNe Ia and Cepheids' observations and found that the H_0 local measurements become dependent on the choice of SN reference colour. These recent investigations hint towards the need of more detailed Cepheid + SNe Ia calibrating data at distances $D_c \gtrsim 50$ Mpc, i.e., at the high end of rung 2 on the distance ladder.

In a recent analysis, Krishnan et al. [416] construct the H_0 diagnostic $\mathcal{H}0(z)$:

$$\mathcal{H}0(z) = \frac{H(z)}{\sqrt{1 - \Omega_{m0} + \Omega_{m0}(1+z)^3}}, \quad (8)$$

to specify the possible deviations from the flat Λ CDM model using the Gaussian process (GP) method [497]. The Gaussian process has been extensively used for cosmological applications, such as the constraint on H_0 [498–502] and the comparison of cosmological models [503]. A more detailed explanation can be discovered from the literature [504–506]. As shown in Figure 5, we are given the reconstructed result of 36 $H(z)$ data (31 CCs + 5 BAOs) using the GP method. From this figure, it can be learned that combining the $H(z)$ data and GP method allows us to obtain a continuous function $f(z)$ to represent the discrete $H(z)$ data. Utilizing the function $f(z)$, the $H(z)$ value at any redshift within a certain range can be obtained, including H_0 at $z = 0$. The effective range mainly depends on the highest redshift of the $H(z)$ data used. Finally, $H(z)$ follows from the continuous function $f(z)$ and the Ω_{m0} is the adopted Planck values [3]. Based on the $H(z)$ data and GP method, they found a running H_0 with redshift z . The main result can be found from Figure 2 in Krishnan et al. [416].

Also employing the $H(z)$ data [499] and the GP method, Hu and Wang [507] reported a late-time transition of H_0 , i.e., H_0 changes from a low value to a high one from an early to late cosmic time that can be used to relieve the H_0 tension. Unlike previous studies [417,487], they processed the $H(z)$ data using a cumulative binning method. An introduction to this method can be found in Figure 1 and Section 2 in Hu and Wang [507]. They found that the redshift of the H_0 transition occurs at $z \sim 0.49$. Without proposing a new cosmological model, their

finding can be used to relieve the H_0 tension with a mitigation level of around 70 percent, and is consistent with the H0LiCOW results in the 1σ range. They also tested the influence of BAOs on the result, and concluded that removing the BAOs data had no substantial effect, i.e., did not make the H_0 transition disappear. Their final results are shown in Figure 6.

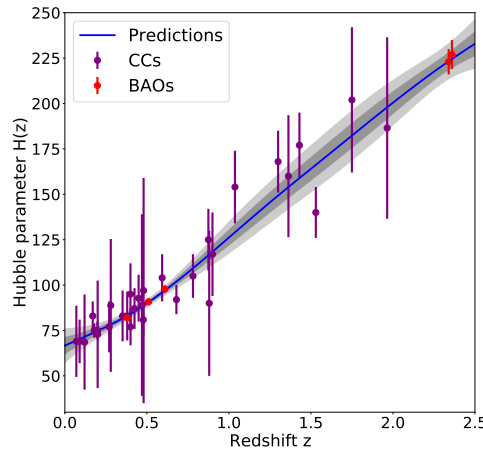


Figure 5. Smoothed $H(z)$ function (blue solid line) with 2σ errors (gray regions) obtained from the 36 $H(z)$ data (31 CCs + 5 BAOs) employing GP method. GP regression is implemented by employing the package *scikit-learn* (<https://scikit-learn.org>) [497] in the Python environment. (Source: Figure 4 in Hu et al. [5].)

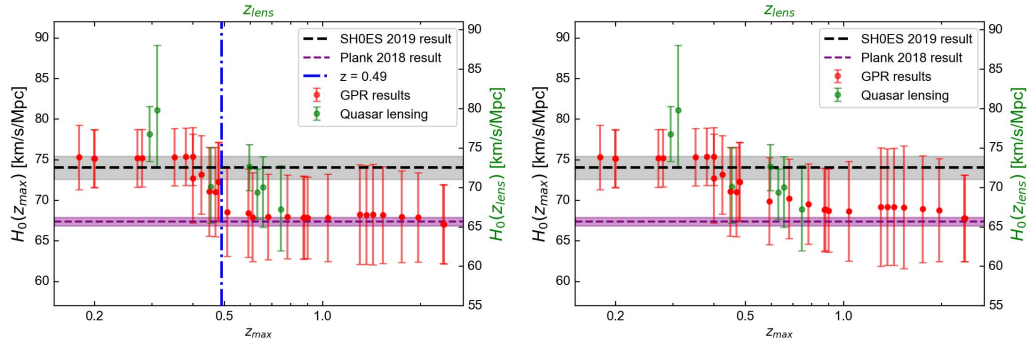


Figure 6. Predictions of $H_0(z_{max})$ adopting the Matérn kernel from the 36 $H(z)$ data (31 CCs + 5 BAOs) binned by the cumulative method. $H_0(z_{max})$ is the H_0 value derived from a data-set with maximal redshift z_{max} . Red points are the predictions of $H_0(z_{max})$ based on our analyses. The gray and purple regions correspond to the results of SH0ES and *Planck* collaborations. Blue dotted line ($z = 0.49$) is the transition redshift. We also show the H_0 results derived from quasar lens observations with green points in $(z_{lens}, H_0(z_{lens}))$ coordinates. (Source: Figures 3 and 4 in Hu and Wang [507].)

Recently, utilizing the latest SNe Ia sample (Pantheon+ sample) and $H(z)$ data, Jia et al. [508] presented a novel non-parametric method to estimate H_0 as a function of the redshift. They found a descending trend of $H_{0,z}$ with the statistical significance of 3.6σ and 5.1σ , corresponding to the equal-number and equal-width binning methods, respectively. Here, $H_{0,z}$ defined as the value of H_0 are derived from the cosmic observations at redshift z . The main results are presented in Figures 1 and 2 of Jia et al. [508]. The evolution of $H_{0,z}$ can effectively relieve the Hubble tension without the early-time modifications. Moreover, the results of the AIC and BIC demonstrate that the observational data favor the $H_{0,z}$ model over the Λ CDM model. Recently,

utilizing a different approach than Jia et al. [508], Malekjani et al. [509] also found a similar H_0 descending trend from the Pantheon+ sample.

The statistical signification of the H_0 descending trend found from the quasar lensing is not high, at only 1.7σ . Moreover, it is not clear that the H_0 descending trend is not caused by systematics. This still provides a new diagnostic for the H_0 tension. The descending trend of H_0 has also been discovered by utilizing the different data-sets and methods, most of which are based on an explicit model (Λ CDM or w_0w_a CDM model) [37,61,416,417,487,491–493,508], except for Hu and Wang [507]. The H_0 descending trend can effectively alleviate the H_0 tension. If this trend is substantiated going forward, a late-time modification consistent with most observations is required. However, some studies are not in favor of modifying the late-time universe [510,511]. Among many late-time solutions, local void [512–515], modified gravity [410,516] and modified cosmological models [260] might be considered as competitive candidates. The local void model has been disfavored by the SNe Ia data [517–519], but can not completely be ruled out. Of course, there is also some evidence supporting the existence of the local void model [520–522]. The reasons for the transition of the Cepheid parameters and the M_B transition of SNe Ia are still unclear. Such a transition may be attributed to either new physics or to unknown systematics hidden in the data [447]. If the source of the demonstrated transitions are physical, it could lead to new cosmological physics beyond the Λ CDM model. In previous studies, there are precedents, e.g., the gravitational constant in the context of a recent first-order phase transition [523–525] to a new vacuum of a scalar-tensor theory, or in the context of a generalization of the symmetron screening mechanism [445]. A similar first-order transition was implemented in early dark energy models [216], attempting to change the last scattering sound horizon scale without affecting other well-constrained cosmological observables. Thus, even though no relevant detailed analysis has been performed so far, there are physical mechanisms that could potentially induce the SNe Ia luminosity transition degree of freedom. In any case, in the face of these evidences that may be new physics beyond the Λ CDM model, one should not just be skeptical and do nothing.

6. Conclusions and Future Prospects

The Λ CDM model as the current standard cosmological model is consistent with almost all of the observational probes available until the present. However, it is not perfect, and there are still many theoretical difficulties and tensions. The significant discrepancy between the H_0 values measured from the local distance ladder and from the cosmic microwave background, i.e., Hubble tension, is the most serious challenge to the standard Λ CDM model. In this review, we have revisited this as the hottest issue, incorporating the latest research.

Until now, there has been a $4\text{--}6\sigma$ discrepancy in H_0 measured by these two approaches, and the discrepancy is still increasing (see Sections 1 and 2 and the reference therein). Initially, possible systematics in the Planck observations and the HST measurements were thought to be responsible for the H_0 tension. However, this possibility has been largely ruled out [35,40,46,88–92,94]. The current arbitration results given by other independent observations (including quasar lensing, Megamaser, GW, FRB, TRGB, etc.) cannot effectively arbitrate the H_0 tension. See Section 3 for details. Many researchers therefore choose to believe that the Hubble tension may be caused by new physics beyond the Λ CDM model [201]. So far, there have been a lot of schemes proposed to solve the H_0 tension (see Perivolaropoulos and Skara [21], Shah et al. [97], Di Valentino et al. [202] for a review). We have reviewed the classifications of solving schemes for the H_0 tension based on previous work by Di Valentino et al. [202] and Shah et al. [97] as well as newer studies (see Section 4.1). According to the research and discussions about solving the H_0 tension, we tend to divide all of the solutions into two categories: sequential and reverse-order schemes. In Section 5, we mainly review the reverse-order schemes, which might hint at new physics beyond the Λ CDM. Some of these schemes have discovered the

late-time H_0 descending trend [37,61,416,417,487,491–493,508] or the late-time H_0 transition [507] that can be used to alleviate the H_0 tension through different independent observations and different methods. The remaining schemes found that considering the new degrees of freedom (parameter transition) can also effectively alleviate the H_0 tension when analyzing the Cepheid and SNe Ia data [444,447,496].

Looking to the future, two new CMB Stage 4 telescopes will be operational in Chile and the South Pole around 2030, which will further extend the spectral resolution. The depth of these surveys will be able to support or rule out many precombination modifications based on the Λ CDM model. The Zwicky Transient Facility and Foundation surveys of nearby SNe Ia will effectively reduce the potential calibration issues of the local distance ladder by resolving the underlying population characteristics, having cleaner selection functions, and providing more galaxies. The H_0 arbitration of independent observations will also be improved. The James Webb Space Telescope (JWST) will greatly expand the range of TRGB observation, and provide continuity in the case of any further degradation of the ageing HST. The VIRGO detector in Italy, and recently the KAGRA detector in Japan will provide more frequent event detections and better sky localization. They will provide a 2% measurement of H_0 within this decade by combining with an improved instrumental calibration. Many thousands of lenses will be detected by the wide-field surveys, such as the Vera Rubin Observatory, Euclid and the Nancy Grace Roman Observatory, and hundreds of which will have accurate time delay measurements [526–528]. Thus, there is a strong incentive to resolve the remaining systematics in the modelling and speed up the analysis pipeline, then clear the relationship between the H_0 descending trend and systematics. The ASKAP and Very Large Array will provide a large number of positioned FRBs in the future, which will provide higher-precision H_0 measurements. In addition, the e-ROSITA all-sky survey, French–Chinese satellite space-based multi-band astronomical variable objects monitor (SVOM) [529], Einstein Probe (EP) [530], and Transient High-Energy Sky and Early Universe Surveyor (THESEUS) [531] space missions together with ground- and space-based multi-messenger facilities will allow us to investigate H_0 tension in the poorly explored high-redshift universe.

Author Contributions: Conceptualization, J.P. and F.Y.; investigation, J.P.; writing—original draft preparation, J.P.; writing—review and editing, J.P. and F.Y.; supervision, F.Y.; All authors have read and agreed to the published version of the manuscript.

Funding: This work was supported by the National Natural Science Foundation of China (grant No. U1831207), the China Manned Spaced Project (CMS-CSST-2021-A12), National Natural Science Foundation of China (grant No. 12273009), Jiangsu Funding Program for Excellent Postdoctoral Talent (20220ZB59) and Project funded by China Postdoctoral Science Foundation (2022M721561).

Data Availability Statement: Not applicable.

Acknowledgments: We thank the anonymous referee for constructive comments. This work was supported by the National Natural Science Foundation of China (grant No. U1831207), the China Manned Spaced Project (CMS-CSST-2021-A12), National Natural Science Foundation of China (grant No. 12273009), Jiangsu Funding Program for Excellent Postdoctoral Talent (20220ZB59) and Project funded by China Postdoctoral Science Foundation (2022M721561).

Conflicts of Interest: The authors declare no conflict of interest.

References

- Alam, S.; Ata, M.; Bailey, S.; Beutler, F.; Bizyaev, D.; Blazek, J.A.; Bolton, A.S.; Brownstein, J.R.; Burden, A.; Chuang, C.H.; et al. The clustering of galaxies in the completed SDSS-III Baryon Oscillation Spectroscopic Survey: Cosmological analysis of the DR12 galaxy sample. *Mon. Not. R. Astron. Soc.* **2017**, *470*, 2617–2652, <https://doi.org/10.1093/mnras/stx721>.

2. Scolnic, D.M.; Jones, D.O.; Rest, A.; Pan, Y.C.; Chornock, R.; Foley, R.J.; Huber, M.E.; Kessler, R.; Narayan, G.; Riess, A.G.; et al. The Complete Light-curve Sample of Spectroscopically Confirmed SNe Ia from Pan-STARRS1 and Cosmological Constraints from the Combined Pantheon Sample. *Astroph. J.* **2018**, *859*, 101, <https://doi.org/10.3847/1538-4357/aab9bb>.
3. Planck Collaboration. Planck 2018 results. VI. Cosmological parameters. *Astron. Astrophys.* **2020**, *641*, A6, <https://doi.org/10.1051/0004-6361/201833910>.
4. Benisty, D.; Staicova, D. Testing late-time cosmic acceleration with uncorrelated baryon acoustic oscillation dataset. *Astron. Astrophys.* **2021**, *647*, A38, <https://doi.org/10.1051/0004-6361/202039502>.
5. Hu, J.P.; Wang, F.Y.; Dai, Z.G. Measuring cosmological parameters with a luminosity-time correlation of gamma-ray bursts. *Mon. Not. R. Astron. Soc.* **2021**, *507*, 730–742, <https://doi.org/10.1093/mnras/stab2180>.
6. DES Collaboration. The first Hubble diagram and cosmological constraints using superluminous supernovae. *Mon. Not. R. Astron. Soc.* **2021**, *504*, 2535–2549, <https://doi.org/10.1093/mnras/stab978>.
7. Brout, D.; Scolnic, D.; Popovic, B.; Riess, A.G.; Carr, A.; Zuntz, J.; Kessler, R.; Davis, T.M.; Hinton, S.; Jones, D.; et al. The Pantheon+ Analysis: Cosmological Constraints. *Astroph. J.* **2022**, *938*, 110, <https://doi.org/10.3847/1538-4357/ac8e04>.
8. DES Collaboration. Dark Energy Survey Year 3 results: Calibration of lens sample redshift distributions using clustering redshifts with BOSS/eBOSS. *Mon. Not. R. Astron. Soc.* **2022**, *513*, 5517–5539. <https://doi.org/10.1093/mnras/stac1160>.
9. Dainotti, M.G.; Nielson, V.; Sarracino, G.; Rinaldi, E.; Nagataki, S.; Capozziello, S.; Gnedin, O.Y.; Bargiacchi, G. Optical and X-ray GRB Fundamental Planes as cosmological distance indicators. *Mon. Not. R. Astron. Soc.* **2022**, *514*, 1828–1856, <https://doi.org/10.1093/mnras/stac1141>.
10. Cao, S.; Ryan, J.; Ratra, B. Cosmological constraints from H II starburst galaxy, quasar angular size, and other measurements. *Mon. Not. R. Astron. Soc.* **2022**, *509*, 4745–4757, <https://doi.org/10.1093/mnras/stab3304>.
11. de Cruz Perez, J.; Park, C.G.; Ratra, B. Current data are consistent with flat spatial hypersurfaces in the Λ CDM cosmological model but favor more lensing than the model predicts. *arXiv* **2022**, arXiv:2211.04268.
12. Liu, Y.; Liang, N.; Xie, X.; Yuan, Z.; Yu, H.; Wu, P. Gamma-Ray Burst Constraints on Cosmological Models from the Improved Amati Correlation. *Astroph. J.* **2022**, *935*, 7, <https://doi.org/10.3847/1538-4357/ac7de5>.
13. Pouroyaghi, S.; Zabihi, N.F.; Malekjani, M. Can high-redshift Hubble diagrams rule out the standard model of cosmology in the context of cosmography? *Phys. Rev. D* **2022**, *106*, 123523, <https://doi.org/10.1103/PhysRevD.106.123523>.
14. Wang, F.Y.; Hu, J.P.; Zhang, G.Q.; Dai, Z.G. Standardized Long Gamma-Ray Bursts as a Cosmic Distance Indicator. *Astroph. J.* **2022**, *924*, 97, <https://doi.org/10.3847/1538-4357/ac3755>.
15. Blanchard, A.; Héloret, J.Y.; Ilić, S.; Lamine, B.; Tutusaus, I. Λ CDM is alive and well. *arXiv* **2022**, arXiv:2205.05017,
16. Berti, E.; Cardoso, V.; Haiman, Z.; Holz, D.E.; Mottola, E.; Mukherjee, S.; Sathyaprakash, B.; Siemens, X.; Yunes, N. Snowmass2021 Cosmic Frontier White Paper: Fundamental Physics and Beyond the Standard Model. *arXiv* **2022**, arXiv:2203.06240,
17. Schmitz, K. Modern Cosmology, an Amuse-Gueule. *arXiv* **2022**, arXiv:2203.04757,
18. Buchert, T.; Coley, A.A.; Kleinert, H.; Roukema, B.F.; Wiltshire, D.L. Observational challenges for the standard FLRW model. *Int. J. Mod. Phys. D* **2016**, *25*, 1630007–244, <https://doi.org/10.1142/S021827181630007X>.
19. Abdalla, E.; Abellán, G.F.; Aboubrahim, A.; Agnello, A.; Akarsu, 'O.; Akrami, Y.; Alestas, G.; Aloni, D.; Amendola, L.; Anchordoqui, L.A.; et al. Cosmology intertwined: A review of the particle physics, astrophysics, and cosmology associated with the cosmological tensions and anomalies. *J. High Energy Astrop.* **2022**, *34*, 49–211, <https://doi.org/10.1016/j.jheap.2022.04.002>.
20. Di Valentino, E.D. Challenges of the Standard Cosmological Model. *Universe* **2022**, *8*, 399. <https://doi.org/10.3390/universe8080399>.
21. Perivolaropoulos, L.; Skara, F. Challenges for Λ CDM: An update. *New Astron. Rev.* **2022**, *95*, 101659, <https://doi.org/10.1016/j.newar.2022.101659>.
22. Aluri, P.K.; Cea, P.; Chingangbam, P.; Chu, M.C.; Clowes, R.G.; Hutsemékers, D.; Kochappan, J.P.; Krasiński, A.; Lopez, A.M.; Liu, L.; et al. Is the Observable Universe Consistent with the Cosmological Principle? *arXiv* **2022**, arXiv:2207.05765,
23. Krishnan, C.; Mondol, R.; Sheikh-Jabbari, M.M. Dipole Cosmology: The Copernican Paradigm Beyond FLRW. *arXiv* **2022**, arXiv:2209.14918,
24. Weinberg, S. The cosmological constant problem. *Rev. Mod. Phys.* **1989**, *61*, 1–23. <https://doi.org/10.1103/RevModPhys.61.1>.
25. Courbin, Val L.; Marlow, Daniel R.; Dementi, A.E. *Critical Problems in Physics*; Princeton University Press: Princeton, United States, 1997.
26. Martin, J. Everything you always wanted to know about the cosmological constant problem (but were afraid to ask). *Comptes Rendus Phys.* **2012**, *13*, 566–665, <https://doi.org/10.1016/j.crhy.2012.04.008>.
27. Burgess, C.P. The Cosmological Constant Problem: Why it's hard to get Dark Energy from Micro-physics. *arXiv* **2013**, arXiv:1309.4133,
28. Velten, H.E.S.; vom Marttens, R.F.; Zimdahl, W. Aspects of the cosmological “coincidence problem”. *Eur. Phys. J. C* **2014**, *74*, 3160, <https://doi.org/10.1140/epjc/s10052-014-3160-4>.
29. Copeland, E.J.; Sami, M.; Tsujikawa, S. Dynamics of Dark Energy. *Int. J. Mod. Phys. D* **2006**, *15*, 1753–1935, <https://doi.org/10.1142/S021827180600942X>.

30. Solà, J. Cosmological constant and vacuum energy: Old and new ideas. *J. Phys. Conf. Ser.* **2013**, *453*, 012015, <https://doi.org/10.1088/1742-6596/453/1/012015>.
31. Weinberg, S. Anthropic bound on the cosmological constant. *Phys. Rev. Lett.* **1987**, *59*, 2607–2610. <https://doi.org/10.1103/PhysRevLett.59.2607>.
32. Susskind, L. The Anthropic Landscape of String Theory. In Proceedings of the Davis Meeting ON Cosmic Inflation, Davis, CA, USA, 22–23 March 2003, p. 26.
33. Planck Collaboration. Planck 2015 results. XIII. Cosmological parameters. *Astron. Astrophys.* **2016**, *594*, A13, <https://doi.org/10.1051/0004-6361/201525830>.
34. Riess, A.G.; Casertano, S.; Yuan, W.; Macri, L.; Anderson, J.; MacKenty, J.W.; Bowers, J.B.; Clubb, K.I.; Filippenko, A.V.; Jones, D.O.; et al. New Parallaxes of Galactic Cepheids from Spatially Scanning the Hubble Space Telescope: Implications for the Hubble Constant. *Astroph. J.* **2018**, *855*, 136, <https://doi.org/10.3847/1538-4357/aaadb7>.
35. Riess, A.G.; Casertano, S.; Yuan, W.; Macri, L.M.; Scolnic, D. Large Magellanic Cloud Cepheid Standards Provide a 1% Foundation for the Determination of the Hubble Constant and Stronger Evidence for Physics beyond Λ CDM. *Astroph. J.* **2019**, *876*, 85, <https://doi.org/10.3847/1538-4357/ab1422>.
36. Riess, A.G. The expansion of the Universe is faster than expected. *Nat. Rev. Phys.* **2020**, *2*, 10–12, <https://doi.org/10.1038/s42254-019-0137-0>.
37. Wong, K.C.; Suyu, S.H.; Chen, G.C.F.; Rusu, C.E.; Millon, M.; Sluse, D.; Bonvin, V.; Fassnacht, C.D.; Taubenberger, S.; Auger, M.W.; et al. H0LiCOW-XIII. A 2.4 per cent measurement of H_0 from lensed quasars: 5.3σ tension between early- and late-Universe probes. *Mon. Not. R. Astron. Soc.* **2020**, *498*, 1420–1439, <https://doi.org/10.1093/mnras/stz3094>.
38. Di Valentino, E. A combined analysis of the H_0 late time direct measurements and the impact on the Dark Energy sector. *Mon. Not. R. Astron. Soc.* **2021**, *502*, 2065–2073, <https://doi.org/10.1093/mnras/stab187>.
39. Riess, A.G.; Casertano, S.; Yuan, W.; Bowers, J.B.; Macri, L.; Zinn, J.C.; Scolnic, D. Cosmic Distances Calibrated to 1% Precision with Gaia EDR3 Parallaxes and Hubble Space Telescope Photometry of 75 Milky Way Cepheids Confirm Tension with Λ CDM. *Astroph. J. Lett.* **2021**, *908*, L6, <https://doi.org/10.3847/2041-8213/abdbaf>.
40. Riess, A.G.; Yuan, W.; Macri, L.M.; Scolnic, D.; Brout, D.; Casertano, S.; Jones, D.O.; Murakami, Y.; Anand, G.S.; Breuval, L.; et al. A Comprehensive Measurement of the Local Value of the Hubble Constant with $1 \text{ km s}^{-1} \text{ Mpc}^{-1}$ Uncertainty from the Hubble Space Telescope and the SH0ES Team. *Astroph. J. Lett.* **2022**, *934*, L7, <https://doi.org/10.3847/2041-8213/ac5c5b>.
41. Basilakos, S.; Nesseris, S. Conjoined constraints on modified gravity from the expansion history and cosmic growth. *Phys. Rev. D* **2017**, *96*, 063517, <https://doi.org/10.1103/PhysRevD.96.063517>.
42. DES Collaboration. Dark Energy Survey year 1 results: Cosmological constraints from galaxy clustering and weak lensing. *Phys. Rev. D* **2018**, *98*, 043526, <https://doi.org/10.1103/PhysRevD.98.043526>.
43. Joudaki, S.; Blake, C.; Johnson, A.; Amon, A.; Asgari, M.; Choi, A.; Erben, T.; Glazebrook, K.; Harnois-Déraps, J.; Heymans, C.; et al. KiDS-450 + 2dFLenS: Cosmological parameter constraints from weak gravitational lensing tomography and overlapping redshift-space galaxy clustering. *Mon. Not. R. Astron. Soc.* **2018**, *474*, 4894–4924, <https://doi.org/10.1093/mnras/stx2820>.
44. Akarsu, O.; Barrow, J.D.; Uzun, N.M. Screening anisotropy via energy-momentum squared gravity: A CDM model with hidden anisotropy. *Phys. Rev. D* **2020**, *102*, 124059, <https://doi.org/10.1103/PhysRevD.102.124059>.
45. Hu, J.P.; Wang, Y.Y.; Wang, F.Y. Testing cosmic anisotropy with Pantheon sample and quasars at high redshifts. *Astron. Astrophys.* **2020**, *643*, A93, <https://doi.org/10.1051/0004-6361/202038541>.
46. Planck Collaboration. Planck 2018 results. VII. Isotropy and statistics of the CMB. *Astron. Astrophys.* **2020**, *641*, A7, <https://doi.org/10.1051/0004-6361/201935201>.
47. Migkas, K.; Pacaud, F.; Schellenberger, G.; Erler, J.; Nguyen-Dang, N.T.; Reiprich, T.H.; Ramos-Caja, M.E.; Lovisari, L. Cosmological implications of the anisotropy of ten galaxy cluster scaling relations. *Astron. Astrophys.* **2021**, *649*, A151, <https://doi.org/10.1051/0004-6361/202140296>.
48. Secrest, N.J.; von Hausegger, S.; Rameez, M.; Mohayaee, R.; Sarkar, S.; Colin, J. A Test of the Cosmological Principle with Quasars. *Astroph. J. Lett.* **2021**, *908*, L51, <https://doi.org/10.3847/2041-8213/abdd40>.
49. Zhao, D.; Xia, J.Q. Constraining the anisotropy of the Universe with the X-ray and UV fluxes of quasars. *Eur. Phys. J. C* **2021**, *81*, 694, <https://doi.org/10.1140/epjc/s10052-021-09491-0>.
50. Akarsu, O.; Dereli, T.; Katircı, N. Λ CDM cosmology with a quiescent anisotropy in a higher dimensional steady state universe. *J. Phys. Conf. Ser.* **2022**, *2191*, 012001, <https://doi.org/10.1088/1742-6596/2191/1/012001>.
51. Kalbouneh, B.; Marinoni, C.; Bel, J. The multipole expansion of the local expansion rate. *arXiv* **2022**, arXiv:2210.11333,
52. Zhao, D.; Xia, J.Q. Testing cosmic anisotropy with the E_p - E_{iso} ('Amati') correlation of GRBs. *Mon. Not. R. Astron. Soc.* **2022**, *511*, 5661–5671, <https://doi.org/10.1093/mnras/stac498>.
53. Akarsu, O.; Di Valentino, E.; Kumar, S.; Özyiğit, M.; Sharma, S. Testing spatial curvature and anisotropic expansion on top of the Λ CDM model. *Phys. Dark Universe* **2023**, *39*, 101162, <https://doi.org/10.1016/j.dark.2022.101162>.

54. Kashlinsky, A.; Atrio-Barandela, F.; Kocevski, D.; Ebeling, H. A Measurement of Large-Scale Peculiar Velocities of Clusters of Galaxies: Results and Cosmological Implications. *Astroph. J. Lett.* **2008**, *686*, L49, <https://doi.org/10.1086/592947>.
55. Watkins, R.; Feldman, H.A.; Hudson, M.J. Consistently large cosmic flows on scales of $100 h^{-1} \text{Mpc}$: A challenge for the standard ΛCDM cosmology. *Mon. Not. R. Astron. Soc.* **2009**, *392*, 743–756, <https://doi.org/10.1111/j.1365-2966.2008.14089.x>.
56. Webb, J.K.; King, J.A.; Murphy, M.T.; Flambaum, V.V.; Carswell, R.F.; Bainbridge, M.B. Indications of a Spatial Variation of the Fine Structure Constant. *Phys. Rev. Lett.* **2011**, *107*, 191101, <https://doi.org/10.1103/PhysRevLett.107.191101>.
57. King, J.A.; Webb, J.K.; Murphy, M.T.; Flambaum, V.V.; Carswell, R.F.; Bainbridge, M.B.; Wilczynska, M.R.; Koch, F.E. Spatial variation in the fine-structure constant—New results from VLT/UVES. *Mon. Not. R. Astron. Soc.* **2012**, *422*, 3370–3414, <https://doi.org/10.1111/j.1365-2966.2012.20852.x>.
58. Wiltshire, D.L.; Smale, P.R.; Mattsson, T.; Watkins, R. Hubble flow variance and the cosmic rest frame. *Phys. Rev. D* **2013**, *88*, 083529, <https://doi.org/10.1103/PhysRevD.88.083529>.
59. Bengaly, C.A.P.; Maartens, R.; Santos, M.G. Probing the Cosmological Principle in the counts of radio galaxies at different frequencies. *J. Cosmol. Astropart. Phys.* **2018**, *2018*, 031, <https://doi.org/10.1088/1475-7516/2018/04/031>.
60. Zhao, D.; Xia, J.Q. A tomographic test of cosmic anisotropy with the recently-released quasar sample. *Eur. Phys. J. C* **2021**, *81*, 948. <https://doi.org/10.1140/epjc/s10052-021-09701-9>.
61. Horstmann, N.; Pietschke, Y.; Schwarz, D.J. Inference of the cosmic rest-frame from supernovae Ia. *Astron. Astrophys.* **2022**, *668*, A34, <https://doi.org/10.1051/0004-6361/202142640>.
62. Luongo, O.; Muccino, M.; Colgáin, E.Ó.; Sheikh-Jabbari, M.M.; Yin, L. Larger H_0 values in the CMB dipole direction. *Phys. Rev. D* **2022**, *105*, 103510, <https://doi.org/10.1103/PhysRevD.105.103510>.
63. Guandalin, C.; Piat, J.; Clarkson, C.; Maartens, R. Theoretical systematics in testing the Cosmological Principle with the kinematic quasar dipole. *arXiv* **2022**, arXiv:2212.04925,
64. Evslin, J. Isolating the Lyman alpha forest BAO anomaly. *J. Cosmol. Astropart. Phys.* **2017**, *2017*, 024, <https://doi.org/10.1088/1475-7516/2017/04/024>.
65. Addison, G.E.; Watts, D.J.; Bennett, C.L.; Halpern, M.; Hinshaw, G.; Weiland, J.L. Elucidating ΛCDM : Impact of Baryon Acoustic Oscillation Measurements on the Hubble Constant Discrepancy. *Astroph. J.* **2018**, *853*, 119, <https://doi.org/10.3847/1538-4357/aaa1ed>.
66. Cuceu, A.; Farr, J.; Lemos, P.; Font-Ribera, A. Baryon Acoustic Oscillations and the Hubble constant: Past, present and future. *J. Cosmol. Astropart. Phys.* **2019**, *2019*, 044, <https://doi.org/10.1088/1475-7516/2019/10/044>.
67. Minami, Y.; Ochi, H.; Ichiki, K.; Katayama, N.; Komatsu, E.; Matsumura, T. Simultaneous determination of the cosmic birefringence and miscalibrated polarisation angles from CMB experiments. *arXiv* **2019**, arXiv:1904.12440,
68. Minami, Y. Determination of miscalibrated polarization angles from observed cosmic microwave background and foreground EB power spectra: Application to partial-sky observation. *Prog. Theor. Exp. Phys.* **2020**, *2020*, 063E01, <https://doi.org/10.1093/ptep/ptaa057>.
69. Minami, Y.; Komatsu, E. New Extraction of the Cosmic Birefringence from the Planck 2018 Polarization Data. *Phys. Rev. Lett.* **2020**, *125*, 221301, <https://doi.org/10.1103/PhysRevLett.125.221301>.
70. Minami, Y.; Komatsu, E. Simultaneous determination of the cosmic birefringence and miscalibrated polarization angles II: Including cross-frequency spectra. *Prog. Theor. Exp. Phys.* **2020**, *2020*, 103E02, <https://doi.org/10.1093/ptep/ptaa130>.
71. Bullock, J.S.; Boylan-Kolchin, M. Small-Scale Challenges to the ΛCDM Paradigm. *Annu. Rev. Astron. Astr.* **2017**, *55*, 343–387, <https://doi.org/10.1146/annurev-astro-091916-055313>.
72. Del Popolo, A.; Le Delliou, M. Small Scale Problems of the ΛCDM Model: A Short Review. *Galaxies* **2017**, *5*, 17, <https://doi.org/10.3390/galaxies5010017>.
73. Salucci, P. The distribution of dark matter in galaxies. *Astron. Astrophys. Rev.* **2019**, *27*, 2, <https://doi.org/10.1007/s00159-018-0113-1>.
74. Di Paolo, C.; Salucci, P. Fundamental properties of the dark and the luminous matter from Low Surface Brightness discs. *arXiv* **2020**, arXiv:2005.03520,
75. Verde, L.; Protopapas, P.; Jimenez, R. Planck and the local Universe: Quantifying the tension. *Phys. Dark Universe* **2013**, *2*, 166–175, <https://doi.org/10.1016/j.dark.2013.09.002>.
76. Fields, B.D. The Primordial Lithium Problem. *Annu. Rev. Nucl. Part. S.* **2011**, *61*, 47–68, <https://doi.org/10.1146/annurev-nucl-10-130445>.
77. Lusso, E.; Piedipalumbo, E.; Risaliti, G.; Paolillo, M.; Bisogni, S.; Nardini, E.; Amati, L. Tension with the flat ΛCDM model from a high-redshift Hubble diagram of supernovae, quasars, and gamma-ray bursts. *Astron. Astrophys.* **2019**, *628*, L4, <https://doi.org/10.1051/0004-6361/201936223>.
78. Risaliti, G.; Lusso, E. Cosmological Constraints from the Hubble Diagram of Quasars at High Redshifts. *Nat. Astron.* **2019**, *3*, 272–277, <https://doi.org/10.1038/s41550-018-0657-z>.
79. Yang, T.; Banerjee, A.; Ó Colgáin, E. Cosmography and flat Λ CDM tensions at high redshift. *Phys. Rev. D* **2020**, *102*, 123532, <https://doi.org/10.1103/PhysRevD.102.123532>.

80. Banerjee, A.; Ó Colgáin, E.; Sasaki, M.; Sheikh-Jabbari, M.M.; Yang, T. On problems with cosmography in cosmic dark ages. *Phys. Lett. B* **2021**, *818*, 136366, <https://doi.org/10.1016/j.physletb.2021.136366>.
81. Hu, J.P.; Wang, F.Y. High-redshift cosmography: Application and comparison with different methods. *Astron. Astrophys.* **2022**, *661*, A71, <https://doi.org/10.1051/0004-6361/202142162>.
82. Antoniou, I.; Perivolaropoulos, L. Constraints on spatially oscillating sub-mm forces from the Stanford Optically Levitated Microsphere Experiment data. *Phys. Rev. D* **2017**, *96*, 104002, <https://doi.org/10.1103/PhysRevD.96.104002>.
83. Perivolaropoulos, L. Submillimeter spatial oscillations of Newton’s constant: Theoretical models and laboratory tests. *Phys. Rev. D* **2017**, *95*, 084050, <https://doi.org/10.1103/PhysRevD.95.084050>.
84. Bowman, J.D.; Rogers, A.E.E.; Monsalve, R.A.; Mozdzen, T.J.; Mahesh, N. An absorption profile centred at 78 megahertz in the sky-averaged spectrum. *Nature* **2018**, *555*, 67–70, <https://doi.org/10.1038/nature25792>.
85. Kraljic, D.; Sarkar, S. How rare is the Bullet Cluster (in a Λ CDM universe)? *J. Cosmol. Astropart. Phys.* **2015**, *2015*, 050–050, <https://doi.org/10.1088/1475-7516/2015/04/050>.
86. Asencio, E.; Banik, I.; Kroupa, P. A massive blow for Λ CDM—The high redshift, mass, and collision velocity of the interacting galaxy cluster El Gordo contradicts concordance cosmology. *Mon. Not. R. Astron. Soc.* **2021**, *500*, 5249–5267, <https://doi.org/10.1093/mnras/staa3441>.
87. Planck Collaboration. Planck 2013 results. XVI. Cosmological parameters. *Astron. Astrophys.* **2014**, *571*, A16, <https://doi.org/10.1051/0004-6361/201321591>.
88. Planck Collaboration. Planck intermediate results. LI. Features in the cosmic microwave background temperature power spectrum and shifts in cosmological parameters. *Astron. Astrophys.* **2017**, *607*, A95, <https://doi.org/10.1051/0004-6361/201629504>.
89. Jones, D.O.; Riess, A.G.; Scolnic, D.M.; Pan, Y.C.; Johnson, E.; Coulter, D.A.; Dettman, K.G.; Foley, M.M.; Foley, R.J.; Huber, M.E.; et al. Should Type Ia Supernova Distances Be Corrected for Their Local Environments? *Astroph. J.* **2018**, *867*, 108, <https://doi.org/10.3847/1538-4357/aae2b9>.
90. Shanks, T.; Hogarth, L.M.; Metcalfe, N. Gaia Cepheid parallaxes and ‘Local Hole’ relieve H_0 tension. *Mon. Not. R. Astron. Soc.* **2019**, *484*, L64–L68, <https://doi.org/10.1093/mnrasl/sly239>.
91. Planck Collaboration. Planck 2018 results. I. Overview and the cosmological legacy of Planck. *Astron. Astrophys.* **2020**, *641*, A1, <https://doi.org/10.1051/0004-6361/201833880>.
92. Rigault, M.; Brinnel, V.; Aldering, G.; Antilogus, P.; Aragon, C.; Bailey, S.; Baltay, C.; Barbary, K.; Bongard, S.; Boone, K.; et al. Strong dependence of Type Ia supernova standardization on the local specific star formation rate. *Astron. Astrophys.* **2020**, *644*, A176, <https://doi.org/10.1051/0004-6361/201730404>.
93. Carneiro, S.; Pigozzo, C.; Alcaniz, J.S. Redshift systematics and the H_0 tension problem. *Eur. Phys. J. Plus* **2022**, *137*, 537, <https://doi.org/10.1140/epjp/s13360-022-02744-1>.
94. de Jaeger, T.; Galbany, L.; Riess, A.G.; Stahl, B.E.; Shappee, B.J.; Filippenko, A.V.; Zheng, W. A 5 per cent measurement of the Hubble-Lemaître constant from Type II supernovae. *Mon. Not. R. Astron. Soc.* **2022**, *514*, 4620–4628, <https://doi.org/10.1093/mnras/stac1661>.
95. Hill, J.C.; McDonough, E.; Toomey, M.W.; Alexander, S. Early dark energy does not restore cosmological concordance. *Phys. Rev. D* **2020**, *102*, 043507, <https://doi.org/10.1103/PhysRevD.102.043507>.
96. D’Amico, G.; Senatore, L.; Zhang, P.; Zheng, H. The Hubble tension in light of the Full-Shape analysis of Large-Scale Structure data. *J. Cosmol. Astropart. Phys.* **2021**, *2021*, 072, <https://doi.org/10.1088/1475-7516/2021/05/072>.
97. Shah, P.; Lemos, P.; Lahav, O. A buyer’s guide to the Hubble constant. *Astron. Astrophys. Rev.* **2021**, *29*, 9, <https://doi.org/10.1007/s00159-021-00137-4>.
98. Verde, L.; Treu, T.; Riess, A.G. Tensions between the early and late Universe. *Nat. Astron.* **2019**, *3*, 891–895, <https://doi.org/10.1038/s41550-019-0902-0>.
99. Weinberg, D.H.; Mortonson, M.J.; Eisenstein, D.J.; Hirata, C.; Riess, A.G.; Rozo, E. Observational probes of cosmic acceleration. *Phys. Rep.* **2013**, *530*, 87–255, <https://doi.org/10.1016/j.physrep.2013.05.001>.
100. Bennett, C.L.; Larson, D.; Weiland, J.L.; Jarosik, N.; Hinshaw, G.; Odegard, N.; Smith, K.M.; Hill, R.S.; Gold, B.; Halpern, M.; et al. Nine-year Wilkinson Microwave Anisotropy Probe (WMAP) Observations: Final Maps and Results. *Astrophys. J. Suppl. S.* **2013**, *208*, 20, <https://doi.org/10.1088/0067-0049/208/2/20>.
101. Knox, L.; Millea, M. Hubble constant hunter’s guide. *Phys. Rev. D* **2020**, *101*, 043533, <https://doi.org/10.1103/PhysRevD.101.043533>.
102. SPT-3G Collaboration. Measurements of the E-mode polarization and temperature-E-mode correlation of the CMB from SPT-3G 2018 data. *Phys. Rev. D* **2021**, *104*, 022003, <https://doi.org/10.1103/PhysRevD.104.022003>.
103. Aiola, S.; Calabrese, E.; Maurin, L.; Naess, S.; Schmitt, B.L.; Abitbol, M.H.; Addison, G.E.; Ade, P.A.R.; Alonso, D.; Amiri, M.; et al. The Atacama Cosmology Telescope: DR4 maps and cosmological parameters. *J. Cosmol. Astropart. Phys.* **2020**, *2020*, 047, <https://doi.org/10.1088/1475-7516/2020/12/047>.
104. Freedman, W.L.; Madore, B.F.; Gibson, B.K.; Ferrarese, L.; Kelson, D.D.; Sakai, S.; Mould, J.R.; Kennicutt, Robert C., J.; Ford, H.C.; Graham, J.A.; et al. Final Results from the Hubble Space Telescope Key Project to Measure the Hubble Constant. *Astroph. J.* **2001**, *553*, 47–72, <https://doi.org/10.1086/320638>.

105. Freedman, W.L.; Madore, B.F.; Scowcroft, V.; Burns, C.; Monson, A.; Persson, S.E.; Seibert, M.; Rigby, J. Carnegie Hubble Program: A Mid-infrared Calibration of the Hubble Constant. *Astroph. J.* **2012**, *758*, 24, <https://doi.org/10.1088/0004-637X/758/1/24>.
106. Lusso, E.; Risaliti, G. The Tight Relation between X-Ray and Ultraviolet Luminosity of Quasars. *Astroph. J.* **2016**, *819*, 154, <https://doi.org/10.3847/0004-637X/819/2/154>.
107. Bisogni, S.; Risaliti, G.; Lusso, E. A Hubble Diagram for Quasars. *Front. Astron. Space Sci.* **2017**, *4*, 68, <https://doi.org/10.3389/fspas.2017.00068>.
108. Lusso, E.; Risaliti, G. Quasars as standard candles. I. The physical relation between disc and coronal emission. *Astron. Astrophys.* **2017**, *602*, A79, <https://doi.org/10.1051/0004-6361/201630079>.
109. Melia, F. Cosmological test using the Hubble diagram of high-z quasars. *Mon. Not. R. Astron. Soc.* **2019**, *489*, 517–523, <https://doi.org/10.1093/mnras/stz2120>.
110. Khadka, N.; Ratra, B. Quasar X-ray and UV flux, baryon acoustic oscillation, and Hubble parameter measurement constraints on cosmological model parameters. *Mon. Not. R. Astron. Soc.* **2020**, *492*, 4456–4468, <https://doi.org/10.1093/mnras/staa101>.
111. Cao, S.; Zajaček, M.; Panda, S.; Martínez-Aldama, M.L.; Czerny, B.; Ratra, B. Standardizing reverberation-measured C IV time-lag quasars, and using them with standardized Mg II quasars to constrain cosmological parameters. *Mon. Not. R. Astron. Soc.* **2022**, *516*, 1721–1740, <https://doi.org/10.1093/mnras/stac2325>.
112. Khadka, N.; Martínez-Aldama, M.L.; Zajaček, M.; Czerny, B.; Ratra, B. Do reverberation-measured H β quasars provide a useful test of cosmology? *Mon. Not. R. Astron. Soc.* **2022**, *513*, 1985–2005, <https://doi.org/10.1093/mnras/stac914>.
113. Khadka, N.; Zajaček, M.; Panda, S.; Martínez-Aldama, M.L.; Ratra, B. Consistency study of high- and low-accreting Mg II quasars: No significant effect of the Fe II to Mg II flux ratio on the radius-luminosity relation dispersion. *Mon. Not. R. Astron. Soc.* **2022**, *515*, 3729–3748, <https://doi.org/10.1093/mnras/stac1940>.
114. Khadka, N.; Ratra, B. Do quasar X-ray and UV flux measurements provide a useful test of cosmological models? *Mon. Not. R. Astron. Soc.* **2022**, *510*, 2753–2772, <https://doi.org/10.1093/mnras/stab3678>.
115. Wang, B.; Liu, Y.; Yuan, Z.; Liang, N.; Yu, H.; Wu, P. Redshift-evolutionary X-Ray and UV Luminosity Relation of Quasars from Gaussian Copula. *Astroph. J.* **2022**, *940*, 174, <https://doi.org/10.3847/1538-4357/ac9df8>.
116. Dainotti, M.G.; Cardone, V.F.; Capozziello, S. A time-luminosity correlation for γ -ray bursts in the X-rays. *Mon. Not. R. Astron. Soc.* **2008**, *391*, L79–L83, <https://doi.org/10.1111/j.1745-3933.2008.00560.x>.
117. Wang, F.Y.; Dai, Z.G.; Liang, E.W. Gamma-ray burst cosmology. *New Astron. Rev.* **2015**, *67*, 1–17, <https://doi.org/10.1016/j.newar.2015.03.001>.
118. Dainotti, M.G.; Del Vecchio, R. Gamma Ray Burst afterglow and prompt-afterglow relations: An overview. *New Astron. Rev.* **2017**, *77*, 23–61, <https://doi.org/10.1016/j.newar.2017.04.001>.
119. Cao, S.; Khadka, N.; Ratra, B. Standardizing Dainotti-correlated gamma-ray bursts, and using them with standardized Amati-correlated gamma-ray bursts to constrain cosmological model parameters. *Mon. Not. R. Astron. Soc.* **2022**, *510*, 2928–2947, <https://doi.org/10.1093/mnras/stab3559>.
120. Cao, S.; Dainotti, M.; Ratra, B. Standardizing Platinum Dainotti-correlated gamma-ray bursts, and using them with standardized Amati-correlated gamma-ray bursts to constrain cosmological model parameters. *Mon. Not. R. Astron. Soc.* **2022**, *512*, 439–454, <https://doi.org/10.1093/mnras/stac517>.
121. Cao, S.; Ratra, B. Using lower redshift, non-CMB, data to constrain the Hubble constant and other cosmological parameters. *Mon. Not. R. Astron. Soc.* **2022**, *513*, 5686–5700, <https://doi.org/10.1093/mnras/stac1184>.
122. Deng, C.; Huang, Y.F.; Xu, F. Pseudo Redshifts of Gamma-Ray Bursts Derived from the L-T-E Correlation. *arXiv* **2022**, arXiv:2212.01990.
123. Jia, X.D.; Hu, J.P.; Yang, J.; Zhang, B.B.; Wang, F.Y. E_{iso}-E_p correlation of gamma-ray bursts: Calibration and cosmological applications. *Mon. Not. R. Astron. Soc.* **2022**, *516*, 2575–2585, <https://doi.org/10.1093/mnras/stac2356>.
124. Liu, Y.; Chen, F.; Liang, N.; Yuan, Z.; Yu, H.; Wu, P. The Improved Amati Correlations from Gaussian Copula. *Astroph. J.* **2022**, *931*, 50, <https://doi.org/10.3847/1538-4357/ac66d3>.
125. Liang, N.; Li, Z.; Xie, X.; Wu, P. Calibrating Gamma-Ray Bursts by Using a Gaussian Process with Type Ia Supernovae. *Astroph. J.* **2022**, *941*, 84, <https://doi.org/10.3847/1538-4357/aca08a>.
126. Li, Z.; Zhang, B.; Liang, N. Constraints on Dark Energy Models with Gamma-Ray Bursts Calibrated from the Observational H(z) Data. *arXiv* **2022**, arXiv:2212.14291,
127. Muccino, M.; Luongo, O.; Jain, D. Constraints on the transition redshift from the calibrated Gamma-ray Burst E_p-E_{iso} correlation. *arXiv* **2022**, arXiv:2208.13700,
128. Luongo, O.; Muccino, M. Intermediate redshift calibration of gamma-ray bursts and cosmic constraints in non-flat cosmology. *Mon. Not. R. Astron. Soc.* **2023**, *518*, 2247–2255, <https://doi.org/10.1093/mnras/stac2925>.
129. Riess, A.G.; Macri, L.M.; Hoffmann, S.L.; Scolnic, D.; Casertano, S.; Filippenko, A.V.; Tucker, B.E.; Reid, M.J.; Jones, D.O.; Silverman, J.M.; et al. A 2.4% Determination of the Local Value of the Hubble Constant. *Astroph. J.* **2016**, *826*, 56, <https://doi.org/10.3847/0004-637X/826/1/56>.

130. Cardona, W.; Kunz, M.; Pettorino, V. Determining H_0 with Bayesian hyper-parameters. *J. Cosmol. Astropart. Phys.* **2017**, *2017*, 056, <https://doi.org/10.1088/1475-7516/2017/03/056>.
131. Burns, C.R.; Parent, E.; Phillips, M.M.; Stritzinger, M.; Krisciunas, K.; Suntzeff, N.B.; Hsiao, E.Y.; Contreras, C.; Anais, J.; Boldt, L.; et al. The Carnegie Supernova Project: Absolute Calibration and the Hubble Constant. *Astroph. J.* **2018**, *869*, 56, <https://doi.org/10.3847/1538-4357/aae51c>.
132. Feeney, S.M.; Mortlock, D.J.; Dalmasso, N. Clarifying the Hubble constant tension with a Bayesian hierarchical model of the local distance ladder. *Mon. Not. R. Astron. Soc.* **2018**, *476*, 3861–3882, <https://doi.org/10.1093/mnras/sty418>.
133. Follin, B.; Knox, L. Insensitivity of the distance ladder Hubble constant determination to Cepheid calibration modelling choices. *Mon. Not. R. Astron. Soc.* **2018**, *477*, 4534–4542, <https://doi.org/10.1093/mnras/sty720>.
134. Dhawan, S.; Jha, S.W.; Leibundgut, B. Measuring the Hubble constant with Type Ia supernovae as near-infrared standard candles. *Astron. Astrophys.* **2018**, *609*, A72, <https://doi.org/10.1051/0004-6361/201731501>.
135. Camarena, D.; Marra, V. Local determination of the Hubble constant and the deceleration parameter. *Phys. Rev. Res.* **2020**, *2*, 013028, <https://doi.org/10.1103/PhysRevResearch.2.013028>.
136. Javanmardi, B.; Mérand, A.; Kervella, P.; Breuval, L.; Gallenne, A.; Nardetto, N.; Gieren, W.; Pietrzyński, G.; Hocdé, V.; Borgniet, S. Inspecting the Cepheid Distance Ladder: The Hubble Space Telescope Distance to the SN Ia Host Galaxy NGC 5584. *Astroph. J.* **2021**, *911*, 12, <https://doi.org/10.3847/1538-4357/abe7e5>.
137. Spergel, D.N.; Verde, L.; Peiris, H.V.; Komatsu, E.; Nolta, M.R.; Bennett, C.L.; Halpern, M.; Hinshaw, G.; Jarosik, N.; Kogut, A.; et al. First-Year Wilkinson Microwave Anisotropy Probe (WMAP) Observations: Determination of Cosmological Parameters. *Astrophys. J. Suppl. S.* **2003**, *148*, 175–194, <https://doi.org/10.1086/377226>.
138. Spergel, D.N.; Bean, R.; Doré, O.; Nolta, M.R.; Bennett, C.L.; Dunkley, J.; Hinshaw, G.; Jarosik, N.; Komatsu, E.; Page, L.; et al. Three-Year Wilkinson Microwave Anisotropy Probe (WMAP) Observations: Implications for Cosmology. *Astrophys. J. Suppl. S.* **2007**, *170*, 377–408, <https://doi.org/10.1086/513700>.
139. Komatsu, E.; Dunkley, J.; Nolta, M.R.; Bennett, C.L.; Gold, B.; Hinshaw, G.; Jarosik, N.; Larson, D.; Limon, M.; Page, L.; et al. Five-Year Wilkinson Microwave Anisotropy Probe Observations: Cosmological Interpretation. *Astrophys. J. Suppl. S.* **2009**, *180*, 330–376, <https://doi.org/10.1088/0067-0049/180/2/330>.
140. Komatsu, E.; Smith, K.M.; Dunkley, J.; Bennett, C.L.; Gold, B.; Hinshaw, G.; Jarosik, N.; Larson, D.; Nolta, M.R.; Page, L.; et al. Seven-year Wilkinson Microwave Anisotropy Probe (WMAP) Observations: Cosmological Interpretation. *Astrophys. J. Suppl. S.* **2011**, *192*, 18, <https://doi.org/10.1088/0067-0049/192/2/18>.
141. Riess, A.G.; Macri, L.; Casertano, S.; Sosey, M.; Lampeitl, H.; Ferguson, H.C.; Filippenko, A.V.; Jha, S.W.; Li, W.; Chornock, R.; et al. A Redetermination of the Hubble Constant with the Hubble Space Telescope from a Differential Distance Ladder. *Astroph. J.* **2009**, *699*, 539–563, <https://doi.org/10.1088/0004-637X/699/1/539>.
142. Riess, A.G.; Macri, L.; Casertano, S.; Lampeitl, H.; Ferguson, H.C.; Filippenko, A.V.; Jha, S.W.; Li, W.; Chornock, R. A 3% Solution: Determination of the Hubble Constant with the Hubble Space Telescope and Wide Field Camera 3. *Astroph. J.* **2011**, *730*, 119, <https://doi.org/10.1088/0004-637X/730/2/119>.
143. Millon, M.; Galan, A.; Courbin, F.; Treu, T.; Suyu, S.H.; Ding, X.; Birrer, S.; Chen, G.C.F.; Shajib, A.J.; Sluse, D.; et al. TDCOSMO. I. An exploration of systematic uncertainties in the inference of H_0 from time-delay cosmography. *Astron. Astrophys.* **2020**, *639*, A101, <https://doi.org/10.1051/0004-6361/201937351>.
144. Kuo, C.Y.; Braatz, J.A.; Reid, M.J.; Lo, K.Y.; Condon, J.J.; Impellizzeri, C.M.V.; Henkel, C. The Megamaser Cosmology Project. V. An Angular-diameter Distance to NGC 6264 at 140 Mpc. *Astroph. J.* **2013**, *767*, 155, <https://doi.org/10.1088/0004-637X/767/2/155>.
145. Reid, M.J.; Braatz, J.A.; Condon, J.J.; Lo, K.Y.; Kuo, C.Y.; Impellizzeri, C.M.V.; Henkel, C. The Megamaser Cosmology Project. IV. A Direct Measurement of the Hubble Constant from UGC 3789. *Astroph. J.* **2013**, *767*, 154, <https://doi.org/10.1088/0004-637X/767/2/154>.
146. Kuo, C.Y.; Braatz, J.A.; Lo, K.Y.; Reid, M.J.; Suyu, S.H.; Pesce, D.W.; Condon, J.J.; Henkel, C.; Impellizzeri, C.M.V. The Megamaser Cosmology Project. VI. Observations of NGC 6323. *Astroph. J.* **2015**, *800*, 26, <https://doi.org/10.1088/0004-637X/800/1/26>.
147. Reid, M.J.; Pesce, D.W.; Riess, A.G. An Improved Distance to NGC 4258 and Its Implications for the Hubble Constant. *Astroph. J. Lett.* **2019**, *886*, L27, <https://doi.org/10.3847/2041-8213/ab552d>.
148. Pesce, D.W.; Braatz, J.A.; Reid, M.J.; Riess, A.G.; Scolnic, D.; Condon, J.J.; Gao, F.; Henkel, C.; Impellizzeri, C.M.V.; Kuo, C.Y.; et al. The Megamaser Cosmology Project. XIII. Combined Hubble Constant Constraints. *Astroph. J. Lett.* **2020**, *891*, L1, <https://doi.org/10.3847/2041-8213/ab75f0>.
149. Abbott, B.P.; Abbott, R.; Abbott, T.D.; Acernese, F.; Ackley, K.; Adams, C.; Adams, T.; Addesso, P.; Adhikari, R.X.; Adya, V.B.; et al. A gravitational-wave standard siren measurement of the Hubble constant. *Nature* **2017**, *551*, 85–88, <https://doi.org/10.1038/nature24471>.
150. Mooley, K.P.; Deller, A.T.; Gottlieb, O.; Nakar, E.; Hallinan, G.; Bourke, S.; Frail, D.A.; Horesh, A.; Corsi, A.; Hotokezaka, K. Superluminal motion of a relativistic jet in the neutron-star merger GW170817. *Nature* **2018**, *561*, 355–359, <https://doi.org/10.1038/s41586-018-0486-3>.

151. Hotokezaka, K.; Nakar, E.; Gottlieb, O.; Nissanke, S.; Masuda, K.; Hallinan, G.; Mooley, K.P.; Deller, A.T. A Hubble constant measurement from superluminal motion of the jet in GW170817. *Nat. Astron.* **2019**, *3*, 940–944, <https://doi.org/10.1038/s41550-019-0820-1>.
152. Hagstotz, S.; Reischke, R.; Lilow, R. A new measurement of the Hubble constant using fast radio bursts. *Mon. Not. R. Astron. Soc.* **2022**, *511*, 662–667, <https://doi.org/10.1093/mnras/stac077>.
153. Wu, Q.; Zhang, G.Q.; Wang, F.Y. An 8 per cent determination of the Hubble constant from localized fast radio bursts. *Mon. Not. R. Astron. Soc.* **2022**, *515*, L1–L5, <https://doi.org/10.1093/mnrasl/slac022>.
154. James, C.W.; Ghosh, E.M.; Prochaska, J.X.; Bannister, K.W.; Bhandari, S.; Day, C.K.; Deller, A.T.; Glowacki, M.; Gordon, A.C.; Heintz, K.E.; et al. A measurement of Hubble’s Constant using Fast Radio Bursts. *Mon. Not. R. Astron. Soc.* **2022**, *516*, 4862–4881, <https://doi.org/10.1093/mnras/stac2524>.
155. Liu, Y.; Yu, H.; Wu, P. Cosmological-model-independent determination of Hubble constant from fast radio bursts and Hubble parameter measurements. *arXiv* **2022**, arXiv:2210.05202.
156. Zhao, Z.W.; Zhang, J.G.; Li, Y.; Zou, J.M.; Zhang, J.F.; Zhang, X. First statistical measurement of the Hubble constant using unlocalized fast radio bursts. *arXiv* **2022**, arXiv:2212.13433.
157. Freedman, W.L.; Madore, B.F.; Hatt, D.; Hoyt, T.J.; Jang, I.S.; Beaton, R.L.; Burns, C.R.; Lee, M.G.; Monson, A.J.; Neeley, J.R.; et al. The Carnegie-Chicago Hubble Program. VIII. An Independent Determination of the Hubble Constant Based on the Tip of the Red Giant Branch. *Astroph. J.* **2019**, *882*, 34, <https://doi.org/10.3847/1538-4357/ab2f73>.
158. Freedman, W.L.; Madore, B.F.; Hoyt, T.; Jang, I.S.; Beaton, R.; Lee, M.G.; Monson, A.; Neeley, J.; Rich, J. Calibration of the Tip of the Red Giant Branch. *Astroph. J.* **2020**, *891*, 57, <https://doi.org/10.3847/1538-4357/ab7339>.
159. Freedman, W.L. Measurements of the Hubble Constant: Tensions in Perspective. *Astroph. J.* **2021**, *919*, 16, <https://doi.org/10.3847/1538-4357/ac0e95>.
160. Vagnozzi, S.; Pacucci, F.; Loeb, A. Implications for the Hubble tension from the ages of the oldest astrophysical objects. *J. High Energy Astrop.* **2022**, *36*, 27–35, <https://doi.org/10.1016/j.jheap.2022.07.004>.
161. Wei, J.J.; Melia, F. Exploring the Hubble Tension and Spatial Curvature from the Ages of Old Astrophysical Objects. *Astroph. J.* **2022**, *928*, 165, <https://doi.org/10.3847/1538-4357/ac562c>.
162. Moresco, M.; Amati, L.; Amendola, L.; Birrer, S.; Blakeslee, J.P.; Cantiello, M.; Cimatti, A.; Darling, J.; Della Valle, M.; Fishbach, M.; et al. Unveiling the Universe with emerging cosmological probes. *Living Rev. Relativ.* **2022**, *25*, 6, <https://doi.org/10.1007/s41114-022-00040-z>.
163. Courbin, F.; Minniti, D. *Gravitational Lensing: An Astrophysical Tool*; Springer: Berlin/Heidelberg, Germany, 2002; Volume 608.
164. Suyu, S.H.; Chang, T.C.; Courbin, F.; Okumura, T. Cosmological Distance Indicators. *Space Sci. Rev.* **2018**, *214*, 91, <https://doi.org/10.1007/s11214-018-0524-3>.
165. Shajib, A.J.; Mozumdar, P.; Chen, G.C.F.; Treu, T.; Cappellari, M.; Knobel, S.; Suyu, S.H.; Bennert, V.N.; Frieman, J.A.; Sluse, D.; et al. TDCOSMO. XIII. Improved Hubble constant measurement from lensing time delays using spatially resolved stellar kinematics of the lens galaxy. *arXiv* **2023**, arXiv:2301.02656.
166. Suyu, S.H.; Halkola, A. The halos of satellite galaxies: The companion of the massive elliptical lens SL2S J08544-0121. *Astron. Astrophys.* **2010**, *524*, A94, <https://doi.org/10.1051/0004-6361/201015481>.
167. Jee, I.; Suyu, S.H.; Komatsu, E.; Fassnacht, C.D.; Hilbert, S.; Koopmans, L.V.E. A measurement of the Hubble constant from angular diameter distances to two gravitational lenses. *Science* **2019**, *365*, 1134–1138, <https://doi.org/10.1126/science.aat7371>.
168. Suyu, S.H.; Treu, T.; Hilbert, S.; Sonnenfeld, A.; Auger, M.W.; Blandford, R.D.; Collett, T.; Courbin, F.; Fassnacht, C.D.; Koopmans, L.V.E.; et al. Cosmology from Gravitational Lens Time Delays and Planck Data. *Astroph. J. Lett.* **2014**, *788*, L35, <https://doi.org/10.1088/2041-8205/788/2/L35>.
169. Chen, G.C.F.; Fassnacht, C.D.; Suyu, S.H.; Rusu, C.E.; Chan, J.H.H.; Wong, K.C.; Auger, M.W.; Hilbert, S.; Bonvin, V.; Birrer, S.; et al. A SHARP view of H0LiCOW: H_0 from three time-delay gravitational lens systems with adaptive optics imaging. *Mon. Not. R. Astron. Soc.* **2019**, *490*, 1743–1773, <https://doi.org/10.1093/mnras/stz2547>.
170. Wong, K.C.; Suyu, S.H.; Auger, M.W.; Bonvin, V.; Courbin, F.; Fassnacht, C.D.; Halkola, A.; Rusu, C.E.; Sluse, D.; Sonnenfeld, A.; et al. H0LiCOW-IV. Lens mass model of HE 0435-1223 and blind measurement of its time-delay distance for cosmology. *Mon. Not. R. Astron. Soc.* **2017**, *465*, 4895–4913, <https://doi.org/10.1093/mnras/stw3077>.
171. Birrer, S.; Treu, T.; Rusu, C.E.; Bonvin, V.; Fassnacht, C.D.; Chan, J.H.H.; Agnello, A.; Shajib, A.J.; Chen, G.C.F.; Auger, M.; et al. H0LiCOW-IX. Cosmographic analysis of the doubly imaged quasar SDSS 1206+4332 and a new measurement of the Hubble constant. *Mon. Not. R. Astron. Soc.* **2019**, *484*, 4726–4753, <https://doi.org/10.1093/mnras/stz200>.
172. Rusu, C.E.; Wong, K.C.; Bonvin, V.; Sluse, D.; Suyu, S.H.; Fassnacht, C.D.; Chan, J.H.H.; Hilbert, S.; Auger, M.W.; Sonnenfeld, A.; et al. H0LiCOW XII. Lens mass model of WFI2033-4723 and blind measurement of its time-delay distance and H_0 . *Mon. Not. R. Astron. Soc.* **2020**, *498*, 1440–1468, <https://doi.org/10.1093/mnras/stz3451>.
173. DES Collaboration. Discovery of the Lensed Quasar System DES J0408-5354. *Astroph. J. Lett.* **2017**, *838*, L15, <https://doi.org/10.3847/2041-8213/aa624e>.

174. Shajib, A.J.; Birrer, S.; Treu, T.; Agnello, A.; Buckley-Geer, E.J.; Chan, J.H.H.; Christensen, L.; Lemon, C.; Lin, H.; Millon, M.; et al. STRIDES: A 3.9 per cent measurement of the Hubble constant from the strong lens system DES J0408-5354. *Mon. Not. R. Astron. Soc.* **2020**, *494*, 6072–6102, <https://doi.org/10.1093/mnras/staa828>.
175. Humphreys, E.M.L.; Reid, M.J.; Moran, J.M.; Greenhill, L.J.; Argon, A.L. Toward a New Geometric Distance to the Active Galaxy NGC 4258. III. Final Results and the Hubble Constant. *Astroph. J.* **2013**, *775*, 13, <https://doi.org/10.1088/0004-637X/775/1/13>.
176. Claussen, M.J.; Heiligman, G.M.; Lo, K.Y. Water-vapour maser emission from galactic nuclei. *Nature* **1984**, *310*, 298–300. <https://doi.org/10.1038/310298a0>.
177. Nakai, N.; Inoue, M.; Miyoshi, M. Extremely-high-velocity H₂O maser emission in the galaxy NGC4258. *Nature* **1993**, *361*, 45–47. <https://doi.org/10.1038/361045a0>.
178. Herrnstein, J.R.; Moran, J.M.; Greenhill, L.J.; Diamond, P.J.; Inoue, M.; Nakai, N.; Miyoshi, M.; Henkel, C.; Riess, A. A geometric distance to the galaxy NGC4258 from orbital motions in a nuclear gas disk. *Nature* **1999**, *400*, 539–541, <https://doi.org/10.1038/22972>.
179. Braatz, J.; Greenhill, L.; Reid, M.; Condon, J.; Henkel, C.; Lo, K.Y. Precision cosmology with H₂O megamasers: Progress in measuring distances to galaxies in the Hubble flow. In *Proceedings of the Astrophysical Masers and Their Environments*; Chapman, J.M.; Baan, W.A., Eds.; Alice Spring, Australia, 2007; Volume 242, pp. 399–401. <https://doi.org/10.1017/S1743921307013452>.
180. Braatz, J.A.; Gugliucci, N.E. The Discovery of Water Maser Emission from Eight Nearby Galaxies. *Astroph. J.* **2008**, *678*, 96–101, <https://doi.org/10.1086/529538>.
181. Gao, F.; Braatz, J.A.; Reid, M.J.; Condon, J.J.; Greene, J.E.; Henkel, C.; Impellizzeri, C.M.V.; Lo, K.Y.; Kuo, C.Y.; Pesce, D.W.; et al. The Megamaser Cosmology Project. IX. Black Hole Masses for Three Maser Galaxies. *Astroph. J.* **2017**, *834*, 52, <https://doi.org/10.3847/1538-4357/834/1/52>.
182. Gao, F.; Braatz, J.A.; Reid, M.J.; Lo, K.Y.; Condon, J.J.; Henkel, C.; Kuo, C.Y.; Impellizzeri, C.M.V.; Pesce, D.W.; Zhao, W. The Megamaser Cosmology Project. VIII. A Geometric Distance to NGC 5765b. *Astroph. J.* **2016**, *817*, 128, <https://doi.org/10.3847/0004-637X/817/2/128>.
183. Pesce, D.W.; Braatz, J.A.; Reid, M.J.; Condon, J.J.; Gao, F.; Henkel, C.; Kuo, C.Y.; Lo, K.Y.; Zhao, W. The Megamaser Cosmology Project. XI. A Geometric Distance to CGCG 074-064. *Astroph. J.* **2020**, *890*, 118, <https://doi.org/10.3847/1538-4357/ab6bcd>.
184. Braatz, J.; Condon, J.; Henkel, C.; Greene, J.; Lo, F.; Reid, M.; Pesce, D.; Gao, F.; Impellizzeri, V.; Kuo, C.Y.; et al. A Measurement of the Hubble Constant by the Megamaser Cosmology Project. In *Proceedings of the Astrophysical Masers: Unlocking the Mysteries of the Universe*; Tarchi, A.; Reid, M.J.; Castangia, P., Eds.; Cambridge University Press: Cambridge, England 2018; Volume 336, pp. 86–91. <https://doi.org/10.1017/S1743921317010249>.
185. LIGO Scientific Collaboration. Advanced LIGO. *Class. Quant. Grav.* **2015**, *32*, 074001, <https://doi.org/10.1088/0264-9381/32/7/074001>.
186. Acernese, F.; Agathos, M.; Agatsuma, K.; Aisa, D.; Allemandou, N.; Allocata, A.; Amarni, J.; Astone, P.; Balestri, G.; Ballardin, G.; et al. Advanced Virgo: A second-generation interferometric gravitational wave detector. *Class. Quant. Grav.* **2015**, *32*, 024001, <https://doi.org/10.1088/0264-9381/32/2/024001>.
187. (LIGO Scientific Collaboration.; Virgo Collaboration.; et al. Gravitational Waves and Gamma-Rays from a Binary Neutron Star Merger: GW170817 and GRB 170817A. *Astroph. J. Lett.* **2017**, *848*, L13, <https://doi.org/10.3847/2041-8213/aa920c>.
188. Goldstein, A.; Veres, P.; Burns, E.; Briggs, M.S.; Hamburg, R.; Kocevski, D.; Wilson-Hodge, C.A.; Preece, R.D.; Poolakkil, S.; Roberts, O.J.; et al. An Ordinary Short Gamma-Ray Burst with Extraordinary Implications: Fermi-GBM Detection of GRB 170817A. *Astroph. J. Lett.* **2017**, *848*, L14, <https://doi.org/10.3847/2041-8213/aa8f41>.
189. Savchenko, V.; Ferrigno, C.; Kuulkers, E.; Bazzano, A.; Bozzo, E.; Brandt, S.; Chenevez, J.; Courvoisier, T.J.L.; Diehl, R.; Domingo, A.; et al. INTEGRAL Detection of the First Prompt Gamma-Ray Signal Coincident with the Gravitational-wave Event GW170817. *Astroph. J. Lett.* **2017**, *848*, L15, <https://doi.org/10.3847/2041-8213/aa8f94>.
190. LIGO Scientific Collaboration.; Virgo Collaboration.; et al. Multi-messenger Observations of a Binary Neutron Star Merger. *Astroph. J. Lett.* **2017**, *848*, L12, <https://doi.org/10.3847/2041-8213/aa91c9>.
191. The LIGO Scientific Collaboration.; the Virgo Collaboration.; the KAGRA Collaboration. Constraints on the cosmic expansion history from GWTC-3. *arXiv* **2021**, arXiv:2111.03604,
192. Mukherjee, S.; Krolewski, A.; Wandelt, B.D.; Silk, J. Cross-correlating dark sirens and galaxies: Measurement of H_0 from GWTC-3 of LIGO-Virgo-KAGRA. *arXiv* **2022**, arXiv:2203.03643,
193. Lorimer, D.R.; Bailes, M.; McLaughlin, M.A.; Narkevic, D.J.; Crawford, F. A Bright Millisecond Radio Burst of Extragalactic Origin. *Science* **2007**, *318*, 777, <https://doi.org/10.1126/science.1147532>.
194. Xiao, D.; Wang, F.; Dai, Z. The physics of fast radio bursts. *Science China Physics, Mechanics, and Astronomy* **2021**, *64*, 249501, <https://doi.org/10.1007/s11433-020-1661-7>.
195. Zhang, B. The Physics of Fast Radio Bursts. *arXiv* **2022**, arXiv:2212.03972.
196. Deng, W.; Zhang, B. Cosmological Implications of Fast Radio Burst/Gamma-Ray Burst Associations. *Astroph. J. Lett.* **2014**, *783*, L35, <https://doi.org/10.1088/2041-8205/783/2/L35>.

197. Shull, J.M.; Smith, B.D.; Danforth, C.W. The Baryon Census in a Multiphase Intergalactic Medium: 30% of the Baryons May Still be Missing. *Astroph. J.* **2012**, *759*, 23, <https://doi.org/10.1088/0004-637X/759/1/23>.
198. McQuinn, M. Locating the “Missing” Baryons with Extragalactic Dispersion Measure Estimates. *Astroph. J. Lett.* **2014**, *780*, L33, <https://doi.org/10.1088/2041-8205/780/2/L33>.
199. Zhang, Z.J.; Yan, K.; Li, C.M.; Zhang, G.Q.; Wang, F.Y. Intergalactic Medium Dispersion Measures of Fast Radio Bursts Estimated from IllustrisTNG Simulation and Their Cosmological Applications. *Astroph. J.* **2021**, *906*, 49, <https://doi.org/10.3847/1538-4357/abceb9>.
200. Zhang, G.Q.; Yu, H.; He, J.H.; Wang, F.Y. Dispersion Measures of Fast Radio Burst Host Galaxies Derived from IllustrisTNG Simulation. *Astroph. J.* **2020**, *900*, 170, <https://doi.org/10.3847/1538-4357/abaa4a>.
201. Vagnozzi, S. New physics in light of the H_0 tension: An alternative view. *Phys. Rev. D* **2020**, *102*, 023518, <https://doi.org/10.1103/PhysRevD.102.023518>.
202. Di Valentino, E.; Mena, O.; Pan, S.; Visinelli, L.; Yang, W.; Melchiorri, A.; Mota, D.F.; Riess, A.G.; Silk, J. In the realm of the Hubble tension-a review of solutions. *Class. Quant. Grav.* **2021**, *38*, 153001, <https://doi.org/10.1088/1361-6382/ac086d>.
203. Sabla, V.I.; Caldwell, R.R. No H_0 assistance from assisted quintessence. *Phys. Rev. D* **2021**, *103*, 103506, <https://doi.org/10.1103/PhysRevD.103.103506>.
204. Kamionkowski, M.; Riess, A.G. The Hubble Tension and Early Dark Energy. *arXiv* **2022**, arXiv:2211.04492,
205. Herold, L.; Ferreira, E.G.M. Resolving the Hubble tension with Early Dark Energy. *arXiv* **2022**, arXiv:2210.16296,
206. Poulin, V.; Smith, T.L.; Karwal, T.; Kamionkowski, M. Early Dark Energy can Resolve the Hubble Tension. *Phys. Rev. Lett.* **2019**, *122*, 221301, <https://doi.org/10.1103/PhysRevLett.122.221301>.
207. Kaloper, N. Dark energy, H_0 and weak gravity conjecture. *Int. J. Mod. Phys. D* **2019**, *28*, 1944017, <https://doi.org/10.1142/S0218271819440176>.
208. Lucca, M. The role of CMB spectral distortions in the Hubble tension: A proof of principle. *Phys. Lett. B* **2020**, *810*, 135791, <https://doi.org/10.1016/j.physletb.2020.135791>.
209. Chudaykin, A.; Gorbunov, D.; Nedelko, N. Exploring an early dark energy solution to the Hubble tension with Planck and SPTPol data. *Phys. Rev. D* **2021**, *103*, 043529, <https://doi.org/10.1103/PhysRevD.103.043529>.
210. Haridasu, B.S.; Viel, M.; Vittorio, N. Sources of H_0 -tension in dark energy scenarios. *Phys. Rev. D* **2021**, *103*, 063539, <https://doi.org/10.1103/PhysRevD.103.063539>.
211. Murgia, R.; Abellán, G.F.; Poulin, V. Early dark energy resolution to the Hubble tension in light of weak lensing surveys and lensing anomalies. *Phys. Rev. D* **2021**, *103*, 063502, <https://doi.org/10.1103/PhysRevD.103.063502>.
212. Berghaus, K.V.; Karwal, T. Thermal friction as a solution to the Hubble tension. *Phys. Rev. D* **2020**, *101*, 083537, <https://doi.org/10.1103/PhysRevD.101.083537>.
213. Alexander, S.; McDonough, E. Axion-dilaton destabilization and the Hubble tension. *Phys. Lett. B* **2019**, *797*, 134830, <https://doi.org/10.1016/j.physletb.2019.134830>.
214. Chudaykin, A.; Gorbunov, D.; Nedelko, N. Combined analysis of Planck and SPTPol data favors the early dark energy models. *J. Cosmol. Astropart. Phys.* **2020**, *2020*, 013, <https://doi.org/10.1088/1475-7516/2020/08/013>.
215. Agrawal, P.; Cyr-Racine, F.Y.; Pinner, D.; Randall, L. Rock ‘n’ Roll Solutions to the Hubble Tension. *arXiv* **2019**, arXiv:1904.01016,
216. Niedermann, F.; Sloth, M.S. Resolving the Hubble tension with new early dark energy. *Phys. Rev. D* **2020**, *102*, 063527, <https://doi.org/10.1103/PhysRevD.102.063527>.
217. Niedermann, F.; Sloth, M.S. New early dark energy. *Phys. Rev. D* **2021**, *103*, L041303. <https://doi.org/10.1103/PhysRevD.103.L041303>.
218. Freese, K.; Winkler, M.W. Chain early dark energy: A Proposal for solving the Hubble tension and explaining today’s dark energy. *Phys. Rev. D* **2021**, *104*, 083533, <https://doi.org/10.1103/PhysRevD.104.083533>.
219. Ye, G.; Piao, Y.S. Is the Hubble tension a hint of AdS phase around recombination? *Phys. Rev. D* **2020**, *101*, 083507, <https://doi.org/10.1103/PhysRevD.101.083507>.
220. Ong, Y.C. An Effective Sign Switching Dark Energy: Lotka-Volterra Model of Two Interacting Fluids. *arXiv* **2022**, arXiv:2212.04429,
221. Akarsu, Ö.; Barrow, J.D.; Escamilla, L.A.; Vazquez, J.A. Graduated dark energy: Observational hints of a spontaneous sign switch in the cosmological constant. *Phys. Rev. D* **2020**, *101*, 063528, <https://doi.org/10.1103/PhysRevD.101.063528>.
222. Lin, M.X.; Benevento, G.; Hu, W.; Raveri, M. Acoustic dark energy: Potential conversion of the Hubble tension. *Phys. Rev. D* **2019**, *100*, 063542, <https://doi.org/10.1103/PhysRevD.100.063542>.
223. Yin, L. Reducing the H_0 tension with exponential acoustic dark energy. *Eur. Phys. J. C* **2022**, *82*, 78, <https://doi.org/10.1140/epjc/s10052-022-10020-w>.
224. Braglia, M.; Ballardini, M.; Emond, W.T.; Finelli, F.; Gümrükçüoğlu, A.E.; Koyama, K.; Paoletti, D. Larger value for H_0 by an evolving gravitational constant. *Phys. Rev. D* **2020**, *102*, 023529, <https://doi.org/10.1103/PhysRevD.102.023529>.
225. Zhao, G.B.; Raveri, M.; Pogosian, L.; Wang, Y.; Crittenden, R.G.; Handley, W.J.; Percival, W.J.; Beutler, F.; Brinkmann, J.; Chuang, C.H.; et al. Dynamical dark energy in light of the latest observations. *Nat. Astron.* **2017**, *1*, 627–632, <https://doi.org/10.1038/s41550-017-0216-z>.
226. Batista, R.C. A Short Review on Clustering Dark Energy. *Universe* **2021**, *8*, 22, <https://doi.org/10.3390/universe8010022>.

227. Heisenberg, L.; Villarrubia-Rojo, H.; Zosso, J. Simultaneously solving the H_0 and σ_8 tensions with late dark energy. *arXiv* **2022**, arXiv:2201.11623.
228. Martinelli, M.; Tutzus, I. CMB Tensions with Low-Redshift H_0 and S_8 Measurements: Impact of a Redshift-Dependent Type-Ia Supernovae Intrinsic Luminosity. *Symmetry* **2019**, *11*, 986. <https://doi.org/10.3390/sym11080986>.
229. Alestas, G.; Kazantzidis, L.; Perivolaropoulos, L. H_0 tension, phantom dark energy, and cosmological parameter degeneracies. *Phys. Rev. D* **2020**, *101*, 123516. <https://doi.org/10.1103/PhysRevD.101.123516>.
230. D’Amico, G.; Senatore, L.; Zhang, P. Limits on wCDM from the EFTofLSS with the PyBird code. *J. Cosmol. Astropart. Phys.* **2021**, *2021*, 006. <https://doi.org/10.1088/1475-7516/2021/01/006>.
231. Yang, W.; Pan, S.; Valentino, E.D.; Saridakis, E.N. Observational Constraints on Dynamical Dark Energy with Pivoting Redshift. *Universe* **2019**, *5*, 219. <https://doi.org/10.3390/universe5110219>.
232. Di Valentino, E.; Melchiorri, A.; Silk, J. Cosmological constraints in extended parameter space from the Planck 2018 Legacy release. *J. Cosmol. Astropart. Phys.* **2020**, *2020*, 013. <https://doi.org/10.1088/1475-7516/2020/01/013>.
233. Vagnozzi, S.; Dhawan, S.; Gerbino, M.; Freese, K.; Goobar, A.; Mena, O. Constraints on the sum of the neutrino masses in dynamical dark energy models with $w(z) \geq -1$ are tighter than those obtained in Λ CDM. *Phys. Rev. D* **2018**, *98*, 083501. <https://doi.org/10.1103/PhysRevD.98.083501>.
234. Du, M.; Yang, W.; Xu, L.; Pan, S.; Mota, D.F. Future constraints on dynamical dark-energy using gravitational-wave standard sirens. *Phys. Rev. D* **2019**, *100*, 043535. <https://doi.org/10.1103/PhysRevD.100.043535>.
235. Yang, W.; Pan, S.; Di Valentino, E.; Saridakis, E.N.; Chakraborty, S. Observational constraints on one-parameter dynamical dark-energy parametrizations and the H_0 tension. *Phys. Rev. D* **2019**, *99*, 043543. <https://doi.org/10.1103/PhysRevD.99.043543>.
236. Li, X.; Shafieloo, A.; Sahni, V.; Starobinsky, A.A. Revisiting Metastable Dark Energy and Tensions in the Estimation of Cosmological Parameters. *Astroph. J.* **2019**, *887*, 153. <https://doi.org/10.3847/1538-4357/ab535d>.
237. Szydłowski, M.; Stachowski, A.; Urbanowski, K. The evolution of the FRW universe with decaying metastable dark energy—a dynamical system analysis. *J. Cosmol. Astropart. Phys.* **2020**, *2020*, 029. <https://doi.org/10.1088/1475-7516/2020/04/029>.
238. Yang, W.; Di Valentino, E.; Pan, S.; Basilakos, S.; Paliathanasis, A. Metastable dark energy models in light of Planck 2018 data: Alleviating the H_0 tension. *Phys. Rev. D* **2020**, *102*, 063503. <https://doi.org/10.1103/PhysRevD.102.063503>.
239. Di Valentino, E.; Mukherjee, A.; Sen, A.A. Dark Energy with Phantom Crossing and the H_0 Tension. *Entropy* **2021**, *23*, 404. <https://doi.org/10.3390/e23040404>.
240. Benevento, G.; Hu, W.; Raveri, M. Can late dark energy transitions raise the Hubble constant? *Phys. Rev. D* **2020**, *101*, 103517. <https://doi.org/10.1103/PhysRevD.101.103517>.
241. Alestas, G.; Kazantzidis, L.; Perivolaropoulos, L. $w-M$ phantom transition at $z_t < 0.1$ as a resolution of the Hubble tension. *Phys. Rev. D* **2021**, *103*, 083517. <https://doi.org/10.1103/PhysRevD.103.083517>.
242. Solà Peracaula, J.; Gómez-Valent, A.; de Cruz Pérez, J.; Moreno-Pulido, C. Running vacuum against the H_0 and σ_8 tensions. *Europhys. Lett.* **2021**, *134*, 19001. <https://doi.org/10.1209/0295-5075/134/19001>.
243. Mavromatos, N.E.; Solà Peracaula, J. Stringy-running-vacuum-model inflation: From primordial gravitational waves and stiff axion matter to dynamical dark energy. *Eur. Phys. J. Spec. Top.* **2021**, *230*, 2077–2110. <https://doi.org/10.1140/epjs/s11734-021-00197-8>.
244. Keeley, R.E.; Joudaki, S.; Kaplinghat, M.; Kirkby, D. Implications of a transition in the dark energy equation of state for the H_0 and σ_8 tensions. *J. Cosmol. Astropart. Phys.* **2019**, *2019*, 035. <https://doi.org/10.1088/1475-7516/2019/12/035>.
245. Dutta, K.; Roy, A.; Ruchika, Sen, A.A.; Sheikh-Jabbari, M.M. Beyond Λ CDM with low and high redshift data: implications for dark energy. *Gen. Relat. Gravit.* **2020**, *52*, 15. <https://doi.org/10.1007/s10714-020-2665-4>.
246. Yang, W.; Pan, S.; Di Valentino, E.; Paliathanasis, A.; Lu, J. Challenging bulk viscous unified scenarios with cosmological observations. *Phys. Rev. D* **2019**, *100*, 103518. <https://doi.org/10.1103/PhysRevD.100.103518>.
247. Elizalde, E.; Khurshudyan, M.; Odintsov, S.D.; Myrzakulov, R. Analysis of the H_0 tension problem in the Universe with viscous dark fluid. *Phys. Rev. D* **2020**, *102*, 123501. <https://doi.org/10.1103/PhysRevD.102.123501>.
248. da Silva, W.J.C.; Silva, R. Growth of matter perturbations in the extended viscous dark energy models. *Eur. Phys. J. C* **2021**, *81*, 403. <https://doi.org/10.1140/epjc/s10052-021-09177-7>.
249. Guo, R.Y.; Zhang, J.F.; Zhang, X. Can the H_0 tension be resolved in extensions to Λ CDM cosmology? *J. Cosmol. Astropart. Phys.* **2019**, *2019*, 054. <https://doi.org/10.1088/1475-7516/2019/02/054>.
250. van Putten, M.H.P.M. Alleviating tension in Λ CDM and the local distance ladder from first principles with no free parameters. *Mon. Not. R. Astron. Soc.* **2020**, *491*, L6–L10. <https://doi.org/10.1093/mnrasl/slz158>.
251. Dai, W.M.; Ma, Y.Z.; He, H.J. Reconciling Hubble constant discrepancy from holographic dark energy. *Phys. Rev. D* **2020**, *102*, 121302. <https://doi.org/10.1103/PhysRevD.102.121302>.
252. Colgáin, E.Ó.; Sheikh-Jabbari, M.M. A critique of holographic dark energy. *Class. Quant. Grav.* **2021**, *38*, 177001. <https://doi.org/10.1088/1361-6382/ac1504>.
253. da Silva, W.J.C.; Silva, R. Cosmological perturbations in the Tsallis holographic dark energy scenarios. *Eur. Phys. J. Plus* **2021**, *136*, 543. <https://doi.org/10.1140/epjp/s13360-021-01522-9>.

254. Ó Colgáin, E.; van Putten, M.H.P.M.; Yavartanoo, H. de Sitter Swampland, H_0 tension & observation. *Phys. Lett. B* **2019**, *793*, 126–129. <https://doi.org/10.1016/j.physletb.2019.04.032>.
255. Ó Colgáin, E.; Yavartanoo, H. Testing the Swampland: H_0 tension. *Phys. Lett. B* **2019**, *797*, 134907. <https://doi.org/10.1016/j.physletb.2019.134907>.
256. Anchordoqui, L.A.; Antoniadis, I.; Lust, D.; Soriano, J.F.; Taylor, T.R. H_0 tension and the string swampland. *Phys. Rev. D* **2020**, *101*, 083532, <https://doi.org/10.1103/PhysRevD.101.083532>.
257. Agrawal, P.; Obied, G.; Vafa, C. H_0 tension, swampland conjectures, and the epoch of fading dark matter. *Phys. Rev. D* **2021**, *103*, 043523, <https://doi.org/10.1103/PhysRevD.103.043523>.
258. Banerjee, A.; Cai, H.; Heisenberg, L.; Colgáin, E.Ó.; Sheikh-Jabbari, M.M.; Yang, T. Hubble sinks in the low-redshift swampland. *Phys. Rev. D* **2021**, *103*, L081305, <https://doi.org/10.1103/PhysRevD.103.L081305>.
259. Miao, H.; Huang, Z. The H_0 Tension in Non-flat QCDM Cosmology. *Astroph. J.* **2018**, *868*, 20, <https://doi.org/10.3847/1538-4357/aae523>.
260. Di Valentino, E.; Ferreira, R.Z.; Visinelli, L.; Danielsson, U. Late time transitions in the quintessence field and the H_0 tension. *Phys. Dark Universe* **2019**, *26*, 100385, <https://doi.org/10.1016/j.dark.2019.100385>.
261. Bag, S.; Sahni, V.; Shafieloo, A.; Shtanov, Y. Phantom Braneworld and the Hubble Tension. *Astroph. J.* **2021**, *923*, 212, <https://doi.org/10.3847/1538-4357/ac307e>.
262. Adler, S.L. Implications of a frame dependent dark energy for the spacetime metric, cosmography, and effective Hubble constant. *Phys. Rev. D* **2019**, *100*, 123503, <https://doi.org/10.1103/PhysRevD.100.123503>.
263. Cai, R.G.; Guo, Z.K.; Li, L.; Wang, S.J.; Yu, W.W. Chameleon dark energy can resolve the Hubble tension. *Phys. Rev. D* **2021**, *103*, L121302, <https://doi.org/10.1103/PhysRevD.103.L121302>.
264. Karwal, T.; Raveri, M.; Jain, B.; Khouri, J.; Trodden, M. Chameleon early dark energy and the Hubble tension. *Phys. Rev. D* **2022**, *105*, 063535, <https://doi.org/10.1103/PhysRevD.105.063535>.
265. Li, X.; Shafieloo, A. A Simple Phenomenological Emergent Dark Energy Model can Resolve the Hubble Tension. *Astroph. J. Lett.* **2019**, *883*, L3, <https://doi.org/10.3847/2041-8213/ab3e09>.
266. Hernández-Almada, A.; Leon, G.; Magaña, J.; García-Aspeitia, M.A.; Motta, V. Generalized emergent dark energy: Observational Hubble data constraints and stability analysis. *Mon. Not. R. Astron. Soc.* **2020**, *497*, 1590–1602, <https://doi.org/10.1093/mnras/staa2052>.
267. Yang, W.; Di Valentino, E.; Pan, S.; Mena, O. Emergent Dark Energy, neutrinos and cosmological tensions. *Phys. Dark Universe* **2021**, *31*, 100762, <https://doi.org/10.1016/j.dark.2020.100762>.
268. Li, X.; Shafieloo, A. Evidence for Emergent Dark Energy. *Astroph. J.* **2020**, *902*, 58, <https://doi.org/10.3847/1538-4357/abb3d0>.
269. Yang, W.; Di Valentino, E.; Pan, S.; Shafieloo, A.; Li, X. Generalized emergent dark energy model and the Hubble constant tension. *Phys. Rev. D* **2021**, *104*, 063521, <https://doi.org/10.1103/PhysRevD.104.063521>.
270. Benoum, H.B.; Yang, W.; Pan, S.; Di Valentino, E. Modified Emergent Dark Energy and its Astronomical Constraints. *arXiv* **2020**, arXiv:2008.09098.
271. Di Valentino, E.; Linder, E.V.; Melchiorri, A. Vacuum phase transition solves the H_0 tension. *Phys. Rev. D* **2018**, *97*, 043528, <https://doi.org/10.1103/PhysRevD.97.043528>.
272. Di Valentino, E.; Linder, E.V.; Melchiorri, A. H_0 ex machina: Vacuum metamorphosis and beyond H_0 . *Phys. Dark Universe* **2020**, *30*, 100733, <https://doi.org/10.1016/j.dark.2020.100733>.
273. Di Valentino, E.; Pan, S.; Yang, W.; Anchordoqui, L.A. Touch of neutrinos on the vacuum metamorphosis: Is the H_0 solution back? *Phys. Rev. D* **2021**, *103*, 123527, <https://doi.org/10.1103/PhysRevD.103.123527>.
274. Carneiro, S.; de Holanda, P.C.; Pigozzo, C.; Sobreira, F. Is the H_0 tension suggesting a fourth neutrino generation? *Phys. Rev. D* **2019**, *100*, 023505, <https://doi.org/10.1103/PhysRevD.100.023505>.
275. Gelmini, G.B.; Kawasaki, M.; Kusenko, A.; Murai, K.; Takhistov, V. Big bang nucleosynthesis constraints on sterile neutrino and lepton asymmetry of the Universe. *J. Cosmol. Astropart. Phys.* **2020**, *2020*, 051, <https://doi.org/10.1088/1475-7516/2020/09/051>.
276. Barenboim, G.; Kinney, W.H.; Park, W.I. Flavor versus mass eigenstates in neutrino asymmetries: Implications for cosmology. *Eur. Phys. J. C* **2017**, *77*, 590, <https://doi.org/10.1140/epjc/s10052-017-5147-4>.
277. D’Eramo, F.; Ferreira, R.Z.; Notari, A.; Bernal, J.L. Hot axions and the H_0 tension. *J. Cosmol. Astropart. Phys.* **2018**, *2018*, 014, <https://doi.org/10.1088/1475-7516/2018/11/014>.
278. Di Luzio, L.; Giannotti, M.; Nardi, E.; Visinelli, L. Corrigendum to “The landscape of QCD axion models” [Phys. Rep. 870 (2020) 1–117]. *Phys. Rep.* **2020**, *870*, 1–117, <https://doi.org/10.1016/j.physrep.2022.06.006>.
279. Xiao, L.; Zhang, L.; An, R.; Feng, C.; Wang, B. Fractional Dark Matter decay: Cosmological imprints and observational constraints. *J. Cosmol. Astropart. Phys.* **2020**, *2020*, 045, <https://doi.org/10.1088/1475-7516/2020/01/045>.
280. Blinov, N.; Keith, C.; Hooper, D. Warm decaying dark matter and the hubble tension. *J. Cosmol. Astropart. Phys.* **2020**, *2020*, 005, <https://doi.org/10.1088/1475-7516/2020/06/005>.

281. Haridasu, B.S.; Viel, M. Late-time decaying dark matter: Constraints and implications for the H_0 -tension. *Mon. Not. R. Astron. Soc.* **2020**, *497*, 1757–1764, <https://doi.org/10.1093/mnras/staa1991>.
282. Pandey, K.L.; Karwal, T.; Das, S. Alleviating the H_0 and σ_8 anomalies with a decaying dark matter model. *J. Cosmol. Astropart. Phys.* **2020**, *2020*, 026, <https://doi.org/10.1088/1475-7516/2020/07/026>.
283. Anchordoqui, L.A. Decaying dark matter, the H_0 tension, and the lithium problem. *Phys. Rev. D* **2021**, *103*, 035025, <https://doi.org/10.1103/PhysRevD.103.035025>.
284. Davari, Z.; Khosravi, N. Can decaying dark matter scenarios alleviate both H_0 and σ_8 tensions? *Mon. Not. R. Astron. Soc.* **2022**, *516*, 4373–4382, <https://doi.org/10.1093/mnras/stac2306>.
285. Hryczuk, A.; Jodłowski, K. Self-interacting dark matter from late decays and the H_0 tension. *Phys. Rev. D* **2020**, *102*, 043024, <https://doi.org/10.1103/PhysRevD.102.043024>.
286. Jodłowski, K. Self-interacting dark matter from late decays and the H_0 tension. In Proceedings of the European Physical Society Conference on High Energy Physics, Online conference, Jointly organized by Universität Hamburg and the research center DESY, 23–30 July, 2021; p. 115, <https://doi.org/10.22323/1.398.0115>.
287. Vattis, K.; Koushiappas, S.M.; Loeb, A. Dark matter decaying in the late Universe can relieve the H_0 tension. *Phys. Rev. D* **2019**, *99*, 121302, <https://doi.org/10.1103/PhysRevD.99.121302>.
288. Clark, S.J.; Vattis, K.; Koushiappas, S.M. Cosmological constraints on late-Universe decaying dark matter as a solution to the H_0 tension. *Phys. Rev. D* **2021**, *103*, 043014, <https://doi.org/10.1103/PhysRevD.103.043014>.
289. Choi, G.; Suzuki, M.; Yanagida, T.T. Quintessence axion dark energy and a solution to the hubble tension. *Phys. Lett. B* **2020**, *805*, 135408, <https://doi.org/10.1016/j.physletb.2020.135408>.
290. Gu, Y.; Khlopov, M.; Wu, L.; Yang, J.M.; Zhu, B. Light gravitino dark matter: LHC searches and the Hubble tension. *Phys. Rev. D* **2020**, *102*, 115005, <https://doi.org/10.1103/PhysRevD.102.115005>.
291. Alcaniz, J.; Bernal, N.; Masiero, A.; Queiroz, F.S. Light dark matter: A common solution to the lithium and H_0 problems. *Phys. Lett. B* **2021**, *812*, 136008, <https://doi.org/10.1016/j.physletb.2020.136008>.
292. Escudero, M.; Hooper, D.; Krnjaic, G.; Pierre, M. Cosmology With a Very Light $L_\mu - L_\tau$ Gauge Boson. *arXiv* **2019**, arXiv:1901.02010,
293. Desai, A.; Dienes, K.R.; Thomas, B. Constraining dark-matter ensembles with supernova data. *Phys. Rev. D* **2020**, *101*, 035031, <https://doi.org/10.1103/PhysRevD.101.035031>.
294. Choi, G.; Suzuki, M.; Yanagida, T.T. Degenerate Sub-keV fermion dark matter from a solution to the Hubble tension. *Phys. Rev. D* **2020**, *101*, 075031, <https://doi.org/10.1103/PhysRevD.101.075031>.
295. Di Valentino, E.; Boehm, C.; Hivon, E.; Bouchet, F.R. Reducing the H_0 and σ_8 tensions with dark matter-neutrino interactions. *Phys. Rev. D* **2018**, *97*, 043513, <https://doi.org/10.1103/PhysRevD.97.043513>.
296. Stadler, J.; Boehm, C.; Mena, O. Comprehensive study of neutrino-dark matter mixed damping. *J. Cosmol. Astropart. Phys.* **2019**, *2019*, 014, <https://doi.org/10.1088/1475-7516/2019/08/014>.
297. Mosbech, M.R.; Boehm, C.; Hannestad, S.; Mena, O.; Stadler, J.; Wong, Y.Y.Y. The full Boltzmann hierarchy for dark matter-massive neutrino interactions. *J. Cosmol. Astropart. Phys.* **2021**, *2021*, 066, <https://doi.org/10.1088/1475-7516/2021/03/066>.
298. Arias-Aragón, F.; Fernández-Martínez, E.; González-López, M.; Merlo, L. Neutrino masses and Hubble tension via a Majoron in MFV. *Eur. Phys. J. C* **2021**, *81*, 28, <https://doi.org/10.1140/epjc/s10052-020-08825-8>.
299. Escudero, M.; Witte, S.J. The hubble tension as a hint of leptogenesis and neutrino mass generation. *Eur. Phys. J. C* **2021**, *81*, 515, <https://doi.org/10.1140/epjc/s10052-021-09276-5>.
300. Huang, G.y.; Rodejohann, W. Solving the Hubble tension without spoiling big bang nucleosynthesis. *Phys. Rev. D* **2021**, *103*, 123007, <https://doi.org/10.1103/PhysRevD.103.123007>.
301. Boyarsky, A.; Ovchynnikov, M.; Sabti, N.; Syvolap, V. When feebly interacting massive particles decay into neutrinos: The N_{eff} story. *Phys. Rev. D* **2021**, *104*, 035006, <https://doi.org/10.1103/PhysRevD.104.035006>.
302. Archidiacono, M.; Hooper, D.C.; Murgia, R.; Bohr, S.; Lesgourgues, J.; Viel, M. Constraining Dark Matter-Dark Radiation interactions with CMB, BAO, and Lyman- α . *J. Cosmol. Astropart. Phys.* **2019**, *2019*, 055, <https://doi.org/10.1088/1475-7516/2019/10/055>.
303. Becker, N.; Hooper, D.C.; Kahlhoefer, F.; Lesgourgues, J.; Schöneberg, N. Cosmological constraints on multi-interacting dark matter. *J. Cosmol. Astropart. Phys.* **2021**, *2021*, 019, <https://doi.org/10.1088/1475-7516/2021/02/019>.
304. Buen-Abad, M.A.; Emami, R.; Schmaltz, M. Cannibal dark matter and large scale structure. *Phys. Rev. D* **2018**, *98*, 083517, <https://doi.org/10.1103/PhysRevD.98.083517>.
305. Freese, K.; Sfakianakis, E.I.; Stengel, P.; Visinelli, L. The Higgs boson can delay reheating after inflation. *J. Cosmol. Astropart. Phys.* **2018**, *2018*, 067, <https://doi.org/10.1088/1475-7516/2018/05/067>.
306. Anchordoqui, L.A.; Bergliaffa, S.E.P. Hot thermal universe endowed with massive dark vector fields and the Hubble tension. *Phys. Rev. D* **2019**, *100*, 123525, <https://doi.org/10.1103/PhysRevD.100.123525>.
307. Flambaum, V.V.; Samsonov, I.B. Ultralight dark photon as a model for early Universe dark matter. *Phys. Rev. D* **2019**, *100*, 063541, <https://doi.org/10.1103/PhysRevD.100.063541>.

308. Carr, B.; Kühnel, F. Primordial Black Holes as Dark Matter: Recent Developments. *Annu. Rev. Nucl. Part. S.* **2020**, *70*, 355–394, <https://doi.org/10.1146/annurev-nucl-050520-125911>.
309. Flores, M.M.; Kusenko, A. Primordial Black Holes from Long-Range Scalar Forces and Scalar Radiative Cooling. *Phys. Rev. Lett.* **2021**, *126*, 041101, <https://doi.org/10.1103/PhysRevLett.126.041101>.
310. Green, A.M.; Kavanagh, B.J. Primordial black holes as a dark matter candidate. *Journal of Physics G Nuclear Physics* **2021**, *48*, 043001, <https://doi.org/10.1088/1361-6471/abc534>.
311. Artymowski, M.; Ben-Dayan, I.; Kumar, U. Emergent dark energy from unparticles. *Phys. Rev. D* **2021**, *103*, L121303, <https://doi.org/10.1103/PhysRevD.103.L121303>.
312. Yao, Y.H.; Meng, X.H. Can interacting dark energy with dynamical coupling resolve the Hubble tension. *arXiv* **2022**, arXiv:2207.05955.
313. Kumar, S.; Nunes, R.C.; Yadav, S.K. Dark sector interaction: A remedy of the tensions between CMB and LSS data. *Eur. Phys. J. C* **2019**, *79*, 576, <https://doi.org/10.1140/epjc/s10052-019-7087-7>.
314. Yang, W.; Pan, S.; Nunes, R.C.; Mota, D.F. Dark calling dark: Interaction in the dark sector in presence of neutrino properties after Planck CMB final release. *J. Cosmol. Astropart. Phys.* **2020**, *2020*, 008, <https://doi.org/10.1088/1475-7516/2020/04/008>.
315. Di Valentino, E.; Melchiorri, A.; Mena, O.; Vagnozzi, S. Interacting dark energy in the early 2020s: A promising solution to the H_0 and cosmic shear tensions. *Phys. Dark Universe* **2020**, *30*, 100666, <https://doi.org/10.1016/j.dark.2020.100666>.
316. Gao, L.Y.; Zhao, Z.W.; Xue, S.S.; Zhang, X. Relieving the H_0 tension with a new interacting dark energy model. *J. Cosmol. Astropart. Phys.* **2021**, *2021*, 005, <https://doi.org/10.1088/1475-7516/2021/07/005>.
317. Wang, L.F.; Zhang, J.H.; He, D.Z.; Zhang, J.F.; Zhang, X. Constraints on interacting dark energy models from time-delay cosmography with seven lensed quasars. *Mon. Not. R. Astron. Soc.* **2022**, *514*, 1433–1440, <https://doi.org/10.1093/mnras/stac1468>.
318. Gómez-Valent, A.; Pettorino, V.; Amendola, L. Update on coupled dark energy and the H_0 tension. *Phys. Rev. D* **2020**, *101*, 123513, <https://doi.org/10.1103/PhysRevD.101.123513>.
319. Yang, W.; Pan, S.; Di Valentino, E.; Nunes, R.C.; Vagnozzi, S.; Mota, D.F. Tale of stable interacting dark energy, observational signatures, and the H_0 tension. *J. Cosmol. Astropart. Phys.* **2018**, *2018*, 019, <https://doi.org/10.1088/1475-7516/2018/09/019>.
320. Di Valentino, E.; Melchiorri, A.; Mena, O.; Vagnozzi, S. Nonminimal dark sector physics and cosmological tensions. *Phys. Rev. D* **2020**, *101*, 063502, <https://doi.org/10.1103/PhysRevD.101.063502>.
321. Banihashemi, A.; Khosravi, N.; Shirazi, A.H. Ginzburg-Landau theory of dark energy: A framework to study both temporal and spatial cosmological tensions simultaneously. *Phys. Rev. D* **2019**, *99*, 083509, <https://doi.org/10.1103/PhysRevD.99.083509>.
322. Pan, S.; Yang, W.; Paliathanasis, A. Non-linear interacting cosmological models after Planck 2018 legacy release and the H_0 tension. *Mon. Not. R. Astron. Soc.* **2020**, *493*, 3114–3131, <https://doi.org/10.1093/mnras/staa213>.
323. Pan, S.; Yang, W.; Di Valentino, E.; Saridakis, E.N.; Chakraborty, S. Interacting scenarios with dynamical dark energy: Observational constraints and alleviation of the H_0 tension. *Phys. Rev. D* **2019**, *100*, 103520, <https://doi.org/10.1103/PhysRevD.100.103520>.
324. Yang, W.; Di Valentino, E.; Mena, O.; Pan, S. Dynamical dark sectors and neutrino masses and abundances. *Phys. Rev. D* **2020**, *102*, 023535, <https://doi.org/10.1103/PhysRevD.102.023535>.
325. Pan, S.; Yang, W.; Singha, C.; Saridakis, E.N. Observational constraints on sign-changeable interaction models and alleviation of the H_0 tension. *Phys. Rev. D* **2019**, *100*, 083539, <https://doi.org/10.1103/PhysRevD.100.083539>.
326. Yang, W.; Pan, S.; Xu, L.; Mota, D.F. Effects of anisotropic stress in interacting dark matter—Dark energy scenarios. *Mon. Not. R. Astron. Soc.* **2019**, *482*, 1858–1871, <https://doi.org/10.1093/mnras/sty2789>.
327. Amirhashchi, H.; Yadav, A.K. Interacting Dark Sectors in Anisotropic Universe: Observational Constraints and H_0 Tension. *arXiv* **2020**, arXiv:2001.03775.
328. Bégué, D.; Stahl, C.; Xue, S.S. A model of interacting dark fluids tested with supernovae and Baryon Acoustic Oscillations data. *Nucl. Phys. B* **2019**, *940*, 312–320, <https://doi.org/10.1016/j.nuclphysb.2019.01.001>.
329. Panpanich, S.; Burikham, P.; Ponglertsakul, S.; Tannukij, L. Resolving Hubble tension with quintom dark energy model. *Chin. Phys. C* **2021**, *45*, 015108. <https://doi.org/10.1088/1674-1137/abc537>.
330. Jesus, J.F.; Escobal, A.A.; Benndorf, D.; Pereira, S.H. Can dark matter-dark energy interaction alleviate the Cosmic Coincidence Problem? *arXiv* **2020**, arXiv:2012.07494.
331. Harko, T.; Asadi, K.; Moshafi, H.; Sheikhhahmadi, H. Observational constraints on the interacting dark energy—Dark matter (IDM) cosmological models. *Phys. Dark Universe* **2022**, *38*, 101131, <https://doi.org/10.1016/j.dark.2022.101131>.
332. Stadler, J.; Boehm, C. Constraints on γ -CDM interactions matching the Planck data precision. *J. Cosmol. Astropart. Phys.* **2018**, *2018*, 009, <https://doi.org/10.1088/1475-7516/2018/10/009>.
333. Yadav, S.K. Constraints on dark matter-photon coupling in the presence of time-varying dark energy. *Mod. Phys. Lett. A* **2020**, *35*, 1950358, <https://doi.org/10.1142/S0217732319503589>.
334. Barkana, R. Possible interaction between baryons and dark-matter particles revealed by the first stars. *Nature* **2018**, *555*, 71–74, <https://doi.org/10.1038/nature25791>.
335. Slatyer, T.R.; Wu, C.L. Early-Universe constraints on dark matter-baryon scattering and their implications for a global 21 cm signal. *Phys. Rev. D* **2018**, *98*, 023013, <https://doi.org/10.1103/PhysRevD.98.023013>.

336. Beltrán Jiménez, J.; Bettoni, D.; Figueruelo, D.; Teppa Pannia, F.A. On cosmological signatures of baryons-dark energy elastic couplings. *J. Cosmol. Astropart. Phys.* **2020**, *2020*, 020, <https://doi.org/10.1088/1475-7516/2020/08/020>.
337. Vagnozzi, S.; Visinelli, L.; Mena, O.; Mota, D.F. Do we have any hope of detecting scattering between dark energy and baryons through cosmology? *Mon. Not. R. Astron. Soc.* **2020**, *493*, 1139–1152, <https://doi.org/10.1093/mnras/staa311>.
338. Blinov, N.; Kelly, K.J.; Krnjajic, G.; McDermott, S.D. Constraining the Self-Interacting Neutrino Interpretation of the Hubble Tension. *Phys. Rev. Lett.* **2019**, *123*, 191102, <https://doi.org/10.1103/PhysRevLett.123.191102>.
339. He, H.J.; Ma, Y.Z.; Zheng, J. Resolving Hubble tension by self-interacting neutrinos with Dirac seesaw. *J. Cosmol. Astropart. Phys.* **2020**, *2020*, 003, <https://doi.org/10.1088/1475-7516/2020/11/003>.
340. Lyu, K.F.; Stamou, E.; Wang, L.T. Self-interacting neutrinos: Solution to Hubble tension versus experimental constraints. *Phys. Rev. D* **2021**, *103*, 015004, <https://doi.org/10.1103/PhysRevD.103.015004>.
341. Kreisch, C.D.; Cyr-Racine, F.Y.; Doré, O. Neutrino puzzle: Anomalies, interactions, and cosmological tensions. *Phys. Rev. D* **2020**, *101*, 123505, <https://doi.org/10.1103/PhysRevD.101.123505>.
342. Brinckmann, T.; Chang, J.H.; LoVerde, M. Self-interacting neutrinos, the Hubble parameter tension, and the cosmic microwave background. *Phys. Rev. D* **2021**, *104*, 063523, <https://doi.org/10.1103/PhysRevD.104.063523>.
343. Berryman, J.M.; Blinov, N.; Brdar, V.; Brinckmann, T.; Bustamante, M.; Cyr-Racine, F.Y.; Das, A.; de Gouvea, A.; Denton, P.B.; Bhupal Dev, P.S.; et al. Neutrino Self-Interactions: A White Paper. *arXiv* **2022**, arXiv:2203.01955.
344. Archidiacono, M.; Gariazzo, S.; Giunti, C.; Hannestad, S.; Tram, T. Sterile neutrino self-interactions: H_0 tension and short-baseline anomalies. *J. Cosmol. Astropart. Phys.* **2020**, *2020*, 029, <https://doi.org/10.1088/1475-7516/2020/12/029>.
345. Ghosh, S.; Khatri, R.; Roy, T.S. Dark neutrino interactions make gravitational waves blue. *Phys. Rev. D* **2018**, *97*, 063529, <https://doi.org/10.1103/PhysRevD.97.063529>.
346. Ghosh, S.; Khatri, R.; Roy, T.S. Can dark neutrino interactions phase out the Hubble tension? *Phys. Rev. D* **2020**, *102*, 123544, <https://doi.org/10.1103/PhysRevD.102.123544>.
347. Yang, W.; Pan, S.; Vagnozzi, S.; Di Valentino, E.; Mota, D.F.; Capozziello, S. Dawn of the dark: Unified dark sectors and the EDGES Cosmic Dawn 21-cm signal. *J. Cosmol. Astropart. Phys.* **2019**, *2019*, 044, <https://doi.org/10.1088/1475-7516/2019/11/044>.
348. Yang, W.; Pan, S.; Paliathanasis, A.; Ghosh, S.; Wu, Y. Observational constraints of a new unified dark fluid and the H_0 tension. *Mon. Not. R. Astron. Soc.* **2019**, *490*, 2071–2085, <https://doi.org/10.1093/mnras/stz2753>.
349. Benetti, M.; Borges, H.; Pigazzoli, C.; Carneiro, S.; Alcaniz, J. Dark sector interactions and the curvature of the Universe in light of Planck’s 2018 data. *arXiv* **2021**, arXiv:2102.10123.
350. Gurzadyan, V.G.; Stepanian, A. H_0 tension: Clue to common nature of dark sector? *Eur. Phys. J. C* **2019**, *79*, 568, <https://doi.org/10.1140/epjc/s10052-019-7081-0>.
351. Gurzadyan, V.G.; Stepanian, A. Hubble tension vs two flows. *Eur. Phys. J. Plus* **2021**, *136*, 235, <https://doi.org/10.1140/epjp/s13360-021-01229-x>.
352. Quiros, I. Selected topics in scalar-tensor theories and beyond. *Int. J. Mod. Phys. D* **2019**, *28*, 1930012–156, <https://doi.org/10.1142/S021827181930012X>.
353. D’Agostino, R.; Nunes, R.C. Measurements of H_0 in modified gravity theories: The role of lensed quasars in the late-time Universe. *Phys. Rev. D* **2020**, *101*, 103505, <https://doi.org/10.1103/PhysRevD.101.103505>.
354. Odintsov, S.D.; Sáez-Chillón Gómez, D.; Sharov, G.S. Analyzing the H_0 tension in $F(R)$ gravity models. *Nuclear Physics B* **2021**, *966*, 115377, <https://doi.org/10.1016/j.nuclphysb.2021.115377>.
355. Wang, D. Can $f(R)$ gravity relieve H_0 and σ_8 tensions? *Eur. Phys. J. C* **2021**, *81*, 482, <https://doi.org/10.1140/epjc/s10052-021-09264-9>.
356. Schiavone, T.; Montani, G. $f(R)$ gravity in the Jordan Frame as a Paradigm for the Hubble Tension. *arXiv* **2022**, arXiv:2211.16737.
357. Nunes, R.C. Structure formation in $f(T)$ gravity and a solution for H_0 tension. *J. Cosmol. Astropart. Phys.* **2018**, *2018*, 052, <https://doi.org/10.1088/1475-7516/2018/05/052>.
358. Yan, S.F.; Zhang, P.; Chen, J.W.; Zhang, X.Z.; Cai, Y.F.; Saridakis, E.N. Interpreting cosmological tensions from the effective field theory of torsional gravity. *Phys. Rev. D* **2020**, *101*, 121301, <https://doi.org/10.1103/PhysRevD.101.121301>.
359. Wang, D.; Mota, D. Can $f(T)$ gravity resolve the H_0 tension? *Phys. Rev. D* **2020**, *102*, 063530, <https://doi.org/10.1103/PhysRevD.102.063530>.
360. Aljaf, M.; Elizalde, E.; Khurshudyan, M.; Myrzakulov, K.; Zhdyranova, A. Solving the H_0 tension in $f(T)$ Gravity through Bayesian Machine Learning. *arXiv* **2022**, arXiv:2205.06252.
361. Escamilla-Rivera, C.; Said, J.L. Cosmological viable models in $f(T, B)$ theory as solutions to the H_0 tension. *Class. Quant. Grav.* **2020**, *37*, 165002, <https://doi.org/10.1088/1361-6382/ab939c>.
362. Paliathanasis, A. Minisuperspace Quantization of $f(T, B)$ Cosmology. *Universe* **2021**, *7*, 150, <https://doi.org/10.3390/universe7050150>.
363. Albuquerque, I.S.; Frusciante, N. A designer approach to $f(Q)$ gravity and cosmological implications. *Phys. Dark Universe* **2022**, *35*, 100980, <https://doi.org/10.1016/j.dark.2022.100980>.
364. Koussour, M.; Pacif, S.K.J.; Bennai, M.; Sahoo, P.K. A new parametrization of Hubble parameter in $f(Q)$ gravity. *arXiv* **2022**, arXiv:2208.04723,

365. Joudaki, S.; Ferreira, P.G.; Lima, N.A.; Winther, H.A. Testing gravity on cosmic scales: A case study of Jordan-Brans-Dicke theory. *Phys. Rev. D* **2022**, *105*, 043522, <https://doi.org/10.1103/PhysRevD.105.043522>.
366. Solà Peracaula, J.; Gómez-Valent, A.; de Cruz Pérez, J.; Moreno-Pulido, C. Brans-Dicke Gravity with a Cosmological Constant Smoothes Out Λ CDM Tensions. *Astroph. J. Lett.* **2019**, *886*, L6, <https://doi.org/10.3847/2041-8213/ab53e9>.
367. Peracaula, J.S.; Gómez-Valent, A.; de Cruz Pérez, J.; Moreno-Pulido, C. Brans-Dicke cosmology with a Λ -term: A possible solution to Λ CDM tensions. *Class. Quant. Grav.* **2020**, *37*, 245003. <https://doi.org/10.1088/1361-6382/abbc43>.
368. Ballardini, M.; Braglia, M.; Finelli, F.; Paoletti, D.; Starobinsky, A.A.; Umlitá, C. Scalar-tensor theories of gravity, neutrino physics, and the H_0 tension. *J. Cosmol. Astropart. Phys.* **2020**, *2020*, 044, <https://doi.org/10.1088/1475-7516/2020/10/044>.
369. Ballesteros, G.; Notari, A.; Rompineve, F. The H_0 tension: ΔG_N vs. ΔN_{eff} . *J. Cosmol. Astropart. Phys.* **2020**, *2020*, 024, <https://doi.org/10.1088/1475-7516/2020/11/024>.
370. Abadi, T.; Kovetz, E.D. Can conformally coupled modified gravity solve the Hubble tension? *Phys. Rev. D* **2021**, *103*, 023530, <https://doi.org/10.1103/PhysRevD.103.023530>.
371. Braglia, M.; Ballardini, M.; Finelli, F.; Koyama, K. Early modified gravity in light of the H_0 tension and LSS data. *Phys. Rev. D* **2021**, *103*, 043528, <https://doi.org/10.1103/PhysRevD.103.043528>.
372. Desmond, H.; Jain, B.; Sakstein, J. Erratum: Local resolution of the Hubble tension: The impact of screened fifth forces on the cosmic distance ladder [Phys. Rev. D 100, 043537 (2019)]. *Phys. Rev. D* **2020**, *101*, 129901. <https://doi.org/10.1103/PhysRevD.101.129901>.
373. Desmond, H.; Sakstein, J. Screened fifth forces lower the TRGB-calibrated Hubble constant too. *Phys. Rev. D* **2020**, *102*, 023007, <https://doi.org/10.1103/PhysRevD.102.023007>.
374. Khosravi, N. Über-gravity and the cosmological constant problem. *Phys. Dark Universe* **2018**, *21*, 21, <https://doi.org/10.1016/j.dark.2018.05.003>.
375. Khosravi, N.; Baghram, S.; Afshordi, N.; Altamirano, N. H_0 tension as a hint for a transition in gravitational theory. *Phys. Rev. D* **2019**, *99*, 103526, <https://doi.org/10.1103/PhysRevD.99.103526>.
376. Zumalacárregui, M. Gravity in the era of equality: Towards solutions to the Hubble problem without fine-tuned initial conditions. *Phys. Rev. D* **2020**, *102*, 023523, <https://doi.org/10.1103/PhysRevD.102.023523>.
377. Heisenberg, L.; Villarrubia-Rojo, H. Proca in the sky. *J. Cosmol. Astropart. Phys.* **2021**, *2021*, 032, <https://doi.org/10.1088/1475-7516/2021/03/032>.
378. Belgacem, E.; Dirian, Y.; Foffa, S.; Maggiore, M. Nonlocal gravity. Conceptual aspects and cosmological predictions. *J. Cosmol. Astropart. Phys.* **2018**, *2018*, 002, <https://doi.org/10.1088/1475-7516/2018/03/002>.
379. Belgacem, E.; Dirian, Y.; Finke, A.; Foffa, S.; Maggiore, M. Gravity in the infrared and effective nonlocal models. *J. Cosmol. Astropart. Phys.* **2020**, *2020*, 010, <https://doi.org/10.1088/1475-7516/2020/04/010>.
380. Linares Cedeño, F.X.; Nucamendi, U. Revisiting cosmological diffusion models in Unimodular Gravity and the H_0 tension. *Phys. Dark Universe* **2021**, *32*, 100807, <https://doi.org/10.1016/j.dark.2021.100807>.
381. Alvarez, P.D.; Koch, B.; Laporte, C.; Rincón, Á. Can scale-dependent cosmology alleviate the H_0 tension? *J. Cosmol. Astropart. Phys.* **2021**, *2021*, 019, <https://doi.org/10.1088/1475-7516/2021/06/019>.
382. De Felice, A.; Mukohyama, S.; Pookkillath, M.C. Addressing H_0 tension by means of VCDM. *Phys. Lett. B* **2021**, *816*, 136201, <https://doi.org/10.1016/j.physletb.2021.136201>.
383. Ganz, A.; Martens, P.; Mukohyama, S.; Namba, R. Bouncing Cosmology in VCDM. *arXiv* **2022**, arXiv:2212.13561.
384. Ratra, B. Tilted spatially nonflat inflation. *Phys. Rev. D* **2022**, *106*, 123524, <https://doi.org/10.1103/PhysRevD.106.123524>.
385. Di Valentino, E.; Mersini-Houghton, L. Testing predictions of the quantum landscape multiverse 2: The exponential inflationary potential. *J. Cosmol. Astropart. Phys.* **2017**, *2017*, 020, <https://doi.org/10.1088/1475-7516/2017/03/020>.
386. Guo, R.Y.; Zhang, X. Constraints on inflation revisited: An analysis including the latest local measurement of the Hubble constant. *Eur. Phys. J. C* **2017**, *77*, 882, <https://doi.org/10.1140/epjc/s10052-017-5454-9>.
387. Keeley, R.E.; Shafieloo, A.; Hazra, D.K.; Souradeep, T. Inflation wars: A new hope. *J. Cosmol. Astropart. Phys.* **2020**, *2020*, 055, <https://doi.org/10.1088/1475-7516/2020/09/055>.
388. Liu, M.; Huang, Z. Band-limited Features in the Primordial Power Spectrum Do Not Resolve the Hubble Tension. *Astroph. J.* **2020**, *897*, 166, <https://doi.org/10.3847/1538-4357/ab982e>.
389. Aresté Saló, L.; Benisty, D.; Guendelman, E.I.; Haro, J.d. Quintessential inflation and cosmological seesaw mechanism: reheating and observational constraints. *J. Cosmol. Astropart. Phys.* **2021**, *2021*, 007, <https://doi.org/10.1088/1475-7516/2021/07/007>.
390. Di Valentino, E.; Melchiorri, A.; Fantaye, Y.; Heavens, A. Bayesian evidence against the Harrison-Zel'dovich spectrum in tensions with cosmological data sets. *Phys. Rev. D* **2018**, *98*, 063508, <https://doi.org/10.1103/PhysRevD.98.063508>.
391. Chiang, C.T.; Slosar, A. Inferences of H_0 in presence of a non-standard recombination. *arXiv* **2018**, arXiv:1811.03624.
392. Hart, L.; Chluba, J. New constraints on time-dependent variations of fundamental constants using Planck data. *Mon. Not. R. Astron. Soc.* **2018**, *474*, 1850–1861, <https://doi.org/10.1093/mnras/stx2783>.
393. Hart, L.; Chluba, J. Updated fundamental constant constraints from Planck 2018 data and possible relations to the Hubble tension. *Mon. Not. R. Astron. Soc.* **2020**, *493*, 3255–3263, <https://doi.org/10.1093/mnras/staa412>.

394. Sekiguchi, T.; Takahashi, T. Early recombination as a solution to the H_0 tension. *Phys. Rev. D* **2021**, *103*, 083507, <https://doi.org/10.1103/PhysRevD.103.083507>.
395. Fung, L.W.H.; Li, L.; Liu, T.; Luu, H.N.; Qiu, Y.C.; Tye, S.H.H. Axi-Higgs cosmology. *J. Cosmol. Astropart. Phys.* **2021**, *2021*, 057, <https://doi.org/10.1088/1475-7516/2021/08/057>.
396. Jedamzik, K.; Saveliev, A. Stringent Limit on Primordial Magnetic Fields from the Cosmic Microwave Background Radiation. *Phys. Rev. Lett.* **2019**, *123*, 021301, <https://doi.org/10.1103/PhysRevLett.123.021301>.
397. Jedamzik, K.; Pogosian, L. Relieving the Hubble Tension with Primordial Magnetic Fields. *Phys. Rev. Lett.* **2020**, *125*, 181302, <https://doi.org/10.1103/PhysRevLett.125.181302>.
398. Banihashemi, A.; Khosravi, N.; Shirazi, A.H. Phase transition in the dark sector as a proposal to lessen cosmological tensions. *Phys. Rev. D* **2020**, *101*, 123521, <https://doi.org/10.1103/PhysRevD.101.123521>.
399. Banihashemi, A.; Khosravi, N.; Shafieloo, A. Dark energy as a critical phenomenon: A hint from Hubble tension. *J. Cosmol. Astropart. Phys.* **2021**, *2021*, 003, <https://doi.org/10.1088/1475-7516/2021/06/003>.
400. Kasai, M.; Futamase, T. A possible solution to the Hubble constant discrepancy: Cosmology where the local volume expansion is driven by the domain average density. *Prog. Theor. Exp. Phys.* **2019**, *2019*, 073E01, <https://doi.org/10.1093/ptep/ptz066>.
401. Yusofi, E.; Ramzanpour, M.A. Cosmological Constant Problem and H_0 Tension in Void-dominated Cosmology. *arXiv* **2022**, arXiv:2204.12180,
402. Akarsu, Ö.; Kumar, S.; Sharma, S.; Tedesco, L. Constraints on a Bianchi type I spacetime extension of the standard Λ CDM model. *Phys. Rev. D* **2019**, *100*, 023532, <https://doi.org/10.1103/PhysRevD.100.023532>.
403. Bolejko, K. Emerging spatial curvature can resolve the tension between high-redshift CMB and low-redshift distance ladder measurements of the Hubble constant. *Phys. Rev. D* **2018**, *97*, 103529, <https://doi.org/10.1103/PhysRevD.97.103529>.
404. Macpherson, H.J.; Lasky, P.D.; Price, D.J. The Trouble with Hubble: Local versus Global Expansion Rates in Inhomogeneous Cosmological Simulations with Numerical Relativity. *Astroph. J. Lett.* **2018**, *865*, L4, <https://doi.org/10.3847/2041-8213/aadf8c>.
405. Heinesen, A.; Buchert, T. Solving the curvature and Hubble parameter inconsistencies through structure formation-induced curvature. *Class. Quant. Grav.* **2020**, *37*, 164001, <https://doi.org/10.1088/1361-6382/ab954b>.
406. Ivanov, M.M.; Ali-Haïmoud, Y.; Lesgourgues, J. H_0 tension or T_0 tension? *Phys. Rev. D* **2020**, *102*, 063515, <https://doi.org/10.1103/PhysRevD.102.063515>.
407. Bengaly, C.A.P.; Gonzalez, J.E.; Alcaniz, J.S. Is there evidence for a hotter Universe? *Eur. Phys. J. C* **2020**, *80*, 936, <https://doi.org/10.1140/epjc/s10052-020-08522-6>.
408. Bose, B.; Lombriser, L. Easing cosmic tensions with an open and hotter universe. *Phys. Rev. D* **2021**, *103*, L081304, <https://doi.org/10.1103/PhysRevD.103.L081304>.
409. Adhikari, S.; Huterer, D. Super-CMB fluctuations and the Hubble tension. *Phys. Dark Universe* **2020**, *28*, 100539, <https://doi.org/10.1016/j.dark.2020.100539>.
410. Capozziello, S.; Benetti, M.; Spallicci, A.D.A.M. Addressing the cosmological H_0 tension by the Heisenberg uncertainty. *Foundations of Physics* **2020**, *50*, 893–899, <https://doi.org/10.1007/s10701-020-00356-2>.
411. Perez, A.; Sudarsky, D.; Wilson-Ewing, E. Resolving the H_0 tension with diffusion. *Gen. Relat. Gravit.* **2021**, *53*, 7, <https://doi.org/10.1007/s10714-020-02781-0>.
412. Berechya, D.; Leonhardt, U. Lifshitz cosmology: Quantum vacuum and Hubble tension. *Mon. Not. R. Astron. Soc.* **2021**, *507*, 3473–3485, <https://doi.org/10.1093/mnras/stab2345>.
413. Ortiz, C. Surface tension: Accelerated expansion, coincidence problem & Hubble tension. *Int. J. Mod. Phys. D* **2020**, *29*, 2050115–2652, <https://doi.org/10.1142/S0218271820501151>.
414. Vishwakarma, R.G. Resolving Hubble tension with the Milne model. *Int. J. Mod. Phys. D* **2020**, *29*, 2043025, <https://doi.org/10.1142/S0218271820430257>.
415. Milne, E.A. *Relativity, gravitation and world-structure*; 1935.
416. Krishnan, C.; Ó Colgáin, E.; Sheikh-Jabbari, M.M.; Yang, T. Running Hubble tension and a H_0 diagnostic. *Phys. Rev. D* **2021**, *103*, 103509, <https://doi.org/10.1103/PhysRevD.103.103509>.
417. Dainotti, M.G.; De Simone, B.; Schiavone, T.; Montani, G.; Rinaldi, E.; Lambiase, G. On the Hubble Constant Tension in the SNe Ia Pantheon Sample. *Astroph. J.* **2021**, *912*, 150, <https://doi.org/10.3847/1538-4357/abeb73>.
418. Marra, V.; Perivolaropoulos, L. Rapid transition of G_{eff} at $z_t \approx 0.01$ as a possible solution of the Hubble and growth tensions. *Phys. Rev. D* **2021**, *104*, L021303, <https://doi.org/10.1103/PhysRevD.104.L021303>.
419. Fosalba, P.; Gaztañaga, E. Explaining cosmological anisotropy: Evidence for causal horizons from CMB data. *Mon. Not. R. Astron. Soc.* **2021**, *504*, 5840–5862, <https://doi.org/10.1093/mnras/staa1193>.
420. Gaztañaga, E. The size of our causal Universe. *Mon. Not. R. Astron. Soc.* **2020**, *494*, 2766–2772, <https://doi.org/10.1093/mnras/staa1000>.
421. Haslbauer, M.; Banik, I.; Kroupa, P. The KBC void and Hubble tension contradict Λ CDM on a Gpc scale—Milgromian dynamics as a possible solution. *Mon. Not. R. Astron. Soc.* **2020**, *499*, 2845–2883, <https://doi.org/10.1093/mnras/staa2348>.

422. Beltrán Jiménez, J.; Bettoni, D.; Brax, P. Screening away the H_0 tension. *Int. J. Mod. Phys. D* **2020**, *29*, 2043010, <https://doi.org/10.1142/S0218271820430105>.
423. Jiménez, J.B.; Bettoni, D.; Brax, P. Charged dark matter and the H_0 tension. *Phys. Rev. D* **2021**, *103*, 103505. <https://doi.org/10.1103/PhysRevD.103.103505>.
424. Cruz, M.; Lepe, S.; Soto, G.E. Phantom cosmologies from QCD ghost dark energy. *Phys. Rev. D* **2022**, *106*, 103508, <https://doi.org/10.1103/PhysRevD.106.103508>.
425. Sola, J.; Gomez-Valent, A.; de Cruz Perez, J.; Moreno-Pulido, C. Running vacuum against the H_0 and σ_8 tensions. *arXiv* **2021**, arXiv:2102.12758,
426. Pan, S.; Yang, W.; Di Valentino, E.; Shafieloo, A.; Chakraborty, S. Reconciling H_0 tension in a six parameter space? *J. Cosmol. Astropart. Phys.* **2020**, *2020*, 062, <https://doi.org/10.1088/1475-7516/2020/06/062>.
427. Liu, Z.; Miao, H. Update constraints on neutrino mass and mass hierarchy in light of dark energy models. *Int. J. Mod. Phys. D* **2020**, *29*, 2050088, <https://doi.org/10.1142/S0218271820500881>.
428. Di Valentino, E.; Gariazzo, S.; Giunti, C.; Mena, O.; Pan, S.; Yang, W. Minimal dark energy: Key to sterile neutrino and Hubble constant tensions? *Phys. Rev. D* **2022**, *105*, 103511, <https://doi.org/10.1103/PhysRevD.105.103511>.
429. Moshafi, H.; Firouzjahi, H.; Talebian, A. Multiple Transitions in Vacuum Dark Energy and H_0 Tension. *Astroph. J.* **2022**, *940*, 121, <https://doi.org/10.3847/1538-4357/ac9c58>.
430. Moshafi, H.; Baghram, S.; Khosravi, N. CMB lensing in a modified Λ CDM model in light of the H_0 tension. *Phys. Rev. D* **2021**, *104*, 063506, <https://doi.org/10.1103/PhysRevD.104.063506>.
431. Yang, W.; Mukherjee, A.; Di Valentino, E.; Pan, S. Interacting dark energy with time varying equation of state and the H_0 tension. *Phys. Rev. D* **2018**, *98*, 123527, <https://doi.org/10.1103/PhysRevD.98.123527>.
432. Carrilho, P.; Moretti, C.; Bose, B.; Marković, K.; Pourtsidou, A. Interacting dark energy from redshift-space galaxy clustering. *J. Cosmol. Astropart. Phys.* **2021**, *2021*, 004, <https://doi.org/10.1088/1475-7516/2021/10/004>.
433. Guo, R.Y.; Feng, L.; Yao, T.Y.; Chen, X.Y. Exploration of interacting dynamical dark energy model with interaction term including the equation-of-state parameter: Alleviation of the H_0 tension. *J. Cosmol. Astropart. Phys.* **2021**, *2021*, 036, <https://doi.org/10.1088/1475-7516/2021/12/036>.
434. Nunes, R.C.; Di Valentino, E. Dark sector interaction and the supernova absolute magnitude tension. *Phys. Rev. D* **2021**, *104*, 063529, <https://doi.org/10.1103/PhysRevD.104.063529>.
435. Chatzidakis, S.; Giacomini, A.; Leach, P.G.L.; Leon, G.; Paliathanasis, A.; Pan, S. Interacting dark energy in curved FLRW spacetime from Weyl Integrable Spacetime. *J. High Energy Astrop.* **2022**, *36*, 141–151, <https://doi.org/10.1016/j.jheap.2022.10.001>.
436. Gariazzo, S.; Di Valentino, E.; Mena, O.; Nunes, R.C. Late-time interacting cosmologies and the Hubble constant tension. *Phys. Rev. D* **2022**, *106*, 023530, <https://doi.org/10.1103/PhysRevD.106.023530>.
437. Anchordoqui, L.A.; Barger, V.; Marfatia, D.; Soriano, J.F. Decay of multiple dark matter particles to dark radiation in different epochs does not alleviate the Hubble tension. *Phys. Rev. D* **2022**, *105*, 103512, <https://doi.org/10.1103/PhysRevD.105.103512>.
438. Vagnozzi, S.; Visinelli, L.; Brax, P.; Davis, A.C.; Sakstein, J. Direct detection of dark energy: The XENON1T excess and future prospects. *Phys. Rev. D* **2021**, *104*, 063023, <https://doi.org/10.1103/PhysRevD.104.063023>.
439. Benisty, D.; Davis, A.C. Dark energy interactions near the Galactic Center. *Phys. Rev. D* **2022**, *105*, 024052, <https://doi.org/10.1103/PhysRevD.105.024052>.
440. Lombriser, L. Consistency of the local Hubble constant with the cosmic microwave background. *Phys. Lett. B* **2020**, *803*, 135303, <https://doi.org/10.1016/j.physletb.2020.135303>.
441. Contarini, S.; Pisani, A.; Hamaus, N.; Marulli, F.; Moscardini, L.; Baldi, M. Voids fill us in on rising cosmology tensions. *arXiv* **2022**, arXiv:2212.07438,
442. Kazantzidis, L.; Perivolaropoulos, L. Hints of a local matter underdensity or modified gravity in the low z Pantheon data. *Phys. Rev. D* **2020**, *102*, 023520, <https://doi.org/10.1103/PhysRevD.102.023520>.
443. Alestas, G.; Perivolaropoulos, L. Late-time approaches to the Hubble tension deforming $H(z)$, worsen the growth tension. *Mon. Not. R. Astron. Soc.* **2021**, *504*, 3956–3962, <https://doi.org/10.1093/mnras/stab1070>.
444. Perivolaropoulos, L.; Skara, F. A Reanalysis of the Latest SH0ES Data for H_0 : Effects of New Degrees of Freedom on the Hubble Tension. *Universe* **2022**, *8*, 502, <https://doi.org/10.3390/universe8100502>.
445. Perivolaropoulos, L.; Skara, F. Gravitational transitions via the explicitly broken symmetron screening mechanism. *Phys. Rev. D* **2022**, *106*, 043528, <https://doi.org/10.1103/PhysRevD.106.043528>.
446. Dhawan, S.; Brout, D.; Scolnic, D.; Goobar, A.; Riess, A.G.; Miranda, V. Cosmological Model Insensitivity of Local H_0 from the Cepheid Distance Ladder. *Astroph. J.* **2020**, *894*, 54, <https://doi.org/10.3847/1538-4357/ab7fb0>.
447. Perivolaropoulos, L.; Skara, F. Hubble tension or a transition of the Cepheid SnIa calibrator parameters? *Phys. Rev. D* **2021**, *104*, 123511, <https://doi.org/10.1103/PhysRevD.104.123511>.
448. Mörtsell, E.; Goobar, A.; Johansson, J.; Dhawan, S. The Hubble Tension Revisited: Additional Local Distance Ladder Uncertainties. *Astroph. J.* **2022**, *935*, 58, <https://doi.org/10.3847/1538-4357/ac7c19>.

449. Smith, T.L.; Poulin, V.; Amin, M.A. Oscillating scalar fields and the Hubble tension: A resolution with novel signatures. *Phys. Rev. D* **2020**, *101*, 063523, <https://doi.org/10.1103/PhysRevD.101.063523>.
450. Sakstein, J.; Trodden, M. Early Dark Energy from Massive Neutrinos as a Natural Resolution of the Hubble Tension. *Phys. Rev. Lett.* **2020**, *124*, 161301, <https://doi.org/10.1103/PhysRevLett.124.161301>.
451. Gogoi, A.; Kumar Sharma, R.; Chanda, P.; Das, S. Early Mass-varying Neutrino Dark Energy: Nugget Formation and Hubble Anomaly. *Astroph. J.* **2021**, *915*, 132, <https://doi.org/10.3847/1538-4357/abfe5b>.
452. Poulin, V.; Smith, T.L.; Bartlett, A. Dark energy at early times and ACT data: A larger Hubble constant without late-time priors. *Phys. Rev. D* **2021**, *104*, 123550, <https://doi.org/10.1103/PhysRevD.104.123550>.
453. Seto, O.; Toda, Y. Comparing early dark energy and extra radiation solutions to the Hubble tension with BBN. *Phys. Rev. D* **2021**, *103*, 123501, <https://doi.org/10.1103/PhysRevD.103.123501>.
454. Ye, G.; Zhang, J.; Piao, Y.S. Resolving both H_0 and S_8 tensions with AdS early dark energy and ultralight axion. *arXiv* **2021**, arXiv:2107.13391,
455. Jiang, J.Q.; Piao, Y.S. Testing AdS early dark energy with Planck, SPTpol, and LSS data. *Phys. Rev. D* **2021**, *104*, 103524, <https://doi.org/10.1103/PhysRevD.104.103524>.
456. Niedermann, F.; Sloth, M.S. Hot new early dark energy: Towards a unified dark sector of neutrinos, dark energy and dark matter. *Phys. Lett. B* **2022**, *835*, 137555, <https://doi.org/10.1016/j.physletb.2022.137555>.
457. Smith, T.L.; Lucca, M.; Poulin, V.; Abellán, G.F.; Balkenhol, L.; Benabed, K.; Galli, S.; Murgia, R. Hints of early dark energy in Planck, SPT, and ACT data: New physics or systematics? *Phys. Rev. D* **2022**, *106*, 043526, <https://doi.org/10.1103/PhysRevD.106.043526>.
458. Fernandez-Martinez, E.; Pierre, M.; Pinsard, E.; Rosauro-Alcaraz, S. Inverse Seesaw, dark matter and the Hubble tension. *Eur. Phys. J. C* **2021**, *81*, 954, <https://doi.org/10.1140/epjc/s10052-021-09760-y>.
459. Seto, O.; Toda, Y. Hubble tension in lepton asymmetric cosmology with an extra radiation. *Phys. Rev. D* **2021**, *104*, 063019, <https://doi.org/10.1103/PhysRevD.104.063019>.
460. Aboubrahim, A.; Klasen, M.; Nath, P. Analyzing the Hubble tension through hidden sector dynamics in the early universe. *J. Cosmol. Astropart. Phys.* **2022**, *2022*, 042, <https://doi.org/10.1088/1475-7516/2022/04/042>.
461. Gu, Y.; Wu, L.; Zhu, B. Axion dark radiation: Hubble tension and the Hyper-Kamiokande neutrino experiment. *Phys. Rev. D* **2022**, *105*, 095008, <https://doi.org/10.1103/PhysRevD.105.095008>.
462. Aloni, D.; Berlin, A.; Joseph, M.; Schmaltz, M.; Weiner, N. A Step in understanding the Hubble tension. *Phys. Rev. D* **2022**, *105*, 123516, <https://doi.org/10.1103/PhysRevD.105.123516>.
463. Ghosh, S.; Kumar, S.; Tsai, Y. Free-streaming and coupled dark radiation isocurvature perturbations: Constraints and application to the Hubble tension. *J. Cosmol. Astropart. Phys.* **2022**, *2022*, 014, <https://doi.org/10.1088/1475-7516/2022/05/014>.
464. Berbig, M.; Jana, S.; Trautner, A. The Hubble tension and a renormalizable model of gauged neutrino self-interactions. *Phys. Rev. D* **2020**, *102*, 115008, <https://doi.org/10.1103/PhysRevD.102.115008>.
465. Choudhury, S.R.; Hannestad, S.; Tram, T. Updated constraints on massive neutrino self-interactions from cosmology in light of the H_0 tension. *J. Cosmol. Astropart. Phys.* **2021**, *2021*, 084, <https://doi.org/10.1088/1475-7516/2021/03/084>.
466. Mazumdar, A.; Mohanty, S.; Parashari, P. Flavour specific neutrino self-interaction: H_0 tension and IceCube. *J. Cosmol. Astropart. Phys.* **2022**, *2022*, 011, <https://doi.org/10.1088/1475-7516/2022/10/011>.
467. Shimon, M. Possible resolution of the Hubble tension with Weyl invariant gravity. *J. Cosmol. Astropart. Phys.* **2022**, *2022*, 048, <https://doi.org/10.1088/1475-7516/2022/04/048>.
468. Petronikolou, M.; Basilakos, S.; Saridakis, E.N. Alleviating H_0 tension in Horndeski gravity. *Phys. Rev. D* **2022**, *106*, 124051, <https://doi.org/10.1103/PhysRevD.106.124051>.
469. Akarsu, Ö.; Kumar, S.; Özülker, E.; Vazquez, J.A. Relaxing cosmological tensions with a sign switching cosmological constant. *Phys. Rev. D* **2021**, *104*, 123512, <https://doi.org/10.1103/PhysRevD.104.123512>.
470. Akarsu, O.; Kumar, S.; Ozulker, E.; Vazquez, J.A.; Yadav, A. Relaxing cosmological tensions with a sign switching cosmological constant: Improved results with Planck, BAO and Pantheon data. *arXiv* **2022**, arXiv:2211.05742,
471. Vagnozzi, S. Consistency tests of Λ CDM from the early integrated Sachs-Wolfe effect: Implications for early-time new physics and the Hubble tension. *Phys. Rev. D* **2021**, *104*, 063524, <https://doi.org/10.1103/PhysRevD.104.063524>.
472. Blinov, N.; Krnjaic, G.; Li, S.W. Realistic model of dark atoms to resolve the Hubble tension. *Phys. Rev. D* **2022**, *105*, 095005, <https://doi.org/10.1103/PhysRevD.105.095005>.
473. Gough, M.P. Information Dark Energy Can Resolve the Hubble Tension and Is Falsifiable by Experiment. *Entropy* **2022**, *24*, 385. <https://doi.org/10.3390/e24030385>.
474. Araki, T.; Asai, K.; Honda, K.; Kasuya, R.; Sato, J.; Shimomura, T.; Yang, M.J.S. Resolving the Hubble tension in a $U(1)_{L_\mu - L_\tau}$ model with the Majoron. *Prog. Theor. Exp. Phys.* **2021**, *2021*, 103B05, <https://doi.org/10.1093/ptep/ptab108>.
475. Schöneberg, N.; Abellán, G.F.; Sánchez, A.P.; Witte, S.J.; Poulin, V.; Lesgourgues, J. The H_0 Olympics: A fair ranking of proposed models. *Phys. Rep.* **2022**, *984*, 1–55, <https://doi.org/10.1016/j.physrep.2022.07.001>.

476. Desmond, H.; Jain, B.; Sakstein, J. Local resolution of the Hubble tension: The impact of screened fifth forces on the cosmic distance ladder. *Phys. Rev. D* **2019**, *100*, 043537, <https://doi.org/10.1103/PhysRevD.100.043537>.
477. Poulin, V. How to Resolve the Hubble tension. In Proceedings of the H_0 2020: Assessing Uncertainties in Hubble’s Constant Across the Universe, Online conference, 22–26 June, 2020; p. 22. <https://doi.org/10.5281/zenodo.4062117>.
478. Addison, G.E. High H_0 Values from CMB E-mode Data: A Clue for Resolving the Hubble Tension? *Astroph. J. Lett.* **2021**, *912*, L1, <https://doi.org/10.3847/2041-8213/abf56e>.
479. Thiele, L.; Guan, Y.; Hill, J.C.; Kosowsky, A.; Spergel, D.N. Can small-scale baryon inhomogeneities resolve the Hubble tension? An investigation with ACT DR4. *Phys. Rev. D* **2021**, *104*, 063535, <https://doi.org/10.1103/PhysRevD.104.063535>.
480. Jedamzik, K.; Pogosian, L.; Zhao, G.B. Why reducing the cosmic sound horizon alone can not fully resolve the Hubble tension. *Commun. Phys.* **2021**, *4*, 123, <https://doi.org/10.1038/s42005-021-00628-x>.
481. Cai, R.G.; Guo, Z.K.; Wang, S.J.; Yu, W.W.; Zhou, Y. No-go guide for the Hubble tension: Late-time solutions. *Phys. Rev. D* **2022**, *105*, L021301, <https://doi.org/10.1103/PhysRevD.105.L021301>.
482. Cai, R.G.; Guo, Z.K.; Wang, S.J.; Yu, W.W.; Zhou, Y. No-go guide for late-time solutions to the Hubble tension: Matter perturbations. *Phys. Rev. D* **2022**, *106*, 063519, <https://doi.org/10.1103/PhysRevD.106.063519>.
483. Escudero, H.G.; Kuo, J.L.; Keeley, R.E.; Abazajian, K.N. Early or phantom dark energy, self-interacting, extra, or massive neutrinos, primordial magnetic fields, or a curved universe: An exploration of possible solutions to the H_0 and σ_8 problems. *Phys. Rev. D* **2022**, *106*, 103517. <https://doi.org/10.1103/PhysRevD.106.103517>.
484. Wang, Y.Y.; Tang, S.P.; Li, X.Y.; Jin, Z.P.; Fan, Y.Z. Prospects of calibrating afterglow modeling of short GRBs with gravitational wave inclination angle measurements and resolving the Hubble tension with a GW-GRB association event. *Phys. Rev. D* **2022**, *106*, 023011, <https://doi.org/10.1103/PhysRevD.106.023011>.
485. Khodadi, M.; Schreck, M. Hubble tension as a guide for refining the early Universe: Cosmologies with explicit local Lorentz and diffeomorphism violation. *arXiv* **2023**, arXiv:2301.03883.
486. Birrer, S.; Shajib, A.J.; Galan, A.; Millon, M.; Treu, T.; Agnello, A.; Auger, M.; Chen, G.C.F.; Christensen, L.; Collett, T.; et al. TDCOSMO. IV. Hierarchical time-delay cosmography—joint inference of the Hubble constant and galaxy density profiles. *Astron. Astrophys.* **2020**, *643*, A165, <https://doi.org/10.1051/0004-6361/202038861>.
487. Krishnan, C.; Colgáin, E.Ó.; Ruchika, Sen, A.A.; Sheikh-Jabbari, M.M.; Yang, T. Is there an early Universe solution to Hubble tension? *Phys. Rev. D* **2020**, *102*, 103525, <https://doi.org/10.1103/PhysRevD.102.103525>.
488. Lloyd, N.M.; Petrosian, V. Synchrotron Radiation as the Source of Gamma-Ray Burst Spectra. *Astroph. J.* **2000**, *543*, 722–732, <https://doi.org/10.1086/317125>.
489. Singal, J.; Petrosian, V.; Lawrence, A.; Stawarz, Ł. On the Radio and Optical Luminosity Evolution of Quasars. *Astroph. J.* **2011**, *743*, 104, <https://doi.org/10.1088/0004-637X/743/2/104>.
490. Dainotti, M.G.; Lenart, A.Ł.; Sarracino, G.; Nagataki, S.; Capozziello, S.; Fraija, N. The X-Ray Fundamental Plane of the Platinum Sample, the Kilonovae, and the SNe Ib/c Associated with GRBs. *Astroph. J.* **2020**, *904*, 97, <https://doi.org/10.3847/1538-4357/abbe8a>.
491. Ó Colgáin, E.; Sheikh-Jabbari, M.M.; Solomon, R.; Bargiacchi, G.; Capozziello, S.; Dainotti, M.G.; Stojkovic, D. Revealing intrinsic flat Λ CDM biases with standardizable candles. *Phys. Rev. D* **2022**, *106*, L041301. <https://doi.org/10.1103/PhysRevD.106.L041301>.
492. Dainotti, M.G.; De Simone, B.D.; Schiavone, T.; Montani, G.; Rinaldi, E.; Lambiase, G.; Bogdan, M.; Ugale, S. On the Evolution of the Hubble Constant with the SNe Ia Pantheon Sample and Baryon Acoustic Oscillations: A Feasibility Study for GRB-Cosmology in 2030. *Galaxies* **2022**, *10*, 24, <https://doi.org/10.3390/galaxies10010024>.
493. Colgáin, E.Ó.; Sheikh-Jabbari, M.M.; Solomon, R.; Dainotti, M.G.; Stojkovic, D. Putting Flat Λ CDM In The (Redshift) Bin. *arXiv* **2022**, arXiv:2206.11447.
494. Schwarz, G. Estimating the Dimension of a Model. *Ann. Stat.* **1978**, *6*, 461–464. <https://doi.org/10.1214/aos/1176344136>.
495. Akaike, H. A new look at the statistical model identification. *IEEE Trans. Autom. Control* **1974**, *19*, 716–723. <https://doi.org/10.1109/TAC.1974.1100705>.
496. Wojtak, R.; Hjorth, J. Intrinsic tension in the supernova sector of the local Hubble constant measurement and its implications. *Mon. Not. R. Astron. Soc.* **2022**, *515*, 2790–2799, <https://doi.org/10.1093/mnras/stac1878>.
497. Pedregosa, F.; Varoquaux, G.; Gramfort, A.; Michel, V.; Thirion, B.; et al. Scikit-learn: Machine Learning in Python. *J. Mach. Learn. Res.* **2011**, *12*, 2825–2830.
498. Gómez-Valent, A.; Amendola, L. H_0 from cosmic chronometers and Type Ia supernovae, with Gaussian Processes and the novel Weighted Polynomial Regression method. *J. Cosmol. Astropart. Phys.* **2018**, *2018*, 051, <https://doi.org/10.1088/1475-7516/2018/04/051>.
499. Yu, H.; Ratra, B.; Wang, F.Y. Hubble Parameter and Baryon Acoustic Oscillation Measurement Constraints on the Hubble Constant, the Deviation from the Spatially Flat Λ CDM Model, the Deceleration-Acceleration Transition Redshift, and Spatial Curvature. *Astroph. J.* **2018**, *856*, 3, <https://doi.org/10.3847/1538-4357/aab0a2>.
500. Liao, K.; Shafieloo, A.; Keeley, R.E.; Linder, E.V. A Model-independent Determination of the Hubble Constant from Lensed Quasars and Supernovae Using Gaussian Process Regression. *Astroph. J. Lett.* **2019**, *886*, L23, <https://doi.org/10.3847/2041-8213/ab5308>.

501. Liao, K.; Shafieloo, A.; Keeley, R.E.; Linder, E.V. Determining Model-independent H_0 and Consistency Tests. *Astroph. J. Lett.* **2020**, *895*, L29, <https://doi.org/10.3847/2041-8213/ab8dbb>.
502. Salti, M.; Ciger, E.; Kangal, E.E.; Zengin, B. Data-driven predictive modeling of Hubble parameter. *Phys. Scripta* **2022**, *97*, 085011, <https://doi.org/10.1088/1402-4896/ac807c>.
503. Melia, F.; Yennapureddy, M.K. Model selection using cosmic chronometers with Gaussian Processes. *J. Cosmol. Astropart. Phys.* **2018**, *2018*, 034, <https://doi.org/10.1088/1475-7516/2018/02/034>.
504. Rasmussen, C.E.; Williams, C.K.I. *Gaussian Processes for Machine Learning*; MIT Press: Cambridge, United States 2006.
505. Frazier, P.I. A Tutorial on Bayesian Optimization. *arXiv* **2018**, arXiv:1807.02811.
506. Schulz, E.; Speekenbrink, M.; Krause, A. A tutorial on Gaussian process regression: Modelling, exploring, and exploiting functions. *J. Math. Psychol.* **2018**, *85*, 1–16. <https://doi.org/https://doi.org/10.1016/j.jmp.2018.03.001>.
507. Hu, J.P.; Wang, F.Y. Revealing the late-time transition of H_0 : Relieve the Hubble crisis. *Mon. Not. R. Astron. Soc.* **2022**, *517*, 576–581, <https://doi.org/10.1093/mnras/stac2728>.
508. Jia, X.D.; Hu, J.P.; Wang, F.Y. The evidence for a decreasing trend of Hubble constant. *arXiv* **2022**, arXiv:2212.00238,
509. Malekjani, M.; Mc Conville, R.; Colgáin, E.; Pourojaghi, S.; Sheikh-Jabbari, M. M. Negative Dark Energy Density from High Redshift Pantheon+ Supernovae. *arXiv* **2023**, arXiv:2301.12725,
510. Krishnan, C.; Mohayaee, R.; Colgáin, E.Ó.; Sheikh-Jabbari, M.M.; Yin, L. Does Hubble tension signal a breakdown in FLRW cosmology? *Class. Quant. Grav.* **2021**, *38*, 184001, <https://doi.org/10.1088/1361-6382/ac1a81>.
511. Keeley, R.E.; Shafieloo, A. Ruling Out New Physics at Low Redshift as a solution to the H_0 Tension. *arXiv* **2022**, arXiv:2206.08440,
512. Keenan, R.C.; Barger, A.J.; Cowie, L.L. Evidence for a ~300 Megaparsec Scale Under-density in the Local Galaxy Distribution. *Astroph. J.* **2013**, *775*, 62, <https://doi.org/10.1088/0004-637X/775/1/62>.
513. Wang, F.Y.; Dai, Z.G. Testing the local-void alternative to dark energy using galaxy pairs. *Mon. Not. R. Astron. Soc.* **2013**, *432*, 3025–3029, <https://doi.org/10.1093/mnras/stt652>.
514. Camarena, D.; Marra, V.; Sakr, Z.; Clarkson, C. A void in the Hubble tension? The end of the line for the Hubble bubble. *Class. Quant. Grav.* **2022**, *39*, 184001, <https://doi.org/10.1088/1361-6382/ac8635>.
515. Yusofi, E.; Khanpour, M.; Khanpour, B.; Ramzanpour, M.A.; Mohsenzadeh, M. Surface tension of cosmic voids as a possible source for dark energy. *Mon. Not. R. Astron. Soc.* **2022**, *511*, L82–L86, <https://doi.org/10.1093/mnrasl/slac006>.
516. Benetti, M.; Capozziello, S.; Lambiase, G. Updating constraints on f(T) teleparallel cosmology and the consistency with big bang nucleosynthesis. *Mon. Not. R. Astron. Soc.* **2021**, *500*, 1795–1805, <https://doi.org/10.1093/mnras/staa3368>.
517. Kenworthy, W.D.; Scolnic, D.; Riess, A. The Local Perspective on the Hubble Tension: Local Structure Does Not Impact Measurement of the Hubble Constant. *Astroph. J.* **2019**, *875*, 145, <https://doi.org/10.3847/1538-4357/ab0ebf>.
518. Luković, V.V.; Haridasu, B.S.; Vittorio, N. Exploring the evidence for a large local void with supernovae Ia data. *Mon. Not. R. Astron. Soc.* **2020**, *491*, 2075–2087, <https://doi.org/10.1093/mnras/stz3070>.
519. Cai, R.G.; Ding, J.E.; Guo, Z.K.; Wang, S.J.; Yu, W.W. Do the observational data favor a local void? *Phys. Rev. D* **2021**, *103*, 123539, <https://doi.org/10.1103/PhysRevD.103.123539>.
520. Böhringer, H.; Chon, G.; Collins, C.A. Observational evidence for a local underdensity in the Universe and its effect on the measurement of the Hubble constant. *Astron. Astrophys.* **2020**, *633*, A19, <https://doi.org/10.1051/0004-6361/201936400>.
521. DES Collaboration. Dark Energy Survey Year 3 results: Imprints of cosmic voids and superclusters in the Planck CMB lensing map. *Mon. Not. R. Astron. Soc.* **2022**, *515*, 4417–4429, <https://doi.org/10.1093/mnras/stac2011>.
522. Krishnan, C.; Mondol, R. H_0 as a Universal FLRW Diagnostic. *arXiv* **2022**, arXiv:2201.13384,
523. Coleman, S. Fate of the false vacuum: Semiclassical theory. *Phys. Rev. D* **1977**, *15*, 2929–2936. <https://doi.org/10.1103/PhysRevD.15.2929>.
524. Callan, Curtis G., J.; Coleman, S. Fate of the false vacuum. II. First quantum corrections. *Phys. Rev. D* **1977**, *16*, 1762–1768. <https://doi.org/10.1103/PhysRevD.16.1762>.
525. Patwardhan, A.V.; Fuller, G.M. Late-time vacuum phase transitions: Connecting sub-eV scale physics with cosmological structure formation. *Phys. Rev. D* **2014**, *90*, 063009, <https://doi.org/10.1103/PhysRevD.90.063009>.
526. Oguri, M.; Marshall, P.J. Gravitationally lensed quasars and supernovae in future wide-field optical imaging surveys. *Mon. Not. R. Astron. Soc.* **2010**, *405*, 2579–2593, <https://doi.org/10.1111/j.1365-2966.2010.16639.x>.
527. Collett, T.E. The Population of Galaxy-Galaxy Strong Lenses in Forthcoming Optical Imaging Surveys. *Astroph. J.* **2015**, *811*, 20, <https://doi.org/10.1088/0004-637X/811/1/20>.
528. LSST Dark Energy Science Collaboration. Strongly lensed SNe Ia in the era of LSST: Observing cadence for lens discoveries and time-delay measurements. *Astron. Astrophys.* **2019**, *631*, A161, <https://doi.org/10.1051/0004-6361/201935370>.
529. Wei, J.; Cordier, B.; Antier, S.; Antilogus, P.; Atteia, J.L.; Bajat, A.; Basa, S.; Beckmann, V.; Bernardini, M.G.; Boissier, S.; et al. The Deep and Transient Universe in the SVOM Era: New Challenges and Opportunities—Scientific prospects of the SVOM mission. *arXiv* **2016**, arXiv:1610.06892,

-
530. Yuan, W.; Zhang, C.; Feng, H.; Zhang, S.N.; Ling, Z.X.; Zhao, D.; Deng, J.; Qiu, Y.; Osborne, J.P.; O'Brien, P.; et al. Einstein Probe—A small mission to monitor and explore the dynamic X-ray Universe. *arXiv* **2015**, arXiv:1506.07735,
531. Amati, L.; O'Brien, P.; Götz, D.; Bozzo, E.; Tenzer, C.; Frontera, F.; Ghirlanda, G.; Labanti, C.; Osborne, J.P.; Stratta, G.; et al. The THESEUS space mission concept: Science case, design and expected performances. *Adv. Space Res.* **2018**, *62*, 191–244, <https://doi.org/10.1016/j.asr.2018.03.010>.

Disclaimer/Publisher's Note: The statements, opinions and data contained in all publications are solely those of the individual author(s) and contributor(s) and not of MDPI and/or the editor(s). MDPI and/or the editor(s) disclaim responsibility for any injury to people or property resulting from any ideas, methods, instructions or products referred to in the content.